Beneath the Surface

New insights into removal processes in the depths of Slow Sand Filters

Trikannad, S.A.

DOI
10.4233/uuid:cf8d9a5c-6478-4466-b09b-22690583334b

Publication date
2024

Document Version
Final published version

Citation (APA)
Trikannad, S. A. (2024). *Beneath the Surface: New insights into removal processes in the depths of Slow Sand Filters*. [Dissertation (TU Delft), Delft University of Technology]. https://doi.org/10.4233/uuid:cf8d9a5c-6478-4466-b09b-22690583334b

BENEATH THE SURFACE

New insights into removal processes in the depths of *Slow Sand Filters*.

SHREYA AJITH TRIKANNAD

Beneath The Surface

New insights into removal processes in the depths of *Slow Sand Filters*

Shreya Ajith Trikannad

Beneath The Surface

New insights into removal processes in the depths of Slow Sand Filters

Dissertation

for the purpose of obtaining the degree of doctor
at Delft University of Technology
by the authority of the Rector Magnificus, prof.dr.ir. T.H.J.J. van der Hagen
chair of the Board of Doctorates
to be defended publicly on
Wednesday 25 September 2024 at 9:30 o'clock

by

Shreya Ajith TRIKANNAD

Master of Science in Civil Engineering
Delft University of Technology, the Netherlands
Born in Mysore, India

This dissertation has been approved by the promotors.

Composition of the doctoral committee:

Rector Magnificus	Chairperson
Prof.dr.ir. J.P. van der Hoek	Delft University of Technology, promotor
Prof.dr.ir. D. van Halem	Delft University of Technology, promotor

Independent members:

Prof.dr. G.J. Medema	Delft University of Technology
Prof.dr.ir. M.K. de Kreuk	Delft University of Technology
Prof. N.J.D Graham	Imperial College London
Dr. C.J. Paul	Lund University
Dr.ir. K. Lekkerkerker-Teunissen	Dunea

Reserve member:

Prof.dr.ir. L.C. Rietveld	Delft University of Technology

This work is part of the NWO-Dunea-Vitens Sand Filtration programme (grant #17831), funded by the Dutch Research Council NWO.

Keywords: Biological filtration, Disinfection, Biological stability, Schmutzdecke, Drinking water
Printed by: Fully Buffered Studios
Cover design by: Sarayu Neelakantan

Table of contents

Acknowledgements

Starting my PhD during the pandemic was nothing short of an epic adventure. This journey has been full of invaluable lessons, and I am grateful for the incredible people who supported me along the way.

First and foremost, I extend my heartfelt thanks to my two promotors, Prof. Jan Peter van der Hoek and Prof. Doris van Halem for giving me the opportunity to pursue this PhD. Jan Peter, you encouraged and supported me to explore my research independently, yet you were always there to steer me back on track when needed. Doris, I appreciate that you always challenged me to push the boundaries of my research. I am glad to know you as a compassionate person, always attentive to my well-being. I feel privileged to have collaborated so closely and I have gained much more than academic knowledge from both of you.

I am also immensely grateful to the people involved in the Sand Filtration programme. Thank you, Valentina, for welcoming me into the world of microbiology. I enjoyed the countless committee meetings and our hands-on work at the pilot-scale installation. Special thanks to Dr. Paul van der Wielen and Prof. Smidt Hauke for sharing their microbiology expertise in this research. To my colleagues Xi, Mandana, Bayan, and Salima from the programme, thank you for making this research even more enjoyable. I cherish our inspiring discussions and the fun times we shared.

Field research in the Netherlands would not have been possible without the cooperation and support from Dunea. I owe a special thanks to Brent and Clemy for their assistance with sampling and operating the pilot-scale filters, and for always being there to answer my questions about slow sand filters. To the WaterLab staff, especially Armand and Jasper, your help and unfading enthusiasm since the very beginning have been invaluable.

Over the past four years, I had the privilege of supervising students who collaborated with me on their MSc and additional theses. Many thanks to Yuwei, Srilekha, Feiyang and Thanisha for their contribution to the multitude of data and ideas presented in this thesis. I would like to thank my colleagues at TU Delft: Mrinal, Dhavissen, Apoorva, Bruno, Mona, Antonella, Erik, Emiel, Simon, Roos, Francesc, Javier, Steef , Carina and Sara with whom I shared offices, lunch breaks at the pond and fun times at PSOR.

I am grateful to my amazing bunch of friends who fill my life with joy and much-needed distractions. Every food and travel adventure with you all helped me stay balanced throughout this journey.

I am blessed to have a supportive family, who constantly encourages and reminds me of my ‘why’ during moments of doubt. Mama and Papa, thank you for believing in my dreams, no matter how distant

or difficult. I owe this success to you.

Most importantly, I want to thank my biggest cheerleader, Sachin for walking this journey with me. You pushed me to aim higher than the sky and made sure we celebrated every win, big or small. I am grateful for every moment of comfort and motivation you provided. This achievement is not just mine, but ours. Thank you for being my rock.

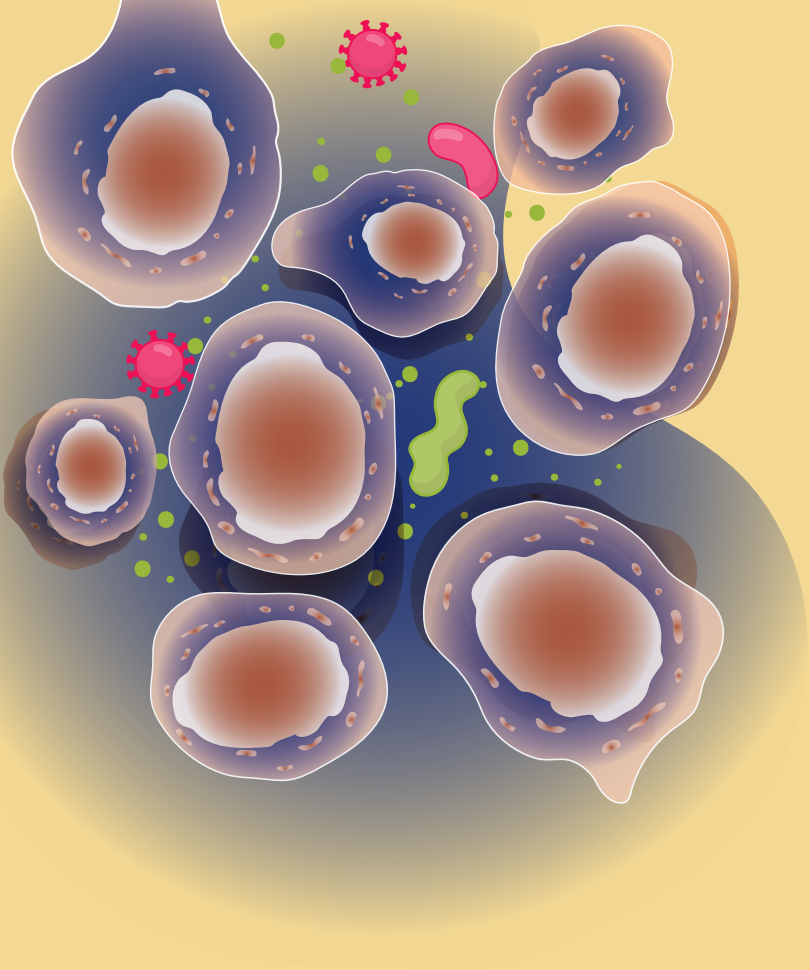

Chapter 1

Introduction

1.1 Drinking water treatment

The quest for safe drinking water has been crucial in human civilization, shaping early urban settlements since 500 BCE (Abkar et al., 2024). Ancient techniques for water purification included the use of clay-fired vessels, filter cloths, carved antlers, and botanicals, illustrating early efforts to make drinking water safe (Smith, 2017). Historical records indicate that natural filtration methods were used millennia ago, with Egyptians digging wells near the Nile to find drinkable water when the river itself was unsuitable for consumption (Hammes et al., 2011).

To date, access to safe drinking water remains a global challenge, particularly in regions burdened by water-borne diseases and lacking treatment infrastructure (Dickin & Gabrielsson, 2023). Droughts induced by climate change and pollution have adversely affected surface and groundwater supplies, subsequently reducing accessibility to drinking water. Contamination with pathogenic microorganisms and chemical compounds can pose acute and chronic health risks and deteriorate the aesthetic properties of water systems (Gil and Galeano, 2019). Thus, drinking water treatment plants play a critical role in supplying safe drinking water to consumers. In industrialized countries and some emerging economies, conventional centralized water treatment systems distribute drinking water to households through carefully monitored pipelines (Prest et al., 2016). However, in resource-limited settings, the feasibility of centralized systems is limited by the costs of treatment and distribution, and the low density of houses (Huang et al., 2021). Instead, on-site water treatment and safe storage, such as point-of-use (POU) technologies, offer a practical solution by treating water at the source before it is consumed (Freitas et al., 2022; Soliman, 2022).

Many drinking water treatment plants around the world use physical-chemical treatment methods, including coagulation-flocculation, sedimentation, (membrane) filtration, chlorination and ultra-violet (UV) disinfection to effectively remove physical, chemical and microbiological contaminants. These methods are often challenged due to their high chemical and energy requirements, high costs, and generation of by-products that require additional treatment (Ray and Jain, 2011). With rising interest in sustainable water treatment and stricter emission and discharge restrictions, there has been a global shift towards biological treatment methods for drinking water.

Biological filtration is among the earliest methods of community-based drinking water purification (Maiyo et al., 2023). This technique involves using a porous filtering medium (e.g., sand, granulated active carbon (GAC), or a synthetic carrier material), where indigenous microorganisms colonize and perform at least one of the essential treatment functions of the process (Maurya et al., 2020). Essentially, drinking water biofilters act as physical strainers in combination with biological processes, offering multiple facets. For instance, biofilms entrap organic matter and microorganisms, enhancing the filter's physical

straining capability. Alternatively, microorganisms can biologically degrade chemical compounds and pathogens, thereby performing a uniquely biological function. Within the context of biofiltration, bacterial presence is not only opportunistic or negative but forms the basis of treatment to produce high-quality drinking water (Hammes et al., 2011). These filters often serve as an alternative or as one of the disinfection processes and have several potential advantages:

- low operating costs
- elimination, rather than sequestration or concentration of contaminants
- simultaneous removal of multiple contaminants
- minimal or no added chemicals
- minimal waste production
- no hazardous waste streams

Contrary to the belief that industrialized countries rely solely on high-tech and energy-intensive water technologies which are unsuitable for rural areas, both Europe (van der Hoek et al., 2013) and North America (Kirisits et al., 2019) commonly use simple and cost-effective (semi) natural and engineered biofiltration systems for drinking water production. These systems vary from centralized, multi-step treatments in industrialized countries to decentralized, point-of-use treatment in remote areas (Figure 1). In the last several decades, variants of biological filters such as rapid sand filters, granular activated carbon filters, river bank filtration and slow sand filters have become popular for removing pathogenic microorganisms and various organic and inorganic pollutants from drinking water (Hammes et al., 2011).

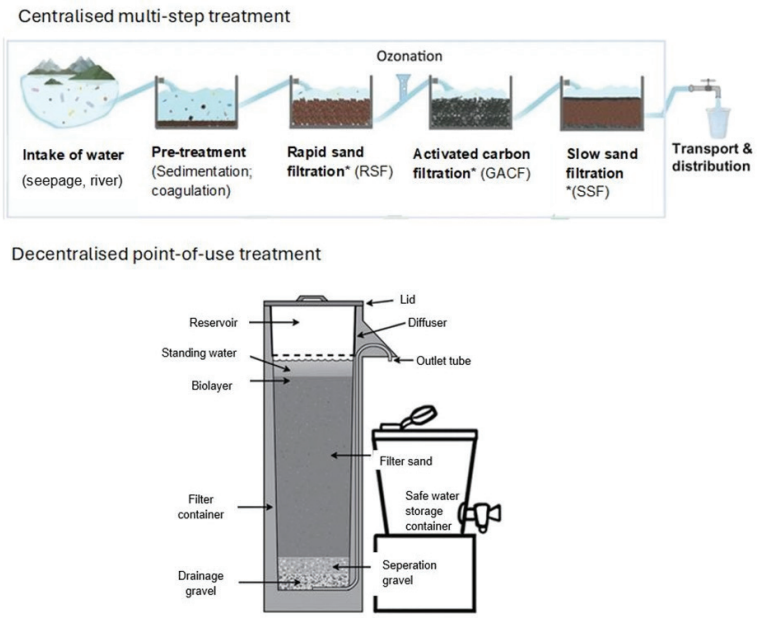

Figure 1 A variety of biofiltration processes (*) are used worldwide for the treatment of drinking water in centralized multi-step treatment systems and as decentralized point-of-use treatment in rural areas. Bai et al., (2023); CAWST. (2012)

1.2 Slow sand filters

Slow sand filters (SSFs) are the oldest community-scale water treatment technology, with possible use occurring as far back as the Roman Empire (Maiyo et al., 2023). The first use of industrial SSF was demonstrated by John Gibb in 1804 in Paisley (Scotland) and then by James Simpson in 1829 (England) (Haig et al., 2011). At that time, SSFs were installed as a strainer for turbidity removal and later for containment of cholera, well before any knowledge of bacteria in drinking water existed (Huisman & Wood, 1974). After John Snow linked cholera and typhoid to water contamination, the use of SSFs was mandated by law for all water sourced from the River Thames in London after 1892 (Maiyo et al., 2023).

This technology operates on the principle of percolation of water through a fine sand bed at low velocities of 0.1-0.3 m/h without backwashing (Abu Hasan et al., 2020). This fosters the growth of indigenous microbial communities, with a thick biofilm layer or *Schmutzdecke* on the filter surface, and thinner biofilms throughout the rest of the filter bed. The development of the *Schmutzdecke* eventually leads to filter clogging and decreased water flow, resulting in mechanical scraping of the top few filter layers (Chan et al., 2018). After scraping, a ripening time is required for the development of a new *Schmutzdecke* in the filter. The primary function of a SSF is to remove turbidity, enteric pathogens and biodegradable organic matter (BOM), with additional functions such as the removal of ammonium (NH_4^+) and organic micropollutants (Gimbel et al., 2017).

SSFs are applied under a variety of conditions and scales from large scale at a drinking water treatment plant to household level. Countries like the Netherlands, Belgium, Egypt, United Kingdom, France, India, Switzerland and Sweden have been using SSFs since the 1900s (Maiyo et al., 2023). In the early 1990s, David Manz adapted the traditional SSF for household level, leading to the development of Household Slow Sand Filter (HSSF) (Freitas et al., 2022). HSSFs are used to remove microbial contaminants such as helminths, protozoa, bacteria and viruses, to reduce diarrhea and cholera cases (Andreoli & Sabogal-Paz, 2020). This innovation has been distributed globally by various organizations, with over 300,000 HSSFs installed across more than 69 countries (CAWST, 2012). Currently, over half a million people in developing countries use SSFs to treat their drinking water (Maiyo et al., 2023). These filters have historically been one of the most important methods to treat water for drinking and eradicate Water, Sanitation, and Hygiene (WASH) challenges. The U.S. Environmental Protection Agency (USEPA) and the World Health Organization (WHO) have also recognized SSFs as an inexpensive and reliable way to provide safe drinking water (Abdiyev et al., 2023).

1.2.1 Pathogens removal

Slow sand filtration is a robust approach to eliminate a wide range of pathogens, achieving a removal of 2−6 $\log_{10}$ oocysts, 2−4 $\log_{10}$ of bacteria, and < 1−3 $\log_{10}$ of viruses (Hijnen et al. 2004; Matuzahroh et al. 2020). Removal occurs through interdependent physical-chemical and biological processes. Physical-chemical pathways include straining, sedimentation, interception, diffusion, adsorption, and flocculation (Haig, 2014). Straining captures particles larger than the filter pores (e.g., bacteria and protozoa). As the biofilm matures and pores narrow, straining becomes more effective. Brownian motion affects particles smaller than 1 µm (e.g., viruses), leading to diffusion and potential attachment to the sand. The attached or deposited particles can detach and penetrate deeper into the filter due to changes in flow or other disturbances, resulting in breakthrough.

Biological processes include predation, inactivation, bio-antagonism, and metabolic decay (Bomo et al., 2004; Haig et al., 2011). Predation, where larger microorganisms, such as protozoa, feed on smaller microorganisms and particles, such as bacteria and viruses, is proposed to play a critical role. Inactivation is caused by microbial exoproducts, such as proteolytic enzymes, and grazing on viruses. Bacterial antagonism involves non-pathogenic organisms outcompeting pathogens for nutrients, resulting in pathogen reduction. Adsorption, although regarded as a physical-chemical process, is enhanced by biological activity, i.e., biofilms on sand. Protozoan grazing of attached bacteria helps in maintaining the sand surface area available for further adsorption.

Several factors such as temperature, source water quality, filter media size and characteristics, media amendment, filter maturity, filter depth, hydraulic retention time (HRT), filtration velocity and mode of operation influence the removal of contaminants in SSFs (Abdiyev et al., 2023; Bai et al., 2023). Specifically, finer grain size, longer bed height, lower HRT and mature media are considered key to efficient removal.

1.2.2 Removal of biological stability parameters

Biologically stable drinking water is obtained by removing bacterial growth-promoting compounds such as biodegradable fractions of dissolved organic carbon (DOC), ammonium (NH_4^+) and phosphate (PO_4^{3-}). This is essential to maintain stable microbial water quality from the point of drinking water production up to the point of consumption, especially in non- chlorinated drinking water systems (Prest et al., 2016).

SSFs have lately gained popularity for their ability to remove biological stability parameters. These filters utilize a combination of physical-chemical (adsorption) and biological (bacterial respiration and

biomass assimilation) processes (Basu et al., 2016). Chemoheterotrophic organisms from diverse phyla remove the biodegradable DOC (e.g., sugars, amino and organic acids) through assimilation, while complex carbon fractions (e.g., polymers, humic substances) are converted to degradable fractions by extracellular enzymes before cellular uptake and metabolism (Sinsabaugh et al., 2003; Nybroe et al., 1992). A diverse range of enzymes capable of degrading complex organic carbon has been found in SSFs indicating the adaptability of filters to different kinds of substrates (Lautenschlager et al., 2014).

NH_4^+ is a common contaminant in groundwater and surface water that is removed biologically in SSFs (Tatari et al., 2014). NH_4^+ is removed by assimilation and by nitrifying bacteria that oxidize NH_4^+ to NO_2^- and subsequently NO_3^- or directly from NH_4^+ to NO_3^-. NH_4^+ oxidizers and NO_2^- oxidizers along with complete NH_4^+ oxidizers known as comammox have been identified in SSFs, thriving at low NH_4^+ concentrations (Bai et al., 2022; Chen et al., 2021).

1.3 This thesis

Although SSFs appear to be simple systems, they are complex environments with several physical, chemical and biological processes occurring simultaneously. Historical SSFs are operated as “black boxes”, with limited understanding of the physical-chemical and biological processes and intricate mechanisms involved in the removal of enteric pathogens and biological stability parameters. These processes occur simultaneously and/or sequentially in the filter, and their intensity varies for different contaminants. For instance, pathogens are removed through straining, attachment to biofilms or sand grains, and microbial inactivation depending on the biological characteristics of sand in the filter, whereas DOC and NH_4^+ are eliminated via biological degradation and/or adsorption and biological oxidation, respectively. Despite recognizing these processes, the exact nature of their interactions and their contribution to removal remains largely unexplored.

Most of the SSF research until now has predominantly focused on the *Schmutzdecke*, while the complex biofilms in the remaining sand bed have been largely neglected. The fact that the *Schmutzdecke* covers only the top few centimeters implies that a considerable proportion of biomass exists on sand in the deeper layers of the filter. In literature, comprehensive studies investigating full-scale SSFs along the filter depth are scarce, likely due to the invasive nature of depth sampling which disrupts the filtration process. Consequently, our understanding of biomass distribution, microbial composition, and the mechanisms of contaminant removal in the deeper layers is limited. The importance of the *Schmutzdecke* emphasized in previous studies that have been conducted in lab or pilot-scale settings might not have fully captured the complex microbial dynamics and process interactions occurring in mature full-scale environments. This thesis challenges the traditional focus on the *Schmutzdecke* and aims to understand the function of the entire filter system in removing enteric pathogens, DOC and NH_4^+.

A development in SSFs is their adoption as the final polishing step to enhance the biological stability of drinking water in a multi-barrier treatment scheme. Thus, SSFs are operated under low loading conditions, which has benefited the filter run time but has prolonged the ripening phase to several weeks or months. The current design and operational parameters, and management strategies based on the historical application of SSFs are scrutinized for their extensive land and water footprint. A thorough understanding of how operational conditions impact the removal kinetics of DOC and NH_4^+ under low loading conditions can reveal process limitations, leading to the development of more efficient and robust design rules for modern SSFs.
The problem description of this thesis has been formulated as follows:

To develop new design rules for low-loaded polishing SSFs, there is a need for a better understanding of the function of the entire filter system, beyond just the Schmutzdecke, in removing enteric pathogens, DOC and NH_4^+.

This problem has been addressed by four main research questions in this thesis.

1.4 Research questions

- How are pathogen transport and removal influenced by different depths of full-scale SSFs? (Chapter 2)
  - What is the contribution of physical-chemical and biological processes to bacteria and viruses removal?

- How do the deeper layers respond to *Schmutzdecke* scraping in full-scale SSFs? (Chapter 3)
  - How does *Schmutzdecke* removal impact microbial biomass and removal processes of DOC and NH_4^+?
  - What effect does scraping have on the microbial community composition in the filter?

- What causes the release of DOC in the deeper layers of SSFs? (Chapter 4)
  - Is the release of DOC influenced by the maturity of the biofilm?
  - What is the composition of released DOC and does it affect effluent quality?

- How do removal kinetics of DOC and NH4+ influence the redesign of SSFs? (Chapter 5)
  - Does a larger grain size result in process limitations for DOC and NH_4^+ removal?
  - Can SSFs be operated at higher loading rates without compromising removal efficiency and effluent quality?
  - How does backwashing affect the recovery of DOC and NH_4^+ removal rates?

1.5 Thesis outline

Chapter 2 sheds light on the pathogen removal capacity and contributing processes at different depths of SSFs, using filter material from a 28-year-old mature full-scale SSF in an innovative experimental setup.

Chapter 3 delves into the recovery of microbial biomass and removal processes of DOC and NH_4^+ after scraping of the *Schmutzdecke* in a full-scale SSF. For this, depth profiles of various chemical and microbial parameters are assessed in operating SSFs over four months after scraping.

In Chapter 4, the first report of the release of DOC in deeper filter layers is presented, examining the potential underlying mechanisms behind this phenomenon in both mature full-scale SSFs and young experimental filters.

Chapter 5 explores the kinetics of DOC and NH_4^+ removal under different operational conditions to identify process limitations and inform redesigning of SSFs.

Chapter 6 provides the concluding remarks of this thesis, with a comprehensive outlook beyond the scope of the individual chapters, along with recommendations for future research.

References

Abdiyev, K., Azat, S., Kuldeyev, E., Ybyraiymkul, D., Kabdrakhmanova, S., Berndtsson, R., ... & Sultakhan, S. (2023). Review of slow sand filtration for raw water treatment with potential application in less-developed countries.
Water, 15(11), 2007.

Abkar, L., Moghaddam, H. S., & Fowler, S. J. (2024). Microbial ecology of drinking water from source to tap.
Science of The Total Environment, 908, 168077.

Agrawal, A., Sharma, N., & Sharma, P. (2021). Designing an economical slow sand filter for households to improve water quality parameters. Materials Today: Proceedings, 43, 1582-1586.

Andreoli, F. C., & Sabogal-Paz, L. P. (2020). Household slow sand filter to treat groundwater with microbiological risks in rural communities. Water Research, 186, 116352.

Bai, X., Dinkla, I. J., & Muyzer, G. (2022). Microbial ecology of biofiltration used for producing safe drinking water. Applied Microbiology and Biotechnology, 106(13), 4813-4829.

Basu, O. D., Dhawan, S., & Black, K. (2016). Applications of biofiltration in drinking water treatment– a review. Journal of Chemical Technology & Biotechnology, 91(3), 585-595.

Bomo, A. M., Stevik, T. K., Hovi, I., & Hanssen, J. F. (2004). Bacterial removal and protozoan grazing in biological sand filters. Journal of environmental quality, 33(3), 1041-1047.

Centre for Affordable Water and Sanitation Technology (CAWST), 2012. Biosand Filter Construction Manual.

Chan, S., Pullerits, K., Riechelmann, J., Persson, K. M., Rådström, P., & Paul, C. J. (2018). Monitoring biofilm function in new and matured full-scale slow sand filters using flow cytometric histogram image comparison (CHIC).
Water research, 138, 27-36.

Chen, L., Zhai, Y., van der Mark, E., Liu, G., van der Meer, W., & Medema, G. (2021). Microbial community assembly and metabolic function in top layers of slow sand filters for drinking water production. Journal of cleaner production, 294, 126342.

Dickin, S., & Gabrielsson, S. (2023). Inequalities in water, sanitation and hygiene: Challenges and opportunities for measurement and monitoring. Water Security, 20, 100143.

Fitriani, N., Ardiyanti, P. E., Kuncoro, E. P., Budiyanto, W. D., Isnadina, D. R. M., Wahyudianto, F. E., & Mohamed, R. M. S. R. (2020). Behavior of schmutzdecke with varied filtration rates of slow sand filter to remove total coliforms.
Heliyon, 6(4).

Freitas, B. L. S., Terin, U. C., Fava, N. D. M. N., Maciel, P. M. F., Garcia, L. A. T., Medeiros, R. C., ... & Sabogal-Paz, L. P. (2022). A critical overview of household slow sand filters for water treatment. Water Research, 208, 117870.

Gil, A., Galeano, L. A., & Vicente, M. Á. (Eds.). (2019). Applications of advanced oxidation processes (AOPs) in drinking water treatment (Vol. 67). Cham: Springer International Publishing.

Gimbel, R., Graham, N., & Collins, M. R. (Eds.). (2006). Recent progress in slow sand and alternative biofiltration processes.

Haig, S. J., Collins, G., Davies, R. L., Dorea, C. C., & Quince, C. (2011). Biological aspects of slow sand filtration: past, present and future. Water Science and Technology: Water Supply, 11(4), 468- 472.

Haig, S. J. (2014). Characterising the functional ecology of slow sand filters through environmental genomics (Doctoral dissertation, University of Glasgow).

Hammes, F., Velten, S., Egli, T., & Juhna, T. (2011). 6.41 Biotreatment of Drinking Water. Reference Module in Earth Systems and Environmental Sciences-Comprehensive Biotechnology, 517-530.

Hasan, H. A., & Muhammad, M. H. (2020). A review of biological drinking water treatment technologies for contaminants removal from polluted water resources. Journal of Water Process Engineering, 33, 101035.

Hijnen, W. A., Schijven, J. F., Bonne, P., Visser, A., & Medema, G. J. (2004). Elimination of viruses, bacteria and protozoan oocysts by slow sand filtration. Water Science and Technology, 50(1), 147- 154.

Huang, Z., Nya, E. L., Cao, V., Gwenzi, W., Rahman, M. A., & Noubactep, C. (2021). Universal access to safe drinking water: Escaping the traps of non-frugal technologies. Sustainability, 13(17), 9645.

Huisman, L., & Wood, W. E. (1974). Slow sand filtration. World Health Organization.

Kirisits, M. J., Emelko, M. B., & Pinto, A. J. (2019). Applying biotechnology for drinking water biofiltration: advancing science and practice. Current opinion in biotechnology, 57, 197-204.

Lautenschlager, K., Hwang, C., Ling, F., Liu, W. T., Boon, N., Köster, O., ... & Hammes, F. (2014). Abundance and composition of indigenous bacterial communities in a multi-step biofiltration- based drinking water treatment plant. Water research, 62, 40-52.

Maiyo, J. K., Dasika, S., & Jafvert, C. T. (2023). Slow sand filters for the 21st century: a review. International Journal of Environmental Research and Public Health, 20(2), 1019.

Maurya, A., Singh, M. K., & Kumar, S. (2020). Biofiltration technique for removal of waterborne pathogens.
In Waterborne pathogens (pp. 123-141). Butterworth-Heinemann.

Nybroe, O., Jørgensen, P. E., & Henze, M. (1992). Enzyme activities in waste water and activated sludge. Water research, 26(5), 579-584.

Prest, E. I., Hammes, F., Van Loosdrecht, M. C., & Vrouwenvelder, J. S. (2016). Biological stability of drinking water: controlling factors, methods, and challenges. Frontiers in microbiology, 7, 45.

Ray, C., & Jain, R. (Eds.). (2011). Drinking water treatment: focusing on appropriate technology and sustainability. Springer Science & Business Media.

Sinsabaugh, R. L., Saiya-Cork, K., Long, T., Osgood, M. P., Neher, D. A., Zak, D. R., & Norby, R. J. (2003). Soil microbial activity in a Liquidambar plantation unresponsive to CO2-driven increases in primary production.Applied Soil Ecology, 24(3), 263-271.

Slezak, L. A., & Sims, R. C. (1984). The application and effectiveness of slow sand filtration in the United States. Journal-American Water Works Association, 76(12), 38-43.

Smith, L. (2017). Historical perspectives on water purification. In Chemistry and water (pp. 421-468). Elsevier.

Wijnja, J., & Nijkamp, J. E. (2022, June). The value of FM for a healthy urban environment: application of

the FM Value Map to Urban FM. In Research Papers for The 21st EuroFM Research Symposium (pp. 47-54). EuroFM: European Facility Management Network.

Tatari, K. (2014). Nitrification biokinetics in rapid sand filters for drinking water treatment. DTU Environment.

van der Hoek, J. P., Bertelkamp, C., Verliefde, A. R. D., & Singhal, N. (2014). Drinking water treatment technologies in Europe: state of the art–challenges–research needs. Journal of Water Supply: Research and Technology—AQUA, 63(2), 124-130.

Verma, S., Daverey, A., & Sharma, A. (2017). Slow sand filtration for water and wastewater treatment– a review. Environmental Technology Reviews, 6(1), 47-58.

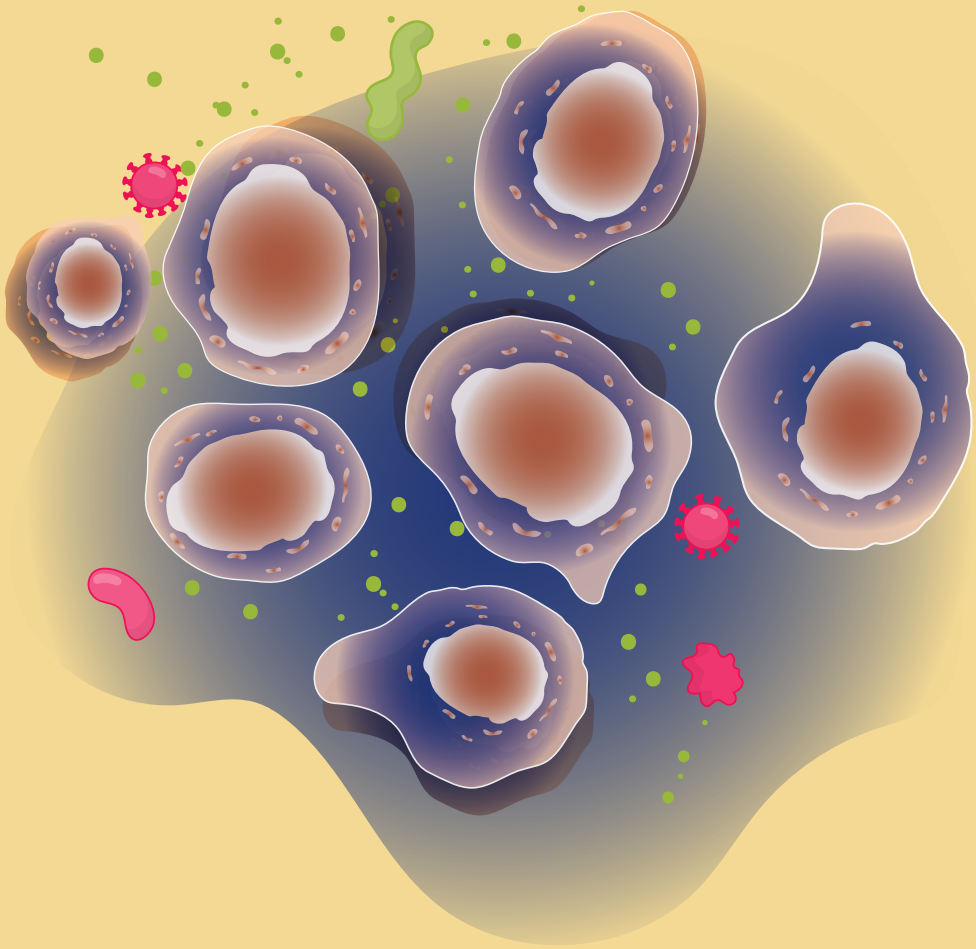

Chapter 2

Contribution of deeper layers in slow sand filters to pathogens removal

This chapter is based on:
Trikannad, S. A., van Halem, D., Foppen, J. W., & van der Hoek, J. P. (2023). The contribution of deeper layers in slow sand filters to pathogens removal. Water Research, 237, 119994.

Abstract

Slow Sand Filtration is popular in drinking water treatment for the removal of a wide range of contaminants (e.g., particles, organic matter, and microorganisms). The *Schmutzdecke* in slow sand filters (SSFs) is known to be essential for pathogen removal, however, this layer is also responsible for increased head loss. Since the role of deeper layers to bacteria and virus removal is poorly understood, this research investigated the removal of *E.coli* WR1 and PhiX 174 at different depths of a full-scale SSF. Filter material from top (0-5 cm), middle (5-20 cm) and deep (20-35 cm) layers of an established filter was used in an innovative experimental set-up to differentiate physical-chemical and biological removal processes. In the analysis, we distinguished between removal by biological activity, biofilm and just sand. In addition, we modelled processes by a one-side kinetic model. The different layers contributed substantially to overall log removal of *E.coli* WR1 (1.4-1.7 $\log_{10}$) and PhiX 174 (0.4-0.6 $\log_{10}$). For *E.coli* WR1, biological activity caused major removal, followed by removal within biofilm and sand, whereas, removal of PhiX 174 mainly occurred within sand followed by biofilm and biological activity. Narrow pore radii in the top layer obtained by micro-computed tomography scanner suggested enhanced retention of bacteria due to constrained transport. The retention rates of *E.coli* WR1 and PhiX 174 in top layer were four and five times higher than deeper layers, respectively (k_{ret} 1.09 min^{-1} vs 0.26 min^{-1} for *E.coli* WR1 and k_{ret} 0.32 min^{-1} vs of 0.06 min^{-1} for PhiX 174). While this higher rate was restricted to the *Schmutzdecke* alone (top 5 cm), the deeper layers extend to around 1 m in full-scale filters. Therefore, the contribution of deeper layers of established SSFs to the overall removal of bacteria and viruses is much more substantial than the *Schmutzdecke*.

2.1 Introduction

Slow sand filtration, one of the earliest water treatment processes, has been a major contributor to drinking water safety (Chan et al., 2018; Chen et al., 2021; Haig et al., 2011). In the past decades, slow sand filters (SSFs) have demonstrated the capacity to effectively remove turbidity, dissolved organic matter and a wide range of enteric pathogens (bacteria, viruses and protozoa). However, in recent times, the focus has also been on the removal of biodegradable organic matter to increase biological stability of drinking water (van der Kooij et al., 2017).

In low-resource settings, intermittently operated SSF, popularly known as the "biosand filter" (BSF) has been a promising household-scale point-of-use (POU) technology for the removal of pathogens from drinking water.
The BSF has been highly successful when measured by user-satisfaction, durability and simplicity of design and operation (Elliott et al., 2011; Napotnik et al., 2020). While SSFs differ from BSF in design and operation, they offer a major benefit of chemical-free turbidity and pathogen removal, compared to any direct competing technologies like membrane filtration, coagulation, ozonation and few more (de Oliveira & Schneider, 2019). Drinking water treatment plants in the Netherlands, the United Kingdom, Sweden, Brazil and many more use SSFs as a third or final treatment step in drinking water production due to their low energy consumption and high efficiency. When drinking water is distributed without residual disinfectants such as chlorine (Sousi et al., 2020) utilities opt for a multi-stage treatment scheme where SSFs are the final treatment step to produce microbiologically safe and biologically stable drinking water (van der Kooij et al., 2017).

While SSFs are known to be safe and robust, there is also consensus that there are a few drawbacks and limitations in operation. The filters have a large land footprint as they are designed to operate at low filtration rates. The *Schmutzdecke*, a dense biofilm in the top layer of SSFs is considered a key barrier for pathogens and other contaminants but overgrowth of biomass in this layer increases head loss in the filter (Andreoli & Sabogal-Paz, 2020; Dizer et al., 2004; Hijnen et al., 2007; Schijven et al., 2013). As a result, cleaning techniques like scraping and wet harrowing are applied which in turn demand a long ripening period of 6-8 weeks to re-establish the *Schmutzdecke* and restore filter performance (Huisman & Wood, 1974; Jenkins et al., 2011).

The importance of *Schmutzdecke* in SSFs is promoted by high microbial abundance, diversity, and a broad range of functions compared to deeper layers of the sand bed (Chen et al., 2021). Stratification of biomass with depth is not surprising as substrate concentration and biomass acting on substrates are highest at the surface of the sand bed. Thus, purification capacity and associated processes may be stratified over the filter height (Chen et al., 2021; Lee et al., 2014; Tatari et al., 2016). Recent investigation

on mature full-scale SSFs showed that removal of the *Schmutzdecke* did not impact coliform counts and flow cytometry bacterial profiles in terms of intact cells and high nucleic acid content (HNA) in effluent water (Chan et al., 2018). They reported that deeper layers in mature filters operating for several years may have extensive biofilms with microbial community required for producing consistent microbial water quality. Generally, during scraping, the *Schmutzdecke* and the top few centimetres (2-5 cm) of sand are removed but deeper layers are retained unaltered. Pfannes et al., (2015) observed 16S rRNA gene copy numbers of around 10^6 copies/mL in the deep sand bed. Although the count is less than 10^{11} copies/mL commonly found in the *Schmutzdecke*, the total volume occupied by the sand bed is much greater than the volume in the *Schmutzdecke*. Oh et al., (2018) observed that microorganisms in the deeper layers grew faster by metabolizing more easily degradable organic matter compared to the microorganisms in the *Schmutzdecke*.

Biofilms in both *Schmutzdecke* and sand bed can entrap cells and support microbial interactions, thus, SSF performance may be a balance between processes in different layers of sand bed (Chan et al., 2018; Pfannes et al., 2015). For example, bacteria and protozoa removal occurred mainly in the *Schmutzdecke* but virus removal improved with filter depth. While the influence of *Schmutzdecke* on pathogens removal and associated mechanisms have been studied extensively (Hijnen et al., 2004; Schijven et al., 2013; Unger and Collins, 2008), the contribution of deeper depths in removal has not received much attention in the past. Previous studies evaluating filter performance have been largely performed on filters at lab or pilot scale where a sand bed microbial community has not had years to establish (Hijnen et al., 2004; Pfannes et al., 2015; Unger and Collins, 2008). In filters without an established microbial community in the deeper layers, changes in treated water quality could be more coupled to the status of the *Schmutzdecke* (Chan et al., 2018). Therefore, understanding of removal processes in both *Schmutzdecke* and deep sand bed in established full-scale filters is crucial to enable improvements in design and operational procedures of SSFs, in terms of new filter designs (bed height) and cleaning procedures for biomass preservation within the filter.

In this study, bacteria and virus removal capacity of *Schmutzdecke* and deeper layers of an established SSF were explored to distinct co-occurring removal processes (including, straining, attachment and microbial inactivation). The top and deeper depths of the filter may be evaluated as separate systems due to vast differences in the physical and biological characteristics of sand that influence microbial transport. Hence, knowledge of stratification of biotic and abiotic-induced processes that aid microbial removal is important for further optimization and promotion of the SSF technology. In this study, it was hypothesized that deeper layers contribute substantially to *E.coli* WR1 and PhiX 174 bacteriophage removal due to a mature biofilm in the sand bed. Therefore in an innovative experimental set-up, the removal capacity and transport of indicator enteric pathogens *E.coli* WR1 and PhiX 174 were investigated at different depths of a full-scale filter. To investigate the contribution of physical, chemical

and biological processes in removal, sand from different depths was investigated directly, after inactivation of microbial activity by sodium azide and after incineration to remove the biofilm. The retention and reentrainment behaviour of *E.coli* WR1 and PhiX 174 at different depths were modelled using a one-site kinetic model. A micro-computed tomography scanner (Micro-CT) and environmental scanning electron microscopy (ESEM) were employed to investigate the influence of porosity and sand characteristics on microbial transport at different depths.

2.2 Materials and Methods

2.2.1 Sampling at full-scale slow sand filter

An established SSF producing drinking water for over 67 years (built in 1955) at a drinking water treatment plant of Dunea (located at Katwijk), a drinking water utility in the Netherlands was used in this study. The plant receives raw water from the river Meuse and is further treated by managed aquifer recharge in the dunes, pellet softening, aeration, rapid sand filtration with powdered activated carbon dosing and lastly slow sand filtration. The SSF in our study has been in operation for approx. 28 years without sand replacement. At the moment of sand sampling, the filter had a sand bed height of 0.9 m with grain size of 0.4-0.6 mm, followed by 0.3 m of gravel layer (4-6 mm) and 0.12 m of underdrains for uniform passage of filtered water. The hydraulic loading was 0.4 m/h. The in-situ water temperature at the treatment plant was mostly stable, between 10-12 °C, as seasonal fluctuation was regulated during dune filtration. Over a period of operation, generally a few years, the filters become clogged with biomass. To restore the water flow, the top layers (2-5 cm) of the SSF including *Schmutzdecke* are removed by mechanical scraping. The filter in this study was last scraped 653 days ago.

During one such scraping event, intact sand samples from mature SSF was sampled up to a depth of 40 cm. Sand was core-sampled from depths 0-5 cm (top), 5-20 cm (middle) and 20-35 cm (deep) by inserting and gently removing a sterile plexiglass cylinder. The cylinder had an inner diameter of 2.5 cm and height of 5 cm for top layer and 15 cm for middle and deep layers, and closed at the top with a rubber stopper. Sampling with the cylindrical cores provided the advantage to take undisturbed in-situ sand samples without impacting the 3D structure and was further transformed into columns for the experiments. Two sand cores from each depth were sampled at two randomly selected locations to be used for duplicate column experiments.

2.2.2 Experimental set-up

The experimental set-up consisted of small plexiglass columns with inner diameter of 2.5 cm and bed height of 5 cm for sand from top layer (0-5 cm) and 15 cm for sand from middle (5-20 cm) and deep layer (20-35 cm). The core-sampled sand from each depth was operated in columns under three conditions to

simulate scenarios of physical, chemical and biological processes in treatment: active biofilm, inactive biofilm and no biofilm. The sand was prepared as per the following:

i) **Active biofilm sand:** Sand directly obtained from the full-scale SSF (as described in section 2.1). The three depths in consideration had different active biomass measured by cellular ATP, with the highest active biomass in the top layer (*Schmutzdecke*-180 ng/g sand) and the lowest in the deep
ii) layer (15 ng/g sand) (Fig S1).
Inactive biofilm sand: Microbial activity on sand from three depths and in the water phase was suppressed by continuously dosing sodium azide at a concentration of 6-mM (390 mg/L) (Elliott et al., 2011). Dosing was continued for three days until no biological activity was detected. The activity was determined by measuring cellular ATP on 1 g of sand using the Deposit & Surface
iii) Analysis kit (DSA) (LuminUltra Technologies Ltd.) according to the manufacturer's protocol.
No biofilm sand: Biofilm on sand from three depths was destroyed by drying sand at 105°C and then ignited at 440°C in a muffle furnace as per British Standard (British Standards Institution, 1990b; Rodgers et al., 2004). The biofilm was burnt off at this temperature, leaving behind a mixture of sand and ash. The sand mixture from 3 depths was washed through a 53 µm sieve and filled into their respective columns.

The influent feeding the full-scale SSFs at the water treatment plant was used as influent for the columns at a filtration rate of 0.4 $m^3/m^2/h$ to replicate full-scale SSF condition. The pore volume and porosity in the columns were determined using deuterium (^2H) as a tracer according to Bertelkamp et al., (2016). Further, the columns were challenged with enteric bacteria and virus indicators *E.coli* WR1 and PhiX 174 bacteriophages respectively.

2.2.3 *E.coli* WR1 and PhiX 174 preparation and enumeration

The experiments were carried out with *E.coli* WR1 (NCTC 13167) and bacteriophage PhiX 174 (ATCC 13706-B1). *E. coli* WR1 is widely used as an indicator of enteric bacteria in drinking water studies (Eisfeld et al., 2022; Schijven et al., 2013) and is used here as a reference for bacterial removal. A highly concentrated suspension of *E. coli* WR1 was prepared by growing in buffered peptone water for 18 h at 37°C, harvested by centrifugation at 3000 g for 5 min and washing in sterile water as per ISO 9308-1. *E.coli* WR1 was enumerated by membrane filtration and incubation onto Chromocult agar for 24 h at 37°C. PhiX 174 is an icosahedral, single-stranded DNA-phage with a diameter of 26 nm and an isoelectric point of 4.4 (Chrysikopoulos & Aravantinou, 2012; Soliman et al., 2020). PhiX 174 is generally seen as a good viral surrogate due to its size and shape resemblance to several human enteroviruses such as poliovirus, norovirus, etc as well as its low hydrophobicity and stability (Bicudo et al., 2021; Oudega et al., 2021). Although PhiX174 may not be an ideal conservative colloidal tracer, somatic coliphages have

gained special importance in Europe in recent years as a reliable viral fecal indicator due to their high prevalence in sewage and persistence in the environment (Oudega et al., 2021). A highly concentrated suspension of PhiX 174 (10^{11} pfu/ml) was prepared and concentrations were assayed as described in ISO-10705.

2.2.4 Spiking of *E.coli* WR1 and PhiX 174

Challenge water was prepared by dosing *E. coli* WR1 or PhiX 174 stock solution to the influent at a concentration of 10^5 to 10^6 cfu/ml and stirred (150 RPM) to prevent settling. The influent concentration was sampled in triplicate: two times before spiked water was distributed and one time after the spiking was done. Challenge experiments with active biofilm, inactive biofilm and no biofilm sand were performed on days 5, 10 and 13, respectively. Spiking was done by lowering the supernatant slightly above the sand bed and dosing the challenge water using a peristaltic pump. After spiking for 2-3 pore volumes (PVs), influent water free of *E.coli* WR1 or PhiX 174 was dosed for the next 8 PVs. Effluent samples were collected in 250 ml sterile bottles every 5 minutes for the first 4-5 PVs and every 10 minutes for the next 5 PVs. The collected samples were refrigerated and further analysed on the same day to yield breakthrough curves.

2.2.5 Micro-computed tomography

The top layer column in active, inactive and no biofilm conditions were subjected to Micro-Computed Tomography (Micro-CT) (Phoenix Nanotom, Boston, MA, USA, 180 kV, 0.5 mA, with a maximum resolution 0.5-1.0 micron). Before imaging, sand columns were disconnected from influent and effluent lines while maintaining the sand bed saturated. ImageJ (http://rsb.info.nih.gov) was used to obtain porosity distribution and calculate pore radius.

2.2.6 Modelling transport of *E.coli* WR1 and PhiX 174

Transport of microorganisms in porous media is described by the advection-dispersion equation with first-order retention and reentrainment (Kianfar et al., 2022; Schijven et al., 2013):

$$\frac{\partial C}{\partial t} + \frac{\rho_b}{\theta}\frac{\partial S}{\partial t} = \lambda_L \nu \frac{\partial^2 C}{\partial x^2} - \nu \frac{\partial C}{\partial x} \quad (1)$$

$$\rho_b \frac{\partial S}{\partial t} = k_{ret}\,\theta C - \rho_b k_{reent} S \quad (2)$$

where C is the concentration of free microorganisms [cfu/ml or pfu/ml], S is the concentration of attached microorganisms [cfu/g or pfu/g], ρ_b is the dry bulk density [kg/m^3], θ is volumetric water content [m^3/m^3], t is time [min], λ_L is the dispersivity (cm^{-1}), v is the pore water velocity [cm. min^{-1}], x is the travelled distance (cm), and k_{ret} and k_{reent} are retention and reentrainment rate co-efficients [min^{-1}], respectively. In this work, retention processes such as unfavourable and favourable attachment, hydrophobic interactions and straining are undertaken together under a single retention rate co-efficient. While, reentrainment rate included detachment from previously (un)favourably attached microorganisms, or detachment of previously hydrophobically retained microorganisms.

2.2.7 Estimating contribution of physical, chemical and biological processes to removal

The contribution to the removal of *E. coli* WR1 and PhiX 174 by intact biofilm (considered as predation, grazing, and enzyme-induced inactivation), biofilm (considered as straining, hydrodynamic interaction, and favorable attachment), and sand alone (considered as favorable and unfavorable attachment) was estimated using Log Reduction Values (LRVs) from "active," "inactive," and "no biofilm" experiments as inputs. The removal induced by intact biofilm was determined by subtracting the LRVs in the "inactive biofilm" experiments from those in the "active biofilm" experiments. The contribution of removal by sand alone was directly obtained from the LRVs in the "no biofilm" experiment. Additionally, biofilm-induced removal was calculated by subtracting the LRVs in the "no biofilm" experiments from those in the "inactive biofilm" experiments. In the "no biofilm" experiments, the effects of biofilm removal and sand repacking (see Section 2.2), which clearly affected the filter bed pore structure were neglected.

2.2.8 Data analysis

Data represents the mean and standard error (SE) of duplicate microbial assays in duplicate columns (n=4). Statistical comparison of means of *E.coli* WR1 and PhiX 174 removal at depths was performed by ANOVA (factor: depth). Pairwise comparison of statistically different means in a series was performed with a pos-hoc Tukey test (p = 0.05). Means for different filter media conditions for each depth were also compared using ANOVA (factor: condition) and further with pos-hoc Tukey test.

2.3 Results

2.3.1 *E.coli* WR1 and PhiX 174 attenuation in active biofilm sand

Fig. 1 shows breakthrough curves (BTCs) of *E.coli* WR1 and PhiX 174 (both data and fitted curves) in top, middle and deep layer columns under active biofilm conditions. All BTCs are characterized by a climbing limb, a plateau phase, a declining limb, and finally a gradual declining tail. The BTCs of *E.coli* WR1 exhibit a very low relative breakthrough concentration in the range of 0.02-0.03 in top, middle and deep

layers, resulting in LRVs of 1.69, 1.52 and 1.41 log_{10}, respectively (Fig.1, Table 1). It is important to note that sand bed height was 5 cm in the top layer column and 15 cm in middle and deep layer columns. As a result, the estimation of log removal per cm showed removal of 0.33 log_{10}/cm in the top layer, substantially higher compared to 0.10-0.12 log_{10}/cm in the middle and deep layer columns. ANOVA tests conducted for removal using depths as the independent variable produced p-values below 0.05 (F = 11.09, p = 0.0001, df = 2) showing that LRVs at three depths were statistically different. The R^2 values between 0.83-0.95, indicated that breakthrough could be well described by one retention rate and one reentrainment rate parameter. *E.coli* WR1 displayed a k_{ret} of 1.09 min^{-1} in the top layer, which was 5 times higher than k_{ret} of 0.26 min^{-1} in the middle and deep layers.

The BTCs of PhiX 174 showed a high relative breakthrough concentration in the range of 0.27-0.39, which was 10 times higher than *E.coli* WR1 relative breakthrough concentration. The BTCs resulted in poor but comparable LRVs of 0.56, 0.41 and 0.42 log_{10} in top, middle and deep layers, respectively (F = 1.91, p = 0.142, df = 2). Further, the estimation of log removal per cm showed removal of 0.12 log_{10}/cm in top layer, 4 times higher than removal of 0.03 log_{10}/cm in middle and deep layers. ANOVA tests performed using depth as an independent variable produced p-values above 0.05 (F = 2.23, p = 0.181, df = 2), meaning that for PhiX 174 the influence of depths in removal is statistically insignificant. The BTCs were well described by one retention rate parameter and one re-entrainment rate parameter shown by R^2 values greater than 0.9. Similar to the observations for *E.coli* WR1, PhiX 174 showed higher k_{ret} of 0.32 min^{-1}, compared to k_{ret} of 0.06 min^{-1} in middle and deep layers.

2.3.2 *E.coli* WR1 and PhiX 174 attenuation in inactive biofilm and no biofilm sand

Upon suppression of microbial activity by sodium azide, LRVs of *E.coli* WR1 in the top, middle and deep layers drastically decreased by 0.80, 0.80 and 0.70 log10 to LRVs of 0.92, 0.71 and 0.69 log_{10}, respectively. It is evident from the BTCs in Fig. 2 that the relative breakthrough concentrations and tails in inactive biofilm condition were at least one order of magnitude higher than the BTCs under active biofilm condition. Statistical testing showed that *E.coli* WR1 removal was significantly lower (by 0.7-0.8 log_{10}) after the suppression of microbial activity (F = 15.36, p = 0.0004, df = 1). Lower removal in inactive biofilm experiments is also reflected by the low retention rates in all three depths.

In the no biofilm experiments, LRVs of *E.coli* WR1 significantly reduced by 0.50, 0.30 and 0.30 log_{10} to 0.42, 0.42 and 0.44 log_{10} in top, middle and deep layers, respectively (F = 16.94, p = 0.0003, df = 2). This was also depicted by a further reduction in k_{ret} as shown in Table 2.

While PhiX 174 displayed a similar behaviour as *E.coli* WR1, the removal was low. The absence of microbial activity caused LRVs to reduce by 0.20, 0.20 and 0.15 log_{10} to 0.46, 0.35 and 0.34 log_{10} in top,

middle and deep layers, respectively also displayed by lower k_{ret}.

Although the variations seem minimal, ANOVA test revealed a statistically significant removal before and after bioactivity inhibition (F = 21.56, p = 0.011, df = 1). No biofilm experiments further reduced LRVs by 0.20, 0.10, 0 $\log_{10}$ to 0.31, 0.26 and 0.28 $\log_{10}$ in top, middle and deep layers, respectively. The influence of loss of biofilm was statistically significant in top and middle layers (F = 11.16, p = 0.0004, df = 1) but not in the deep layer (F= 1.13, p = 0.05, df = 1) (Table 2).

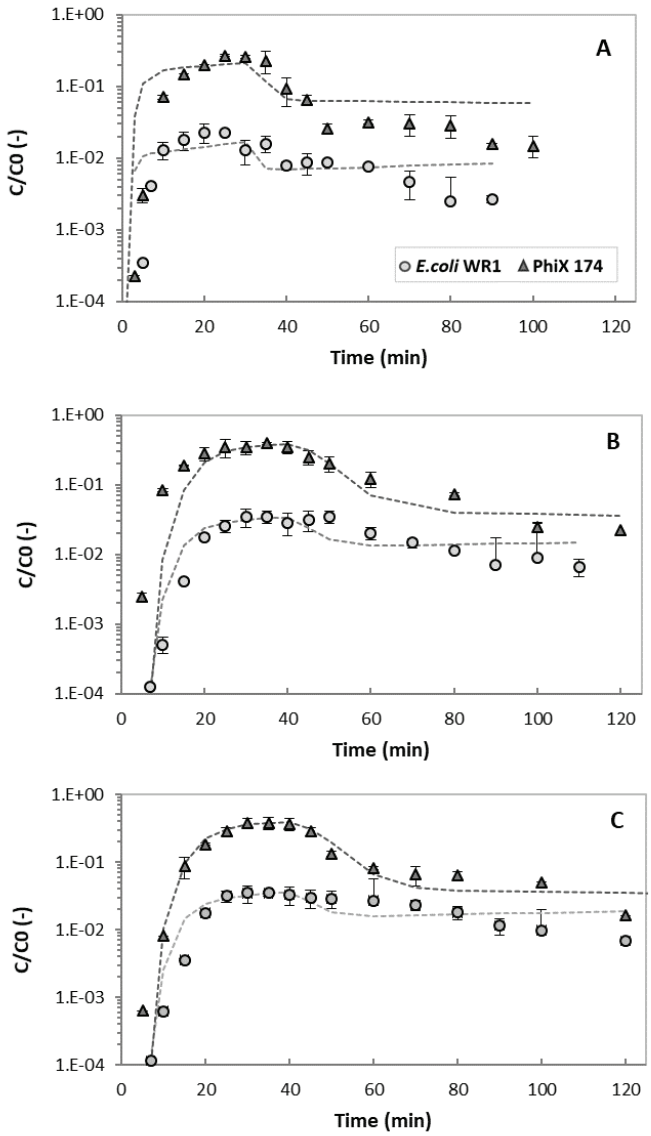

Figure.1. Breakthrough curves of E.coli WR1 and PhiX 174 in top (A), middle (B) and deep (C) layer columns under active biofilm condition. Data represents the mean and standard error (SE.) of duplicate microbial assays in duplicate columns (n=4). Dotted lines are fitted models obtained from Hydrus-1D and the symbols are corresponding experimental data (in the same colour as the dotted lines)

Table 1 Model parameters for E.coli WR1 and PhiX 174 BTCs in top, middle and deep layer columns under active biofilm condition

Condition	Model organism	Depths	Hydrus-1D results					Calculated results		
			k_{ret} (min^{-1})		k_{reent} (min^{-1})		R^2	C/C_0 peak	$-\log_{10}(C/C_0)/x$	$-\log_{10}(C/C_0)$
			EST.	SE.	EST.	SE.				
Active biofilm	*E.coli* WR1	Top	1.09	0.07	0.01	0.002	0.83	0.02	0.33	1.69
		Middle	0.26	0.01	0.01	0.001	0.93	0.03	0.12	1.52
		Deep	0.26	0.01	0.01	0.001	0.93	0.04	0.10	1.41
	PhiX 174	Top	0.32	0.04	0.01	0.004	0.95	0.27	0.12	0.56
		Middle	0.06	0.004	0.004	0.003	0.90	0.39	0.03	0.41
		Deep	0.06	0	0.004	0.002	0.94	0.38	0.03	0.42

Data represents the mean and standard error (SE.) of duplicate microbial assays in duplicate columns (n=4). R^2= coefficient of determination to evaluate model fit to the data; $-\log_{10}(C/C_0)$= overall log removal per column; x= distance in cm; $-\log_{10}(C/C_0)/x$= log removal per cm; EST.= estimated value

Table 2 Model parameters for E.coli WR1 and PhiX 174 BTCs in top, middle and deep layer columns in inactive biofilm and no biofilm conditions

Condition	Model organism	Depths	Hydrus-1D results					Calculated results		
			k_{ret} (min^{-1})		k_{reent} (min^{-1})		R^2	C/C_0 peak	$-\log_{10}(C/C_0)/x$	$-\log_{10}(C/C_0)$
			EST.	SE.	EST.	SE.				
Inactive biofilm	*E.coli* WR1	Top	0.57	0.06	0.01	0.004	0.95	0.12	0.18	0.92
		Middle	0.10	0.01	0.01	0.002	0.97	0.19	0.05	0.72
		Deep	0.10	0.01	0.01	0.002	0.98	0.2	0.05	0.70
	PhiX 174	Top	0.27	0.03	0.02	0.004	0.96	0.35	0.09	0.46
		Middle	0.03	0.004	0.01	0.004	0.91	0.45	0.02	0.35
		Deep	0.04	0.003	0.01	0.003	0.93	0.46	0.02	0.34
No biofilm	*E.coli* WR1	Top	0.23	0.03	0.01	0.004	0.94	0.38	0.08	0.42
		Middle	0.05	0.003	0.01	0.002	0.95	0.38	0.03	0.42
		Deep	0.06	0.004	0.01	0.002	0.98	0.37	0.03	0.43
	PhiX 174	Top	0.17	0.02	0.01	0.004	0.98	0.49	0.06	0.31
		Middle	0.03	0.01	0.01	0.01	0.83	0.55	0.02	0.26
		Deep	0.03	0.004	0.01	0.01	0.90	0.53	0.02	0.28

Data represents the mean and standard error (SE.) of duplicate microbial assays in duplicate columns (n=4). R^2= coefficient of determination to evaluate model fit to the data; $-\log_{10}(C/C_0)$= overall log removal per column; x= distance in cm; $-\log_{10}(C/C_0)/x$= log removal per cm; EST.= estimated value

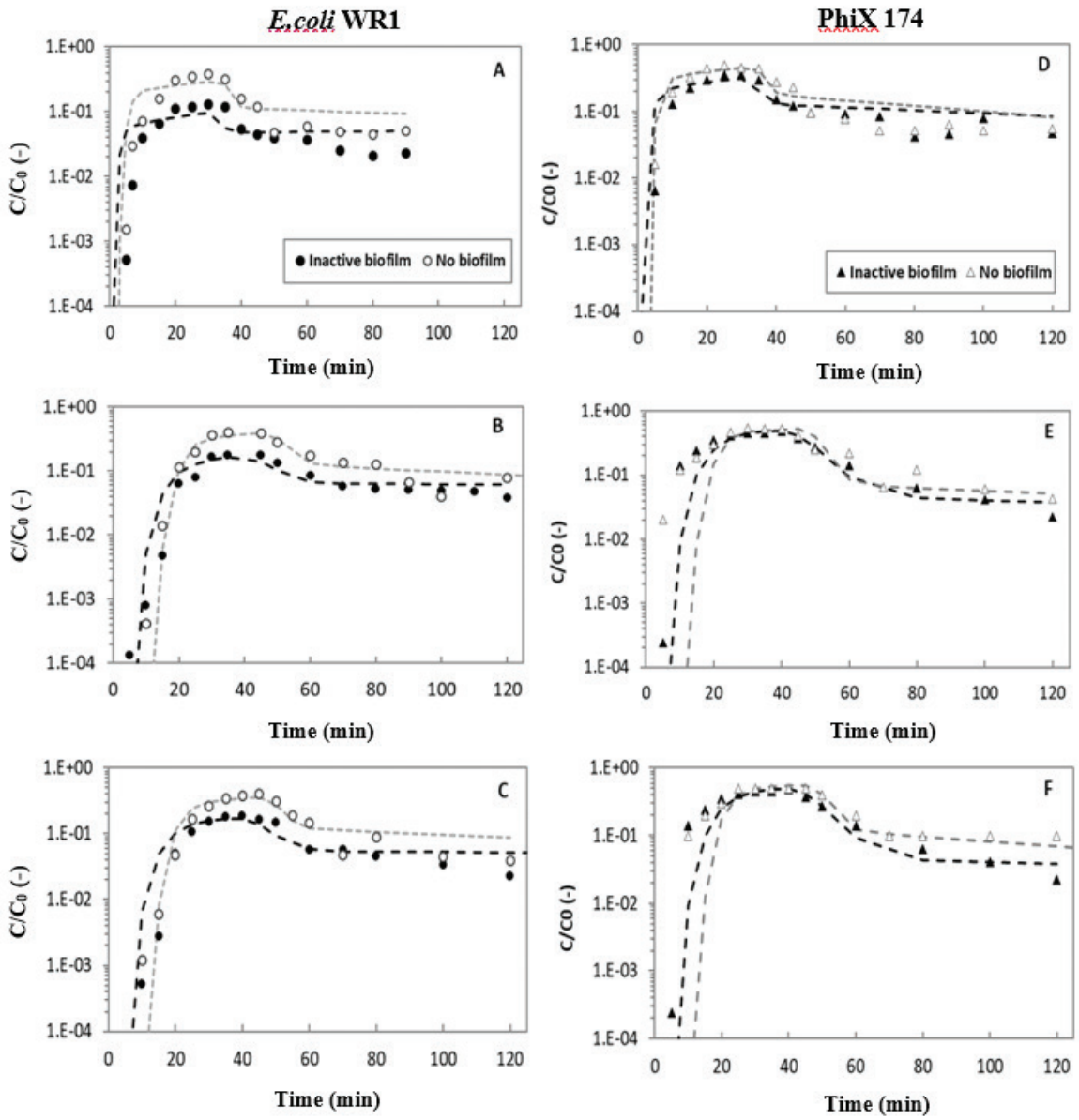

Figure. 2 Breakthrough curves of E.coli WR1 and PhiX 174 in top (A,D), middle (B,E) and deep (C,F) layer columns in inactive biofilm and no biofilm conditions. Data represents the mean and standard error (SE.) of duplicate microbial assays in duplicate columns (n=4). Dotted lines are fitted models obtained from Hydrus-1D and the symbols are corresponding experimental data (in the same colour as the dotted lines).

2.3.3 Micro-computed tomography scanner

The biofilm-dense *Schmutzdecke* may influence porosity in the top layer and alter flow path. Micro-CT was used to directly characterize the pore structure and porosity distribution in the top layer column in active, inactive and no biofilm conditions. A comparison of porosity profiles (Fig. 3A) shows that porosity in both active and inactive biofilm columns is significantly lower than in columns without biofilm. In active biofilm column, porosity increased along the filter height; the lowest porosity of 0.27 was recorded near the column inlet which increased to 0.32 almost at the bottom of the sand bed (5 cm). The inactive biofilm column depicted the same trend in porosity distribution. On the other hand, column without biofilm showed a consistent porosity in the range of 0.38-0.40 throughout the height of the sand bed. Further investigation on pore radius showed that pore radii in the column with no biofilm spanned between 15-75 µm, with a median around 35 µm (Fig. 3C). In active and inactive biofilm columns, pore radii ranged between 1-35 µm, with a median of 15 µm (Fig. 3C). In active and inactive biofilm columns, pore radii of 1 µm, which are in the range of average size of *E.coli* WR1 made up 0.03-0.07% of the total pore volume.

2.4 Discussion

2.4.1 Significance of mature biofilm

This study showed that top, middle and deep layers of mature SSF caused substantial removal of *E.coli* WR1 (1.4-1.7 $\log_{10}$) and PhiX 174 (0.4-0.6 $\log_{10}$) indicating the significance of mature biofilms in the sand bed. *Schmutzdecke* is described as a visibly thick, brownish slimy layer, unlike the biofilms in deeper layers that can only be visualized under the microscope. Hence, a general assumption is that pathogen removal by microbial activity associated processes like predation, grazing or enzyme induced inactivation occurs mainly in the *Schmutzdecke* where biological activity is the highest (Chen et al., 2021; Schijven et al., 2013). Complementary to the previous observations, it was found that microbial activity in intact biofilm contributed to 0.70-0.80 $\log_{10}$ of *E.coli* WR1 removal at all three depths (Table 3). Meanwhile, the intact biofilm slightly influenced PhiX 174 removal with 0.10 $\log_{10}$ at all three depths. In biological filters, stratification of biomass and bioactivity is observed due to environmental and chemical gradients (e.g., DOC, NH_4^+) (Chen et al., 2021). Despite these variations, the substantial contribution of deeper depths to overall bacteria and virus removal suggests the importance of a well-functioning biofilm in the sand bed.

Mature biofilms in filters functioning over a while have been reported to own different physical and biological properties such as thickness, morphology and microbial community composition compared to young biofilms in newly established filters (Boe-Hansen et al., 2002; Bai et al., 2022; Haig et al., 2015). In this study, we observed that biofilm associated removal by straining, hydrodynamic interaction, and

favourable attachment contributed to *E.coli* WR1 removal of 0.5 $\log_{10}$ in the top layer and 0.3 $\log_{10}$ in middle and deep layers (Table 3). The contribution to PhiX 174 removal was rather low, between 0.1-0.2 $\log_{10}$. Earlier studies showed *Schmutzdecke* thickness as one of the major factors increasing pathogen removal in SSFs (Schijven et al., 2013). Increased biofilm thickness by biomass accumulation is a consequence of filter ageing or maturation (Elliot et al., 2011; Hijnen et al., 2007; Schijven et al., 2013). Enhanced attachment and straining of bacteria and viruses have been observed for biofilms with higher thickness compared to relatively thin biofilms (Afrooz & Boehm, 2016). The favourable retention of bacteria and viruses in biofilm coated surface vs no biofilm surface is shown by higher retention rates in the former, thus depicting different transport behaviour (Fig. 1 and 2).

Biological properties of biofilm such as microbial community abundance, diversity and evenness increase with filter maturation (Haig et al., 2015). In newly built SSFs where biofilm has not had years to develop, *Schmutzdecke* microbial community may be distinctive from that of the sand bed. In such young filters, treatment performance may be more coupled to the status of the *Schmutzdecke* (Chan et al., 2018). In mature SSFs, this will not be the case and consequent temporal changes are marginal (Haig et al., 2015). E.g., the overall community composition in the first 50 cm of the sand bed is similar for bacteria, archaea, and eukaryotes (Li et al., 2017; Wakelin et al., 2011; Haig et al., 2015). Even at low abundance, eukaryotic communities are strongly related to the removal of pathogenic bacteria by grazing and predation (Weber-Shirk and Dick 1997a; Stott et al. 2001; Haig et al. 2015). Based on these observations, biological removal processes may be prominent even in the deeper layers and not restricted to the *Schmutzdecke* as previously assumed.

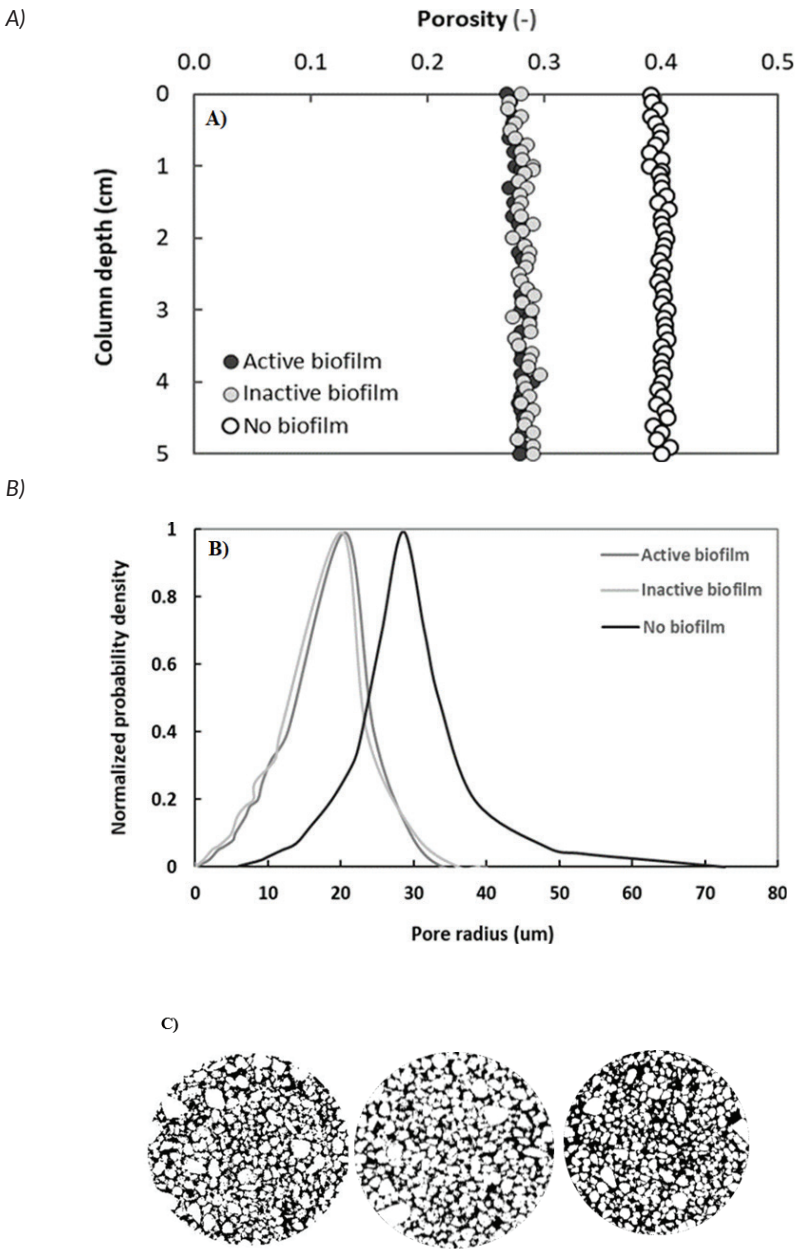

Figure. 3 Top layer column analysed using Micro-computed tomography scanner under active, inactive and no biofilm conditions. A) Porosity distribution along the column bed height, B) normalized probability density of pore radius, C) Micro-CT slices from 1 cm depth in the top layer showing intensity response of sand grains (white) and flow channels or pores (black).

Table 3 Contribution of intact biofilm, biofilm and sand to overall removal of E.coli WR1 and PhiX 174 at different depths

Model organism	Filter depths	Microbial log removal			
		Per depth	Intact biofilm	Biofilm	Sand only
E.coli WR1	Top	1.69 ± 0.317	0.77 ± 0.254	0.50 ± 0.317	0.42 ± 0.254
	Middle	1.52 ± 0.317	0.81 ± 0.317	0.29 ± 0.317	0.42 ± 0.317
	Deep	1.41 ± 0.254	0.72 ± 0.190	0.25± 0.254	0.44 ± 0.254
PhiX 174	Top	0.56 ± 0.317	0.1 ± 0.254	0.14 ± 0.190	0.32 ± 0.254
	Middle	0.41 ± 0.254	0.06 ± 0.254	0.09 ± 0.190	0.26 ± 0.254
	Deep	0.42 ± 0.317	0.08 ± 0.254	0.06 ± 0.190	0.28 ± 0.190

Data represents the mean values from duplicate column experiments (n=2). 95%-confidence intervals are given between brackets

2.4.2 Retention processes at different depths

Active and inactive biofilm on sand increased retention of *E.coli* WR1 as seen by higher k_{ret} values compared to no biofilm experiments at all three depths. The top layer caused four times higher k_{ret} of *E.coli* WR1, compared to middle and deep layers (1.09 min^{-1} vs 0.26 min^{-1}). Similarly, for PhiX 174, the influence of active and inactive biofilm was prominent in top layer, i.e., 5 times higher k_{ret} in top layer than deeper layers. It is worthy to note that *E.coli* WR1 retention was greater than PhiX 174 at all three depths, however, the change in k_{ret} between top and deeper layers was greater for the latter. This highlights the value of top layer, in terms of surface functionality and biological activity on sand in virus removal. These observations indicate varying contribution of different retention processes at different depths for each type of microorganism.

From the modelling results it can be infered, based on literature, that retention processes like straining, hydrophobic interactions, and favourable and unfavourable attachment are occurring (Afrooz et al., 2018; Fu et al., 2023). Straining is caused when microbes are trapped in pore throats that are too small to allow passage (Foppen et al., 2005). It was observed that biofilms decreased the pore radii sizes in the top layer from 15-70 µm to 0.5-35 µm. With narrow pores, chances of *E.coli* WR1 retention by straining is higher due to a higher chance of collision with biofilm and large size of bacteria (He et al., 2020; Foppen et al., 2007). Additionally, strained bacteria would not be reentrained unless biofilm sloughing happens which is not the case in our experiments as shown by 100 times lower k_{reent} of *E.coli* than k_{ret} in the top layer. However, for viruses, physical straining within the biofilm is unlikely due to their small size, supported by relatively lower k_{ret} in the top layer. The fact that *Schmutzdecke* removal (scraping) reduced bacteria LRVs and not viruses in earlier studies (Hijnen et al.,2007; Schijven et al., 2013) may support the argument that straining may be an important retention mechanism for bacteria in the top layer, although role of other (biological) retention mechanisms such as predation, grazing, enzyme induced inactivation and attachment to biofilm cannot be excluded. Enhanced retention of *E.coli* WR1 and PhiX 174 in biofilms may also be supported by Extracellular Polymeric Substances (EPS) in biofilms. EPS components- proteins and polysaccharides could bind and form hydrophobic interaction with bacterial surface functional groups such as teichoic acids and phospholipids (Fu et al., 2023; Xiao and Wiesner, 2013). In addition, positively charged amine groups in EPS promote electrostatic attraction with negatively charged bacteria and viruses allowing for favourable attachment (Guo et al., 2015).

In middle and deep layers, the biomass levels were much lower than in the top layer suggesting the presence of relatively thin biofilms. k_{ret} in both depths was slightly higher in the presence of biofilm indicating their influence on retention processes. Porosity distribution in middle and deep layers was not investigated in this study but the trend of increasing porosity with depth in top layer suggests that microbial retention by straining may not be critical in deeper depths. However, the contribution of

hydrophobic interactions, and favourable and unfavourable attachment cannot be overlooked. This study did not quantify the exact contribution of different retention processes to *E.coli* WR1 and PhiX removal as such an effort was beyond the scope of the present study.

Interestingly, k_{ret} of *E.coli* WR1 and PhiX 174 in no biofilm experiments was not negligible. Under no biofilm condition, removal is determined by clean bed collisions and the classic colloid filtration mechanisms (interception, Brownian diffusion, and gravitational deposition) of which interception and Brownian diffusion are likely most important for bacteria and virus removal, respectively (Afrooz et al., 2018; Bradford et al., 2003). At neutral pH as in the experiments, colloids (*E.coli* WR1/PhiX 174) and sand grain surface are both negatively charged and therefore repulsive (Tripathi et al., 2011). However, when the distance between colloids and sand grain is small enough (less than a few nm), the attractive Van der Waals force may become dominant, thus causing attachment (Foppen et al., 2005). On the other hand, favourable attachment of negatively charged bacteria/viruses can occur on patches of positively charged surfaces on sand grains. Hence, the higher intensity of k_{ret} for both *E.coli* WR1 and PhiX 174 in top layer may be attributed to relatively high concentration of Fe and Mn (oxides) in top layer sand as shown in Fig. S2 and S3 (B). Despite these differences, similar removal of *E.coli* WR1 and PhiX 174 at different bed heights in top, middle and deep layers is likely caused by small sticking efficiency variations within the bacterium and virus population. Despite the variation in sticking efficiencies as reported in literature, Hijnen et al. (2004) and Schijven et al. (2013) observed that removal data of *E.coli* WR1 *were* concomitant with removal of thermotolerant coliforms and naturally present *E.coli* bacteria in pilot and full-scale filter studies. In terms of viruses, Elliott et al. (2008) observed higher reduction of human enteric virus (echovirus 12) than bacteriophages (MS2 and PRD1) in BSF, suggesting that virus removal depends upon the specific viral agent.

2.4.3 Balanced contribution of *Schmutzdecke* and deeper layers to microbial removal

In this study, it was hypothesised that deeper layers in established SSFs contribute to substantial removal of bacteria and viruses due to mature biofilm in the sand bed. The estimated LRVs showed that *E.coli* WR1 removal was 0.33 $\log_{10}$/cm in top layer and 0.10 $\log_{10}$/cm in middle and middle-deep layers. Similarly, PhiX 174 removal was 0.12 $\log_{10}$/cm and 0.03 $\log_{10}$/cm for top and middle-deep layers, respectively. Although log removal/cm in deeper layers is 3.3 and 4 times lower than in top layer for *E.coli* WR1 and PhiX 174, respectively, the total volume of the deep sand is many times greater than that occupied by the *Schmutzdecke*/top layer. The study of Pfannes et al. (2015) showed that effective removal of fecal indicators occurred due to the *Schmutzdecke* in 14 week-old SSFs, however, microbial communities in influent and effluent water were indistinguishable by t-RFLP analysis of bacterial 16S rRNA. In (immature) filters where a deep sand bed biofilm was unable to transform the influent water for any number of reasons (time, inoculation), the influence of *Schmutzdecke* on filter function might have

been more obvious (Chan et al., 2018). In mature SSFs, functional microbial community was observed to be highly similar even when sampled from different depths (Haig et al., 2015). Thus, biofilms in both *Schmutzdecke* and deep sand bed is essential for shaping the produced water quality.

Based on the finding that deeper layers of SSFs are important for bacteria and virus removal, it is recommended that reducing the height of the filter bed by repetitive scraping is avoided where possible. By doing so, the treatment capacity of the deep sand bed in mature SSFs can be utilized, particularly after *Schmutzdecke* scraping, preventing lengthy filter downtime. Also, traditional practice to switch the deeper layers to the top when renewing the filter bed might need reconsideration, as disturbing the deeper bed biofilm might have negative effects on filter perfomance. The filters in this study were operated at relatively high filtration rates of 0.4 m/h (typical filtration rates- 0.05-0.2 m/h) (Haig et al., 2014; Schijven et al., 2013) and grain size of 0.4-0.6 mm (typical grain sizes- 0.15-0.3mm) (Schijven et al., 2013) which might have influenced the stratification of microbial processes. It is therefore encouraged to consider varying filtration rates and grain sizes (both lower and higher than the values in this study) as to further investigate the benefit on bacteria and virus removal.

This research also showed that bacteria and virus attenuation could be improved by microbial activity, also in the deeper layers. The microorganisms inhabiting the biofilm is driven by environmental and chemical gradients (e.g., DOC, NH_4^+) (Bai et al., 2022; Chen et al., 2021). Typically, SSFs in many parts of the world operate without extensive pre- treatment. Thus, greater loads of particulate matter, organics, nutrients and microorganisms are introduced for continued development of biological activity in the filter. As a result, the contribution of microbial mechanisms could be greater, favouring pathogen removal. However, more efforts should be made to explore the influence of influent water quality and microbial community composition on pathogen removal in mature SSFs. Regardless, filter operational procedures, specifically cleaning practices that aim towards biomass preservation would benefit optimized performance. For instance, partial retention of *Schmutzdecke* in the filter, in-situ hydraulic rinsing may be considered as alternatives to the conventional scraping to shorten the ripening process.

2.5 Conclusions

This study examined the removal capacity of two important indicator enteric pathogens *E.coli* WR1 and PhiX 174 at different depths of an established full-scale SSF. Filter material collected from selected depths was studied in an innovative experimental setup to differentiate physical, chemical and biological removal processes. The main findings were:

- *Schmutzdecke* and deeper layers of established SSF showed substantial contribution to *E.coli* WR1 and PhiX 174 log removal.

- *E.coli* WR1 removal was caused by active biofilm led processes like predation, grazing, enzyme induced inactivation at all three depths indicating the importance of mature biofilms in the sand bed. Furthermore, removal by straining, hydrodynamic interaction, favourable and unfavourable attachment by (inactive) biofilm and sand contributed to overall removal.
- In contrast, active and inactive biofilm marginally influenced PhiX 174 removal, mainly in the top layer. However, PhiX 174 removal was found to be mostly influenced by Brownian diffusion as the engine of collisions with the sand surface.
- One-site kinetic retention model showed higher retention rates for *E.coli* WR1 and PhiX 174 in the top layer. Physical-chemical factors, such as pore radii and, Mn and Fe oxides and biological factors like dense biomass were identified as potential impactors for better retention of bacteria and viruses in the top layer.
- The knowledge of underestimated removal capacity of deeper sand bed is a valuable contribution to optimizing the design and operation of SSFs in drinking water utilities.

2.6 Supplementary information

2.6.1 Characterization of filter sand grains and water analysis

Sand (0.5 g) from different depths after biofilm ignition was dissolved in 25 mL demi water and 6.25 mL concentrated HNO_3 (69-70%) by heating the suspension to 98°C for 4 hours (Gude et al., 2015). After cooling down, the acidified water was analysed for Fe and Mn using inductively coupled plasma mass spectrometry (ICP-MS).

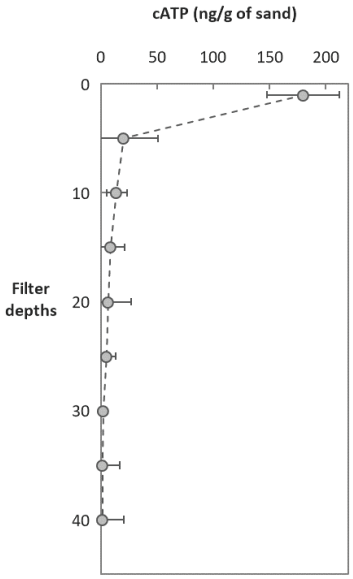

Figure S1 ATP concentration on filter material obtained from the first 40 cm of full-scale SSF

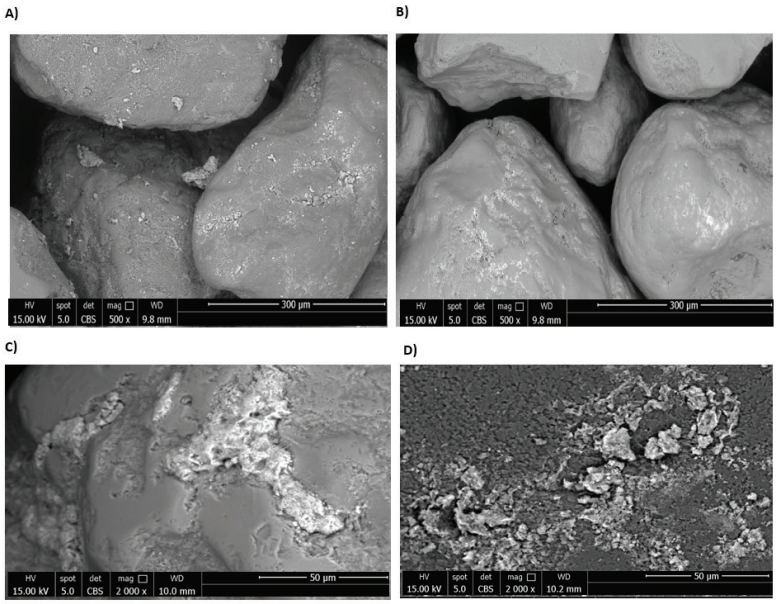

Figure S2 ESEM pictures of Fe and Mn deposits (A) Sand grains from top layer; (B) Sand grains from deep layers; (C,D) Fe precipitates on top layer sand grains.

Top, middle and deep layer sand samples without biofilm were inspected with Environmental Scanning Electron Microscopy coupled with Energy Dispersive X-ray Spectroscopy (ESEM-EDX). Deposits of iron (Fe) and manganese (Mn) were observed in the form of scattered deposits over the surface of sand grains as shown in Fig. S2 (A) and (B). The top layer sand showed high concentrations of Fe, around 6 mg/g of sand compared to middle and deep layers which had a concentration <3 mg/g of sand (Fig. S3 (A)). Also for Mn, the highest concentration was observed in the top layer, but Mn content on sand was much lower than for Fe. As discussed in Section 2.1, the water entering the treatment plant is pre-treated by dune filtration and rapid sand filtration, and breakthrough of trace amounts (micrograms per liter) of iron, and manganese in the filtrate are typically observed. The mature full-scale SSF used in this study showed removal of Fe and Mn by 75% and 85%, respectively as shown in Fig. S3 (B).

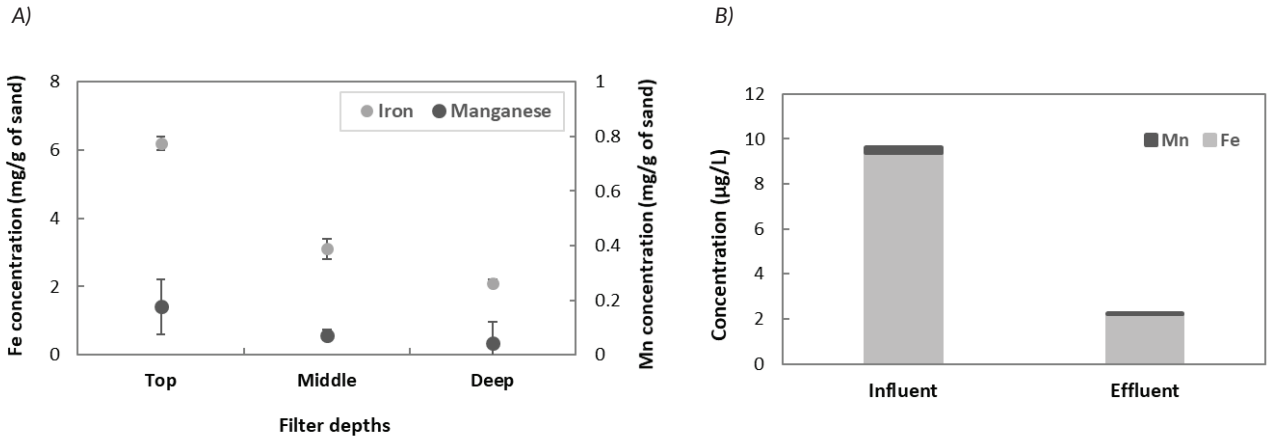

Figure S3 (A) Fe and Mn concentrations on sand from top, middle and deep layers; (B) Fe and Mn concentrations in the influent and effluent of mature full-scale SSF.

References

Afrooz, A. R. M. N., & Boehm, A. B. (2016). Escherichia coli removal in biochar-modified biofilters: Effects of biofilm. PLoS ONE, 11(12), 1–17.

Afrooz, A. R. M. N., Pitol, A. K., Kitt, D., & Boehm, A. B. (2018). Role of microbial cell properties on bacterial pathogen and coliphage removal in biochar-modified stormwater biofilters. Environmental Science: Water Research and Technology, 4(12), 2160–2169.

Andreoli, F. C., & Sabogal-Paz, L. P. (2020). Household slow sand filter to treat groundwater with microbiological risks in rural communities. Water Research, 186, 116352.

Bai, X., Dinkla, I. J. T., & Muyzer, G. (2022). Microbial ecology of biofiltration used for producing safe drinking water. Applied Microbiology and Biotechnology, 106(13–16), 4813–4829.

Bertelkamp, C., Verliefde, A. R. D., Reynisson, J., Singhal, N., Cabo, A. J., de Jonge, M., & Van der Hoek, J. P. (2016). A predictive multi-linear regression model for organic micropollutants, based on a laboratory-scale column study simulating the river bank filtration process. Journal of Hazardous Materials, 304, 502–511.

Bicudo, B., van Halem, D., Trikannad, S. A., Ferrero, G., & Medema, G. (2021). Low voltage iron electrocoagulation as a tertiary treatment of municipal wastewater: removal of enteric pathogen indicators and antibiotic-resistant bacteria. Water Research, 188, 116500.

Boe-Hansen, R., Albrechtsen, H. J., Arvin, E., & Jørgensen, C. (2002). Dynamics of biofilm formation in a model drinking water distribution system. Journal of Water Supply: Research and Technology - AQUA, 51(7), 399–406.

Bradford, S. A., Simunek, J., Bettahar, M., Van Genuchten, M. T., & Yates, S. R. (2003). Modeling colloid attachment, straining, and exclusion in saturated porous media. Environmental Science and Technology, 37(10), 2242–2250.

British Standards Institution. 1990b. Determination by mass-loss on ignition. British standard methods of test for soils for civil engineering purposes. Chemical and electro-chemical tests. BS 1377:3:1990:4. BSI, London.

Chan, S., Pullerits, K., Riechelmann, J., Persson, K. M., Rådström, P., & Paul, C. J. (2018). Monitoring biofilm

function in new and matured full-scale slow sand filters using flow cytometric histogram image comparison (CHIC). Water Research, 138, 27–36.

Chen, L., Zhai, Y., van der Mark, E., Liu, G., van der Meer, W., & Medema, G. (2021). Microbial community assembly and metabolic function in top layers of slow sand filters for drinking water production. Journal of Cleaner Production, 126342.

Chrysikopoulos, C. V., & Aravantinou, A. F. (2012). Virus inactivation in the presence of quartz sand under static and dynamic batch conditions at different temperatures. Journal of Hazardous Materials, 233–234, 148–157.

de Oliveira, F. F., & Schneider, R. P. (2019). Slow sand filtration for biofouling reduction in seawater desalination by reverse osmosis. Water research, 155, 474-486.

Dizer, H., Grützmacher, G., Bartel, H., Wiese, H. B., Szewzyk, R., & López-Pila, J. M. (2004). Contribution of the colmation layer to the elimination of coliphages by slow sand filtration. Water Science and Technology, 50(2), 211–214.

Eisfeld, C., Schijven, J. F., van der Wolf, J. M., Medema, G., Kruisdijk, E., & van Breukelen, B. M. (2022). Removal of bacterial plant pathogens in columns filled with quartz and natural sediments under anoxic and oxygenated conditions. Water Research, 220(February), 118724.

Elliott, M. A., DiGiano, F. A., & Sobsey, M. D. (2011). Virus attenuation by microbial mechanisms during the idle time of a household slow sand filter. Water Research, 45(14), 4092–4102.

Elliott, M. A., Stauber, C. E., Koksal, F. A. T. M. A., DiGiano, F. A., & Sobsey, M. D. (2008). Reductions of E. coli, echovirus type 12 and bacteriophages in an intermittently operated household- scale slow sand filter. Water research, 42(10-11), 2662-2670.

Foppen, J. W. A., Mporokoso, A., & Schijven, J. F. (2005). Determining straining of Escherichia coli from breakthrough curves. Journal of Contaminant Hydrology, 76(3–4), 191–210.

Foppen, J.W., van Herwerden, M., Schijven, J., 2007. Transport of Escherichia coli in saturated porous media: dual mode deposition and intra- population heterogeneity. Water Research 41 (8), 1743–1753.

Fu, J., Gao, B., Xu, H., Hao, S., Ren, J., Wu, J., & Sun, Y. (2023). Effects of biofilms on the retention and transport of PFOA in saturated porous media. Journal of Hazardous Materials, 443(PB), 130392.

Guo, J. S., Zhang, P., Chen, Y. P., Shen, Y., Hu, X., Yan, P., Yang, J. X., Fang, F., Li, C., Gao, X., & Wang, G. X. (2015). Microbial attachment and adsorption-desorption kinetic of tightly bound extracellular polymeric substances on model organic surfaces. Chemical Engineering Journal, 279, 516– 521.

Haig, S. J., Collins, G., Davies, R. L., Dorea, C. C., & Quince, C. (2011). Biological aspects of slow sand filtration: Past, present and future. Water Science and Technology: Water Supply, 11(4), 468–472.

Haig, S. J., Quince, C., Davies, R. L., Dorea, C. C., & Collins, G. (2015). The relationship between microbial community evenness and function in slow sand filters. MBio, 6(5), He, L., Rong, H., Wu, D., Li, M., Wang, C., & Tong, M. (2020). Influence of biofilm on the transport and deposition behaviors of nano- and micro-plastic particles in quartz sand. Water Research, 178, 115808.

Hijnen, W. A. M., Dullemont, Y. J., Schijven, J. F., Hanzens-Brouwer, A. J., Rosielle, M., & Medema, G. (2007). Removal and fate of Cryptosporidium parvum, Clostridium perfringens and small-sized centric diatoms (Stephanodiscus hantzschii) in slow sand filters. Water Research, 41(10), 2151–2162.

Hijnen, W. A. M., Schijven, J. F., Bonné, P., Visser, A., & Medema, G. J. (2004). Elimination of viruses, bacteria and protozoan oocysts by slow sand filtration. Water Science and Technology, 50(1), 147–154. https://doi.org/10.2166/wst.2004.0044

Huisman, L., & Wood, W. E. (1974). Slow sand filtration. WORLD HEALTH ORGANIZATION.

Jenkins, M. W., Tiwari, S. K., & Darby, J. (2011). Bacterial, viral and turbidity removal by intermittent slow sand filtration for household use in developing countries: Experimental investigation and modeling. Water Research.

Kianfar, B., Tian, J., Rozemeijer, J., van der Zaan, B., Bogaard, T. A., & Foppen, J. W. (2022). Transport characteristics of DNA-tagged silica colloids as a colloidal tracer in saturated sand columns; role of solution chemistry, flow velocity, and sand grain size. Journal of Contaminant Hydrology, 246(December 2021), 103954.

Li, Q., Yu, S., Li, L., Liu, G., Gu, Z., Liu, M., ... & Ren, L. (2017). Microbial communities shaped by treatment processes in a drinking water treatment plant and their contribution and threat to drinking water safety. Frontiers in Microbiology, 8, 2465.

Lee, C. O., Boe-Hansen, R., Musovic, S., Smets, B., Albrechtsen, H. J., & Binning, P. (2014). Effects of dynamic operating conditions on nitrification in biological rapid sand filters for drinking water treatment.

Maurya, A., Singh, M. K., & Kumar, S. (2020). Biofiltration technique for removal of waterborne pathogens. In Waterborne Pathogens (pp. 123-141). Butterworth-Heinemann.

Napotnik, J.A., Baker, D., Jellison, K.L., 2020. Influence of sand depth and pause period on microbial removal in traditional and modified biosand filters. Water Res, 116577.

Oh, S., Hammes, F., & Liu, W. T. (2018). Metagenomic characterization of biofilter microbial communities in a full-scale drinking water treatment plant. Water research, 128, 278-285.

Oudega, T. J., Lindner, G., Derx, J., Farnleitner, A. H., Sommer, R., Blaschke, A. P., & Stevenson, M. E. (2021). Upscaling Transport of Bacillus subtilis Endospores and Coliphage phiX174 in Heterogeneous Porous Media from the Column to the Field Scale. Environmental Science and Technology, 55(16), 11060–11069.

Pfannes, K. R., Langenbach, K. M. W., Pilloni, G., Stührmann, T., Euringer, K., Lueders, T., Neu, T. R., Müller, J. A., Kästner, M., & Meckenstock, R. U. (2015). Selective elimination of bacterial faecal indicators in the Schmutzdecke of slow sand filtration columns. Applied Microbiology and Biotechnology, 99(23), 10323–10332.

Rodgers, M., Mulqueen, J., & Healy, M. G. (2004). Surface Clogging in an Intermittent Stratified Sand Filter. Soil Science Society of America Journal.

Schijven, J. F., Van den Berg, H. H. J. L., Colin, M., Dullemont, Y., Hijnen, W. A. M., Magic-Knezev, A., Oorthuizen, W. A., & Wubbels, G. (2013). A mathematical model for removal of human pathogenic viruses and bacteria by slow sand filtration under variable operational conditions. Water Research, 47(7), 2592–2602.

Soliman, M. Y. M., Medema, G., Bonilla, B. E., Brouns, S. J. J., & van Halem, D. (2020). Inactivation of RNA and DNA viruses in water by copper and silver ions and their synergistic effect. Water Research X, 9, 100077.

Soliman, M. Y. M., van Halem, D., & Medema, G. (2020). Virus removal by ceramic pot filter disks: Effect of biofilm growth and surface cleaning. International Journal of Hygiene and Environmental Health, 224(December 2019).

Sousi, M., Liu, G., Salinas-Rodriguez, S. G., Chen, L., Dusseldorp, J., Wessels, P., ... & van der Meer, W. (2020). Multi-parametric assessment of biological stability of drinking water produced from

groundwater: Reverse osmosis vs. conventional treatment. Water research, 186, 116317.

Stott R, May E, Matsushita E, Warren A (2001) Protozoan predation as a mechanism for the removal of cryptosporidium oocysts from wastewaters in constructed wetlands. Water Sci Technol 44:191–198.

Tatari, K., Smets, B. F., & Albrechtsen, H. J. (2016). Depth investigation of rapid sand filters for drinking water production reveals strong stratification in nitrification biokinetic behavior. Water Research, 101, 402–410.

Tripathi, S., Champagne, D., & Tufenkji, N. (2011). Transport Behavior of Selected Nanoparticles with different Surface Coatings in Granular Porous Media coated with Pseudomonas aeruginosa Biofilm. Environmental Science & Technology, 46(13), 6942–6949.

Unger, M. C., & Collins, M. R. (2006, November). The Role of the Schmutzdecke in Pathogen Removal in Slow Sand and Riverbank Filtration. In Proc. 2006 AWWA Ann. Conf., San Antonio.

van der Kooij, D., Veenendaal, H. R., van der Mark, E. J., & Dignum, M. (2017). Assessment of the microbial growth potential of slow sand filtrate with the biomass production potential test in comparison with the assimilable organic carbon method. Water Research, 125, 270–279.

Wakelin, S., Page, D., Dillon, P., Pavelic, P., Abell, G. C. J., Gregg, A. L., & Anderson, G. (2011). Microbial community structure of a slow sand filter schmutzdecke: a phylogenetic snapshot based on rRNA sequence analysis. Water Science and Technology: Water Supply, 11(4), 426-436.

Weber-Shirk, M. L., & Dick, R. I. (1997a). Biological mechanisms in slow sand filters. Journal American Water Works Association, 89(1), 87–100.

Weber-Shirk, M. L., & Dick, R. I. (1997b). Physical-chemical mechanisms in slow sand filters. Journal American Water Works Association, 89(1), 87–100.

Xiao, Y., & Wiesner, M. R. (2013). Transport and retention of selected engineered nanoparticles by porous media in the presence of a biofilm. Environmental science & technology, 47(5), 2246-2253.

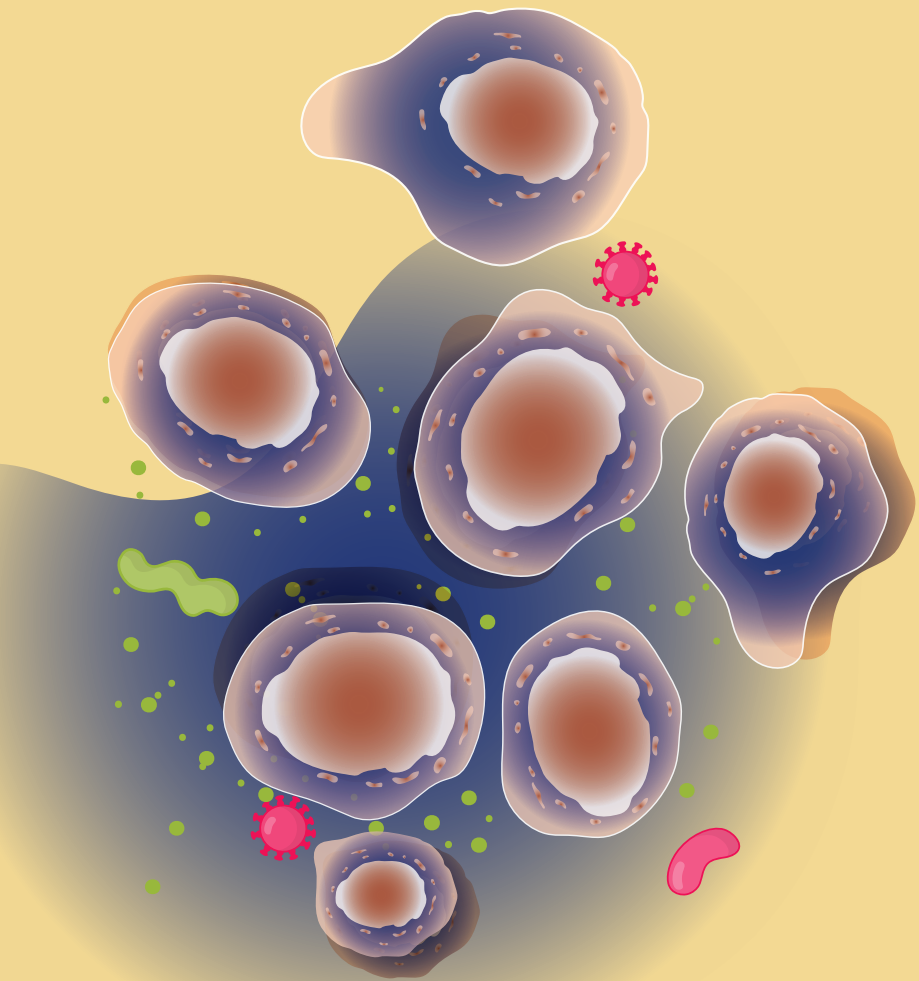

Chapter 3

Recovery of full-scale slow sand filters performance after scraping

This chapter is based on:
Trikannad, S. A., Attiani, V., van der Wielen, P. W., Smidt, H., van der Hoek, J. P., & van Halem, D. (2024). Recovery of microbial biomass and purification performance after scraping of full-scale slow sand filters. Journal of Water Process Engineering, 60, 105101.

Abstract

Slow sand filters (SSFs) are widely used in drinking water production to improve microbial safety and biological stability of water. Full-scale SSFs are maintained by scraping the biomass-rich top layers of sand. The period of downtime required for filter recovery after scraping is a major challenge due to limited knowledge of the re-stabilisation of purification processes. This study examined the recovery of microbial biomass, and removal of dissolved organic carbon (DOC) and ammonium (NH_4^+) in water phase and/or on sand along the depth of a scraped full- scale SSF. Scraping reduced microbial biomass on sand in the top layers, while the main prokaryotic taxa remained unaltered. Cellular ATP (cATP) and intact cell counts (ICC) in water sampled from the top layers increased, indicating a temporary disruption in functionality for 37 days. However, stable concentrations of cATP and ICC and similar microbial community composition in the effluent after scraping revealed that deeper layer biofilms offset any scraping effect. Consistent DOC and NH_4^+ removal after scraping showed that deeper layers effectively performed the role of the top layer. These findings highlight the resilience and robustness of microbial communities in mature full-scale SSFs and their contribution to water treatment efficiency after disturbances caused by scraping.

3.1 Introduction

Water utilities aim to produce microbiologically safe and biologically stable drinking water to prevent microbial regrowth during distribution (Prest et al., 2016). Slow sand filters (SSFs) are a third or final polishing step in drinking water production to remove turbidity, pathogens, dissolved organic carbon (DOC) and ammonium (NH_4^+) (Haig et al., 2011; van der Kooij et al., 2017). SSFs are energy-efficient, require no additional chemicals and produce minimal waste, making them a sustainable choice for drinking water production in both developed and developing countries (Huisman and Wood, 1974).

SSFs purify water by interdependent biological and physical-chemical processes, and the indigenous microbial community that inhabit the sand bed play a crucial role (Bai et al., 2022; Haig et al., 2015; Oh et al., 2018). The *Schmutzdecke*, a highly active, biomass-rich top layer forms a primary barrier for several contaminants. Excessive biomass accumulation over time restricts hydraulic flow in the filter, thus, the top few layers are periodically scraped (Symons, 2006). In full-scale SSFs, *Schmutzdecke* scraping often leads to a downtime or ripening period until filter activity recovers and effluent quality meets regulatory standards. This period can be lengthy or short, depending on filter age and maturity of microbial communities on sand (Chan et al., 2018).

Former investigations performed in lab and pilot-scale SSFs showed that scraping invariably reduced *E.coli* and coliforms removal (Collins and Unger, 2008). A full-scale SSF study found minimal effect of *Schmutzdecke* removal on total organic carbon (TOC) and bacterial indicator removal (Chan et al., 2018). A lab-scale investigation showed that scraping significantly changed microbial community composition in the top layer but did not compromise turbidity and total coliform removal (De Souza et al., 2021). These inconsistencies may result from differences in filter maturity in young lab/pilot-scale filters which might not accurately represent well-established full-scale SSFs. Despite some insights on the impact of scraping, knowledge on re-stabilisation of DOC and NH_4^+ removal processes after scraping, from a biological stability perspective is limited. Moreover, the recovery of microbial communities during ripening of mature full-scale SSFs has not been thoroughly explored.

DOC in water primarily consists of refractory (i.e. poorly biodegradable) compounds, biodegradable dissolved organic carbon (BDOC) and easily assimilable organic carbon (AOC) (Brandt et al., 2017, Schurer et al., 2022). BDOC and AOC fractions in drinking water can stimulate bacterial regrowth during distribution (van der Wielen et al., 2023). Slowly biodegradable organic carbon fractions such as biopolymers negatively affect the biological stability of drinking water (Park et al., 2016). Due to the importance of both slowly and easily biodegradable organic carbon fractions, DOC is widely measured amongst other biostability parameters such as AOC, BDOC, biomass and Biofilm Formation Rate (BFR)

(Hammes et al., 2010, Hubner et al., 2012; Schurer et al., 2022). Typically in SSFs, DOC is removed by a combination of biological (bacterial respiration and biomass assimilation) and physical- chemical processes (Haig, 2014; Lautenschlager et al., 2014; Velten et al., 2011). NH_4^+ is removed by assimilation and by nitrifying microorganisms that oxidize NH_4^+ to NO_2^- and subsequently NO_3^- (Tatari et al., 2013) or directly from NH_4^+ to NO_3^- (van Kessel et al., 2015). Since both DOC and NH_4^+ removal depend on microbial activity, it is important to examine how scraping influences recovery of the removal processes.

The knowledge of filter ripening is often limited due to the inability of current routine analyses to describe the recovery of microbial communities and purification processes in real or near-real time. After scraping, the effluent of full-scale SSFs is typically monitored for heterotrophic plate counts (HPC) and the absence of pathogen indicator organisms like *Escherichia coli*, total coliforms, enterococci and *Clostridium*. When SSFs are at the end of the treatment train and receive a low microbial load, pathogen indicators might not always be detected in the influent (van der Kooij et al., 2017). Earlier studies have emphasized the ability of rapid methods such as flow cytometry (FCM) for assessing prokaryote cell numbers and adenosine triphosphate (ATP) for detecting changes in cell numbers and active biomass in water treatment (Adomat et al., 2020; Chan et al., 2018; de Vera et al., (2019); Prest et al., 2013; Sousi et al., 2020). Chan et al. showed that abnormal changes in bacterial profiles of SSF effluent measured by FCM could indicate disturbances in the treatment process(Chan et al., 2018).

The objective of this study was to evaluate the recovery of microbial biomass and communities and the removal of DOC and NH_4^+ after scraping in a mature full-scale SSF. To this end, a scraped full-scale SSF was compared with an unscraped full-scale SSF and monitored throughout the ripening process. This is the first study examining depth profiles of operating full-scale SSFs for changes in ATP, cell counts, 16S ribosomal RNA (rRNA) gene copies, microbial community composition in water and on filter sand, and DOC and NH_4^+ in the water phase.

3.2 Materials and Methods

3.2.1 Description of SSFs

Two full-scale SSFs at a drinking water treatment plant in Scheveningen (The Netherlands) of drinking water company Dunea were investigated in this study. The plant receives raw water from the river Meuse and is further treated by managed aquifer recharge in the dunes, pellet softening, aeration, rapid sand filtration with powdered activated carbon dosing and slow sand filtration before distribution. Both SSFs, located in the same production line, were built in 1955 and have been producing drinking water for the last 28 years without sand replacement. The operational parameters and influent water characteristics of both filters are shown in Table 1. The SSFs become clogged every few years due to excessive biofilm accumulation in the *Schmutzdecke* layer and, consequently, filters are scraped every few

years to remove the clogged top layer of the filter. One of the filters in this study (Scraped filter) was scraped after 5.3 years of continuous operation by removing the top 10 cm of the sand bed, while the second filter (Control filter), which was last scraped 4.6 years ago, was used as a control.

3.2.2 Sand Sampling

On day 0, the supernatant water was lowered below the filter bed to allow for sand scraping in the scraped filter. Just before scraping, a sand core was sampled from the scraped filter by using a sterile aluminium sediment sampler. The sand core was divided into different sections (0-2 cm, 0-5cm, 10-15 cm, and 20-25 cm) and collected into 15 ml sterile falcon tubes. The selected filter depths represent the *Schmutzdecke* (0-2 cm), top (0-5 cm) and middle (10-15 and 20-25 cm) layers of the sand bed. The sand sampling depth was restricted to 25 cm to prevent sampling disturbances in the deep sand bed, which could negatively affect the quality of the produced drinking water. Hence, the sand sampling is not representative of the overall filter bed performance but gives a good indication of what happens in the first 25 cm of the sand bed.

After restarting the filter, only the top 0-2 cm sand layer was sampled using a telescopic sampler from scraped and control SSFs on the same day and around the same time. Sand from the surface layer was sampled on days 1, 8, 15, 28, 36, 52, 80, 100, and 120 after scraping, to better understand biomass recovery during operation (Fig. 1A). The sand collected on days 0, 8, 15, 28 and 52 was used for microbial community composition analysis. Two replicate samples were collected from the sampling point and transported to the laboratory in Styrofoam boxes containing icepacks. The first replicate samples were stored at −20°C on the same day for DNA extraction. Other replicate samples were stored at 4°C and used for cellular ATP (cATP) and cell count measurements on the same day.

Table 1 Operational parameters, influent and effluent characteristics of scraped and control full-scale SSFs. Historical data refer to average and standard deviation of the biweekly concentrations between June 2020 and August 2022.

	Unit	Scraped filter	Control filter
Filter bed height	m	0.95	0.8
Height of supernatant	m	1	1
Filter area	m^2	2383	2359
Filtration rate	m/h	0.4	0.4
Grain size	mm	0.3-0.6	0.3-0.6
Age of media	years	28	28
Time since last scraping	years	5.3	4.6

Historical data		Influent	Effluent	
Temperature	ºC	14.2 ± 2.68	14.5 ± 2.68	14.3 ± 2.68
ATP	pg/ml	6.24 ± 0.08	1.5 ± 0.08	1.41± 0.07
ICC	cells/ml	2.66 x 105 ± 0.03	1.66 x 10^5 ± 0.03	1.70 x 10^5 ± 0.03
TCC	cells/ml	4.70 x 105 ± 0.04	2.70 x 10^5 ± 0.04	2.59 x 10^5 ± 0.03
AOC	µg C/L	5.45 ± 0.04	3.7 ± 0.04	3.8 ± 0.05
DOC	mg C/L	3.65 ± 0.02	2.65 ± 0.02	2.7 ± 0.03
NO_3^-	mg N/L	0.98 ± 0.01	1.20 ± 0.01	1.25 ± 0.02
NH_4^+	mg N/L	0.009	0.006	0.006
NO_2^-	mg N/L	0.001	0.001	0.001
Turbidity	NTU	2.11 ± 0.01	1.36 ± 0.01	1.39 ± 0.01
Coliforms	CFU/L	0 ± 2	0	0
Escherichia coli	CFU/L	0 ± 1	0	0
Sulfite-reducing clostridia	CFU/L	0 ± 1	0	0

CFU- Colony Forming Unit

3.2.3 Water sampling

The water used to measure the chemical and microbial biomass parameters was sampled from both filters at influent, effluent and at four different depths (15, 25, 35 and 55 cm) (Fig. 1B). The water was collected using sampling ports provided on the filter wall with 30 cm long pipes penetrating the sand bed. The first water sampling over the height was conducted one day before scraping, (i.e., day -1) as the filter had to be drained completely on day 0 for the scraping. Thereafter, water was sampled on days 8, 15, 28 and 37 after scraping (Fig. 1A).

The water used for the microbial community analysis was sampled from the influent and effluent points of the scraped filter. The water was collected in duplicates of 1 L using sterile plastic bottles (Identipack, the Netherlands) 6 days before and 15 days after scraping. The samples were transported to the laboratory in Styrofoam boxes containing icepacks and were filtered with 0.2 µm filter (Isopore TM PC membrane, 47 mm hydrophilic, Merck, Millipore) within 24 h from sampling to collect microorganisms. The filters were stored at −20°C until DNA extraction.

3.2.4 Water analyses

Microbial cATP, which is indicative of the active biomass, was measured using Quench- Gone aqueous test kit and a LB9509 luminometer (Aqua Tools, France) as per the manufacturer's protocol. Flow-cytometry analysis was carried out with BD AccuriC6® FCM (BD Biosciences, Belgium) at Het Waterlaboratorium (Haarlem, the Netherlands). Sample volumes of 260 µL were drawn at a flow rate of 200–400 mL/min and mixed with fluorescent stain (SYBR®Green, propidium iodide). After incubation (10 min, 37°C), samples were analysed (FL1 channel at 525 nm, FL3 channel at 721 nm) using fixed gates to separate cells and background signals and additionally to distinguish between so-called high nucleic acid (HNA) and low nucleic acid (LNA) content cells. Here on, cATP and ICC measured in water will be referred to as $cATP_w$ and ICC_w.

DOC (Limit of Detection [LOD]=0.1 mg/L) was measured with a Shimadzu TOC- VCPH/CPN analyser with a standard deviation of 0.1 mg/L immediately or within one day after sampling. 30 mL of sample was filtered through 0.45 µm filters (SPARTAN™, Whatman, Germany) that had been flushed twice with demineralized water. Samples for NH_4^+ (LOD=0.01 mg/L) and NO_3^- (LOD=0.1 mg/L) were immediately filtered through a 0.22 µm nanopore filter and measured within 12 h using Ion Chromatography (Dionex ICS-2100, Thermo, USA) equipped with an AS17-Column with a detection limit of 0.01 mg/L.

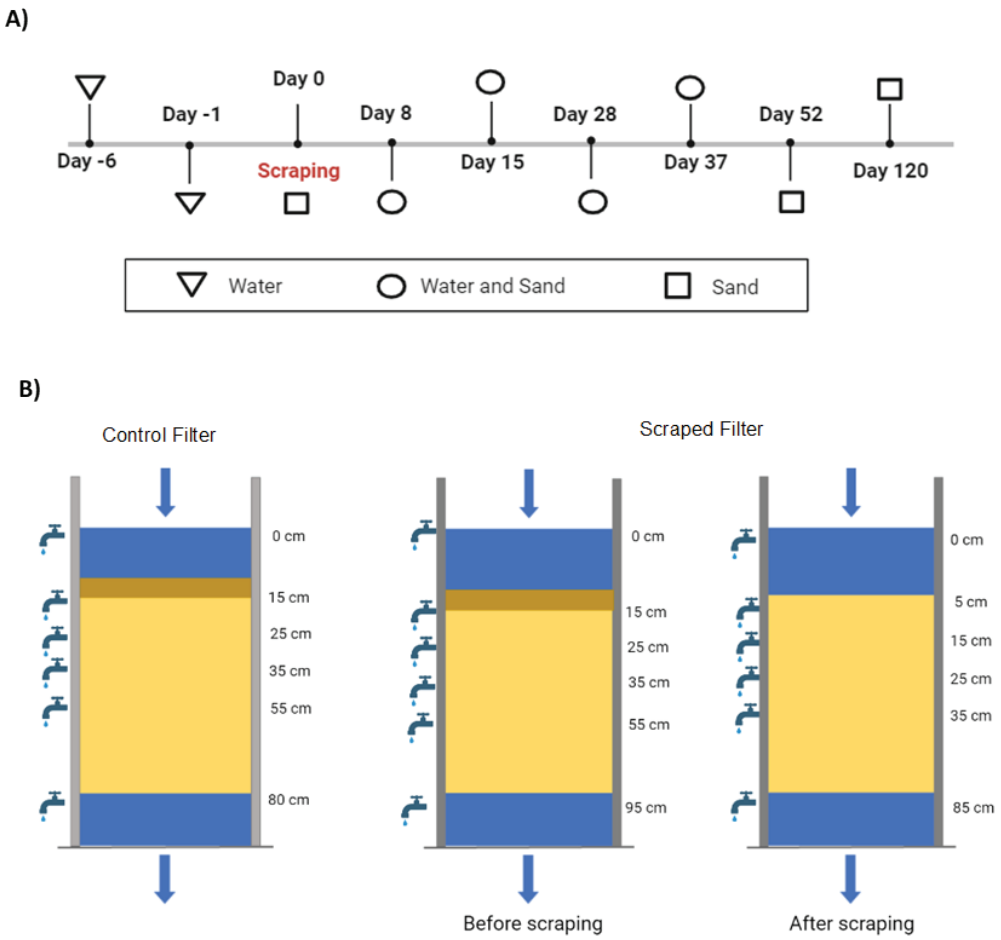

Figure 1 Overview of sand and water sampling in scraped and control SSFs, (B) Schematic diagram of the SSFs and sampling points

3.2.5 Sand analyses

cATP was measured on filter sand with 1 g of wet media sample, following the Deposit and Surface Analysis test kit method from LuminUltra Technologies. Measurements were read using a luminometer. ICC measurement was conducted at Het Waterlaboratorium (Haarlem, the Netherlands) following the protocol described by Liu et al. (2013). cATP and ICC measured on sand will be referred to as $cATP_s$ and ICC_s.

3.2.6 Molecular analysis

3.2.6.1 DNA isolation and library preparation

The DNA from water samples was extracted using the DNeasy PowerBiofilm Kit (QIAGEN, Hilden, Germany) according to the manufacturer's instruction except for the first step for which the thawed filters were placed directly into the PowerBeads tubes. The DNA from sand samples was isolated with the Powersoil Pro kit (QIAGEN, Hilden, Germany) using a range of 0.5-1 g of sand as starting material. The amount of sand used was noted for future reference and normalization. A negative control consisting of one empty PowerBead Pro Tube was included during DNA extraction for quality control. For both water and sand samples, the bead beating step was performed using the FastPrep-24 5G bead beating grinder and lysis system (MP Biomedicals, Irvine, United States), and by applying one cycle at 4.0 m/s for 45 s. After DNA extraction, DNA concentrations were measured fluorometrically (Qubit dsDNA BR assay, Invitrogen) and the DNA was stored at −20°C.

The hypervariable region V4 (~290 bp) of the bacterial and archaeal 16S rRNA gene was amplified from the extracted DNA with a PCR reaction prepared with 10 µL of 5X Phusion Green HF Buffer (Thermo Scientific, US), 1 µL of 10 µM barcoded primers 515F-n (5'- GTGYCAGCMGCCGCGGTAA-3') and 806R-n (5'- GGACTACNVGGGTWTCTAAT-3') (Apprill, McNally, Parsons, & Weber, 2015; Parada, Needham, & Fuhrman, 2016), 1 µL of 10 mM dNTPs mix (Promega Corporation, US), 0.5 µL of 2 U/µL Phusion Green Hot Start II HF DNA polymerase (Thermo Scientific, US), the DNA template (final concentration of ~20 ng/µL DNA) and Nuclease-free water to reach a final volume of 50 µL. Positive controls, non-template controls (only PCR mix) and negative controls (PCR mix and Nuclease-free water instead of the template DNA) were included in the PCR analyses for quality check. The amplification program included an initial step of 98°C for 30 s, then 28 cycles at 98°C for 10 s, followed by an annealing step at 50°C for 10 s and elongation step at 72°C for 10 s, and a final extension at 72°C for 7 min. The presence and length of PCR products were verified by gel electrophoresis. Subsequently, PCR products were purified using CleanPCR magnetic beads kit (CleanNA, Netherlands) according to the manufacturer's protocol. Purified products were quantified fluorometrically (Qubit dsDNA BR assay, Invitrogen) and quantified using the Qubit dsDNA BR Assay kit (Invitrogen by Thermo Fisher Scientific,

Eugene, OR, USA). The clean samples were pooled in equimolar amounts into libraries, including negative and positive controls. After pooling, the mixed libraries were purified and concentrated again using CleanPCR magnetic beads to a concentration final volume of 40 µL. The final purified PCR products including those amplified from SSFs samples, positive and negative controls were sequenced on an Illumina Novaseq 6000 platform at Novogene (Cambridge, United Kingdom). Raw 16S rRNA gene sequences with barcode and primer removed and supporting metadata were deposited in the European Nucleotide Archive (http://www.ebi.ac.uk/ena) under accession number PRJEB72542.

3.2.6.2 qPCR

Quantitative PCR (qPCR) was used to measure the copy numbers of the total bacterial 16S rRNA genes of the DNA from sand and water samples. The DNA concentrations were adjusted to 1 ng/µL by diluting original extracts in DNase/RNase free water before use as the template in qPCR. The qPCR mix was composed of iQTM SYBR Green Supermix (Bio-Rad Laboratories, USA), universal primers targeting the 16S rRNA gene (1369F 5'- CGGTGAATACGTTCYCGG-3' and 1492R 5'-GGWTACCTTGTTACGACTT-3'; 123 bp), 1 µL of DNA template and sterile nuclease-free water in a total volume of 10 µL. Each sample was assayed in technical triplicates by using a C1000 Thermal Cycler (CFX384 Real-Time system, Bio-Rad Laboratories, USA) with the following protocol: 95°C for 10 min followed by 40 cycles of 95°C for 15s, 60°C for 30 s and 72°C for 15s each; then one cycle of 95°C for 1 min; and a stepwise increase of temperature from 60°C to 95°C (at 0.5°C per 5s) to obtain melt curve data. The qPCR data was analysed using CFX Maestro 2.3 (Bio-Rad) and Microsoft Excel (version 2021).

3.2.6.3 Bioinformatic analysis of 16S rRNA gene sequence data

NG-Tax 2.0 was used for processing of 16S rRNA gene sequence data with default settings (Poncheewin et al., 2020; Ramiro-Garcia et al., 2016). Subsequently, amplicon sequence variants (ASVs) were identified on a per sample basis. Taxonomic assignment of ASVs was performed referring to the SILVA 138.1 database (Quast et al., 2013). All bioinformatic analyses were conducted in R (version 4.2.1) using the packages *phyloseq* (v 1.42.0) (McMurdie & Holmes, 2013), *microViz* (v 0.11.0) (Barnett, 2021), *ggplot2* (v 3.4.3), *ggsignif* (v 0.6.4) (Ahlmann-Eltze & Patil, 2021), *dplyr* (v 1.1.3), *speedyseq* (v 0.5.3.9018) (McLaren, 2023), *RColorBrewer* (v 1.1.3) (Neuwirth, 2022) and *vegan* (v 2.6.4) (Oksanen et al., 2014).

3.2.7 Statistical analysis

Statistical analysis was performed on all quantitative data (cATP, cell counts, DOC, NH_4^+ and 16S rRNA gene copies) using one-way ANOVA, followed by the Bonferroni post-hoc correction.

3.3 Results

3.3.1 Microbial biomass and activity

Total bacterial 16S rRNA gene copies (via qPCR), $cATP_s$ and ICC_s were used as complementary indicators to measure the total biomass in sand and water. While qPCR accounts for both dead and viable cells, $cATP_s$ indicates active biomass and ICC_s cells with an intact membrane.

Before scraping, the top 0-2 cm sand layer in the scraped filter showed the highest 16S rRNA gene copy numbers compared to its deeper sections (Fig. 2A). During scraping, the top 10 cm of the sand bed was removed from the filter. Eight days after scarping, the bacterial biomass on the top layer of sand was significantly lower as compared to the filter before scraping and the control filter (Fig. 2B, C and S2) (qPCR, $cATP_s$ and ICC_s $p=0.004$). The 16S rRNA gene copies and $cATP_s$ in the top layer sand (0-2 cm) decreased by 13 and 6 times, respectively. However, the biomass concentrations in the top layer of scraped filter gradually increased over time as filtration progressed, approaching the level prior to scraping. In comparison, the top layer of the control filter maintained stable biomass throughout the experimental period (qPCR, $cATP_s$ and ICC_s $p=0.09$) (Fig. 2B and C).

Microbial biomass in water along the filter height was assessed using $cATP_w$ and ICC_w (Fig. 3). One day before scraping, both filters showed a decrease in $cATP_w$ and ICC_w with depth. After scraping, $cATP_w$ and ICC_w were significantly higher within the top 25 cm of the scraped filter on days 8 and 15, in contrast to the control filter ($p=0.0002$). At 5 cm depth, the concentrations of HNA and LNA cells within the ICC and cATP increased significantly ($p=0.006$) by 68%, 14% and 50%, respectively compared to the influent (0 cm). Despite this breakthrough of biomass in the top layers, the effluent ATP and ICC concentrations remained stable throughout (Fig. S3). From day 28, the disturbed depth profile of the biomass parameters in the scraped filter began shifting towards the concentrations obtained before scraping and in the control SSF, suggesting complete restoration by day 37. In the scraped filter, bacterial biomass in the effluent water, measured with qPCR, was significantly lower than in the influent water both before and 15 days after scraping (qPCR $p=0.004$) (Fig. 2D).

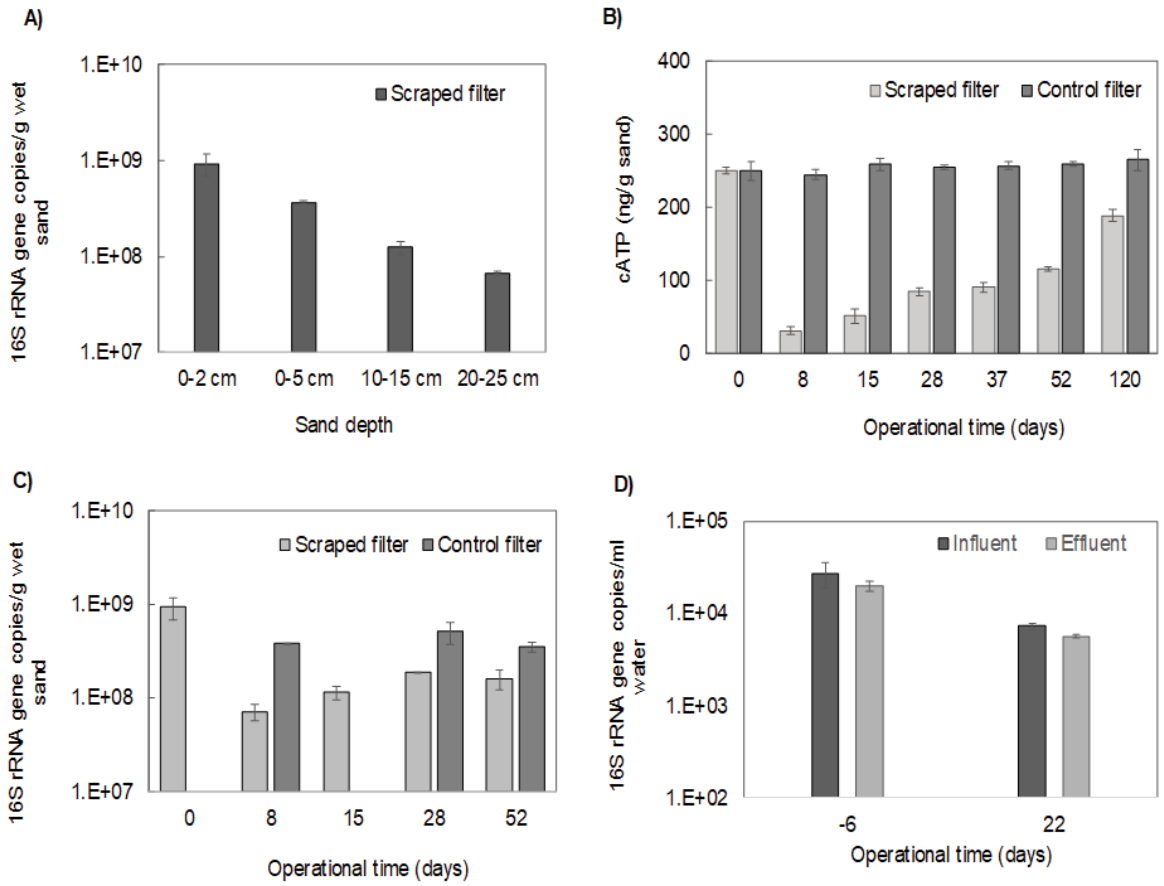

Figure 2 Microbial biomass in sand samples. A) Total bacterial 16S rRNA gene copies in sand at different depths of scraped filter before scraping, B) cATPs in the top sand layer (0-2cm) of control and scraped filter during operation, C) Total bacterial 16S rRNA gene copies in the top layer (0-2cm) of control and scraped filter, D) Total bacterial 16S rRNA gene copies in water influent and effluent of the scraped filter 6 days before and 15 days after scraping. The measurements

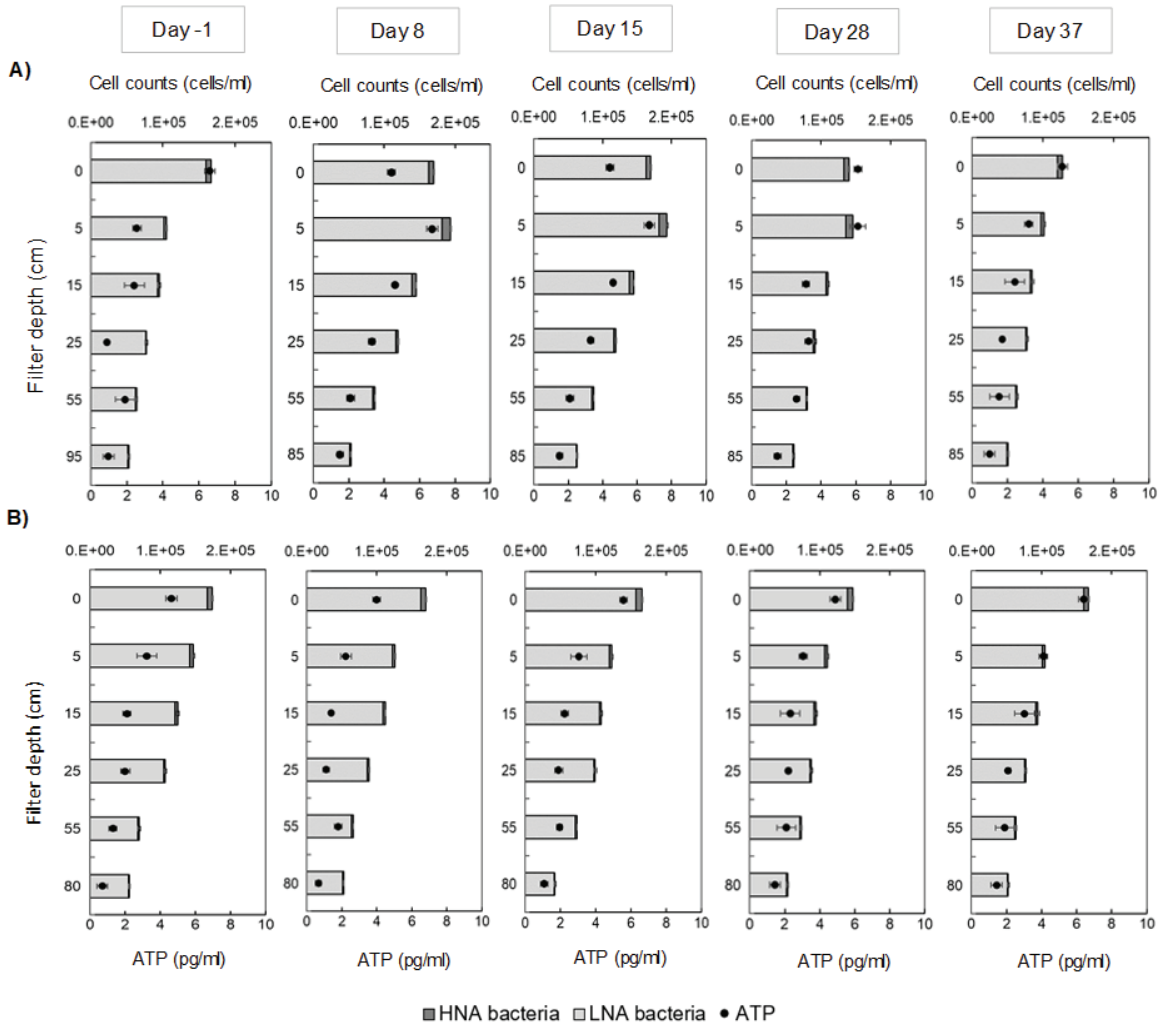

Figure 3 Depth profiles of cATPw, HNA and LNA cells within ICCw in water in scraped (A) and control (B) filters during filter operation. Measurements were carried out in triplicates; error bars represent standard deviation.

3.3.2 Microbial community composition

The microbial communities of the influent and effluent water and sand were dominated by different taxa (Table S1). The families *Methylomonadaceae* (11.9%), *Comamonadaceae* (5.9 %), *Gallionellaceae* (5.8%) and *Methylopilaceae* (4.7%) were only abundant in the influent, whereas an unclassified family within the order PLTA-13 (16.6%), *Gemmataceae* (7.6%), *Pirellulaceae* (4.8%), A4b (2.5%) and *Entotheonellaceae* (2.1%) were mainly present in the sand samples. Finally, *Omnitrophaceae* (9.2%), as well as unclassified families within the order *Rokubacteriales* (6.4%) and the class *Thermodesulfovibrionia* (5.8%) were only dominant in the water influent and, thus, did not reflect the microbial community of the sand.

3.3.2.1 Sand

The top 2 cm of the scraped filter before scraping (day 0) and the control filter had similar dominant taxa (Table S1). The PCoA plot of the beta-diversity analysis (Fig. 4) also indicated that these two filters had a similar community since both samples were almost identical on the first axis of the PCoA plot which explained 76% of the data variance. After scraping, the sand microbial community composition of the scraped filter shifted to the left side of the plot already at day 8, indicating a notable impact of scraping on the community composition in the top layer. However, after scraping the community in the top 2 cm resembled the composition in the deeper layers (10-15 and 20-25 cm) in the filter before scraping (Fig. 6). This shift can be attributed to the fact that approximately 10 cm of sand is manually removed during the scraping process, making the 10 cm depth of the pre-scraped filter the new surface (0 -2 cm) in the filter after scraping.

Scraping changed the relative abundance of some of the dominant taxa in the top layer of the SSF, with mainly an increase in an unclassified family within the order PLTA13, whereas *Gemmataceae* and A4b decreased. Despite these shifts, the main taxa like PLTA13, *Nitrospiraceae*, *Gemmataceae*, *Vicinamibacteriales*, *Pirellulaceae*, *Vicinamibacteriaceae*, *Nitrosomonadaceae*, *Nitrosopumilaceae*, A4b and *Hyphomicrobiaceae* remained prevalent both before and after scraping (Table 2 and Fig. 5). However, a substantial decrease in the overall biomass load occurred in the top layer as shown in Fig. 2B, demonstrating that although the relative abundance for most taxa remained similar, the absolute abundance of these taxa decreased due to scraping.

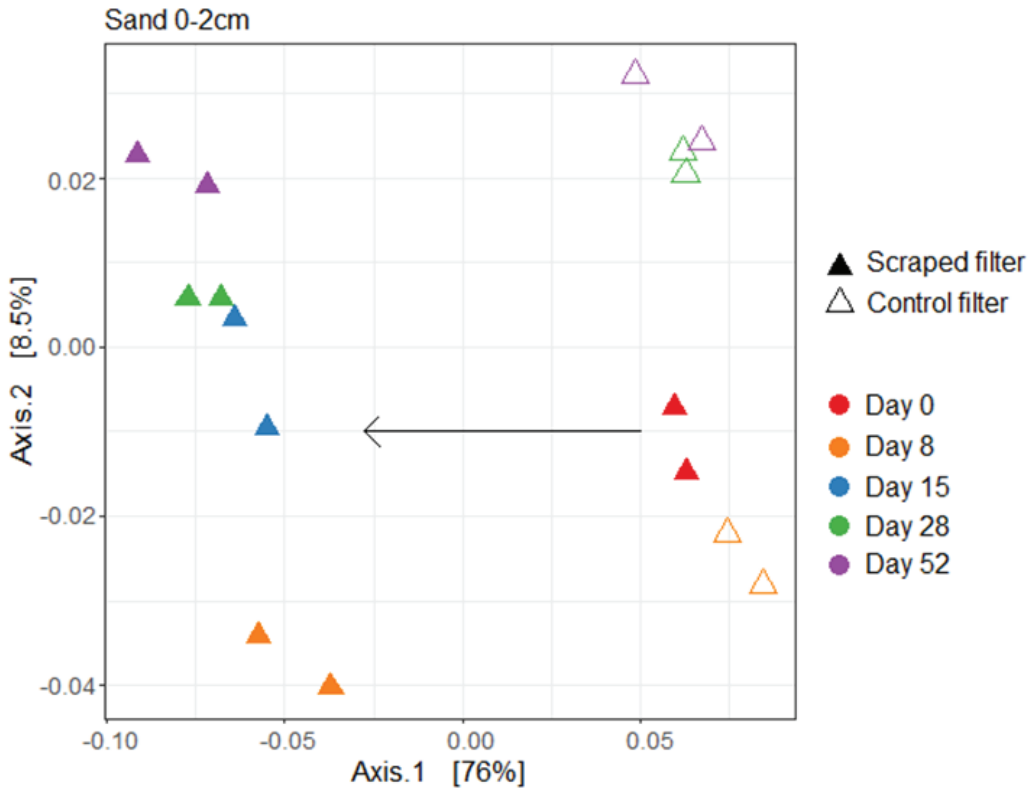

Figure 4 PCoA plot showing the temporal variation in Beta Diversity (Weighted UniFrac) analysis of sand samples (0-2 cm) collected from scraped and unscraped.

3.3.2.2 Water

The microbial community composition of the effluent water before (day -6) and 15 days after scraping was comparable, and both were distinctly different from the community in the influent water (Fig. 5 and Fig. 6). This observation was further supported by the results of the PERMANOVA test, indicating a significant difference between sampling points (influent and effluent) (p=0.031). Additionally, there was no significant difference in microbial community composition when considering the sampling day (p=0.655).

Table 2 Heatmap of the dominant 35 taxa at family level that are present in the sand 0-2 cm of scraped and control filters. For family-level taxa that are only classified at higher taxonomic level (order, class, phylum), those are indicated.

	RELATIVE ABUNDANCE							
	Scraped filter					Control filter		
	Day 0	Day 8	Day 15	Day 28	Day 52	Day 8	Day 28	Day 52
PLTA13--Order	4.9	17.1	19.5	19.6	24.7	4.4	6.4	6.9
Nitrospira	12.6	6.1	11.0	11.5	9.6	5.3	9.4	10.7
Gemmataceae--Family	12.0	6.8	5.9	6.1	2.4	11.5	10.2	10.2
Vicinamibacterales--Order	4.3	5.0	3.6	3.7	3.1	6.8	5.0	5.6
Vicinamibacteraceae--Family	2.7	3.6	2.2	2.6	3.2	5.3	4.0	5.2
A4b--Family	7.0	1.7	0.8	0.9	0.9	5.8	4.2	4.4
Pirellulaceae--Family	1.4	3.0	2.9	2.5	2.0	1.5	2.0	0.9
BD2-11_terrestrial_group--Class	1.5	1.5	1.9	2.2	2.0	1.0	2.3	2.0
TRA3-20--Family	1.8	2.5	1.8	2.0	3.0	1.5	0.8	0.9
Nitrosopumilaceae--Family	0.2	2.7	2.6	4.6	3.2	0.1	0.1	0.2
Blastocatellaceae--Family	2.0	0.8	0.5	0.7	1.2	1.6	1.6	4.0
Latescibacterota--Phylum	0.7	0.6	1.3	1.5	2.3	1.4	2.7	2.0
Subgroup_17--Order	1.1	1.6	1.7	1.8	2.6	0.8	1.3	1.5
RCP2-54--Phylum	2.3	2.3	1.4	1.7	1.5	1.9	0.7	0.6
SWB02	1.3	1.0	1.0	1.3	1.0	2.6	2.2	2.0
OM190--Class	1.6	0.7	1.7	2.0	2.0	0.7	2.0	1.3
MND1	0.9	1.1	1.4	1.7	2.6	0.5	1.6	2.1
RBG-13-54-9--Order	0.7	0.7	2.0	2.4	2.4	0.3	1.3	1.9
Comamonadaceae--Family	1.3	0.3	0.7	0.9	1.2	1.1	1.9	3.4
Gaiellales--Order	0.6	1.9	2.0	1.7	1.2	1.0	1.2	0.8
Pedomicrobium	1.4	0.7	0.7	0.6	0.9	2.6	1.7	1.8
Entotheonellaceae--Family	1.7	2.1	0.7	0.8	0.7	1.3	1.4	1.4
NB1-j--Phylum	1.5	1.6	1.8	1.6	1.3	0.4	0.3	0.2
Anaerolineaceae--Family	1.1	0.1	0.0	0.0	0.0	1.9	3.4	2.2
Subgroup_9--Order	1.1	2.1	1.8	1.2	1.0	0.4	0.4	0.1
MB-A2-108--Class	0.7	1.5	1.6	1.3	0.7	0.9	1.0	0.4
B1-7BS--Family	1.3	0.9	0.4	0.5	0.5	1.9	1.2	1.1
Gemmata	0.8	0.8	0.9	0.8	0.6	1.5	1.1	1.2
Pirellula	0.9	1.3	0.9	0.8	0.9	1.1	0.8	0.9
Pir4_lineage	0.7	1.1	1.1	0.9	0.9	0.9	0.9	0.8
mle1-7	0.6	0.9	1.3	1.3	1.8	0.2	0.6	0.6
S085--Order	0.5	0.4	0.7	0.4	0.6	1.1	2.1	1.5
Planctomycetales--Order	1.2	0.6	0.4	0.5	0.5	0.7	1.1	1.6
IS-44	0.7	0.6	0.9	0.7	1.2	0.6	0.8	1.2
Rhizobiales_Incertae_Sedis--Family	1.0	0.9	0.6	0.5	0.5	1.3	0.7	0.6

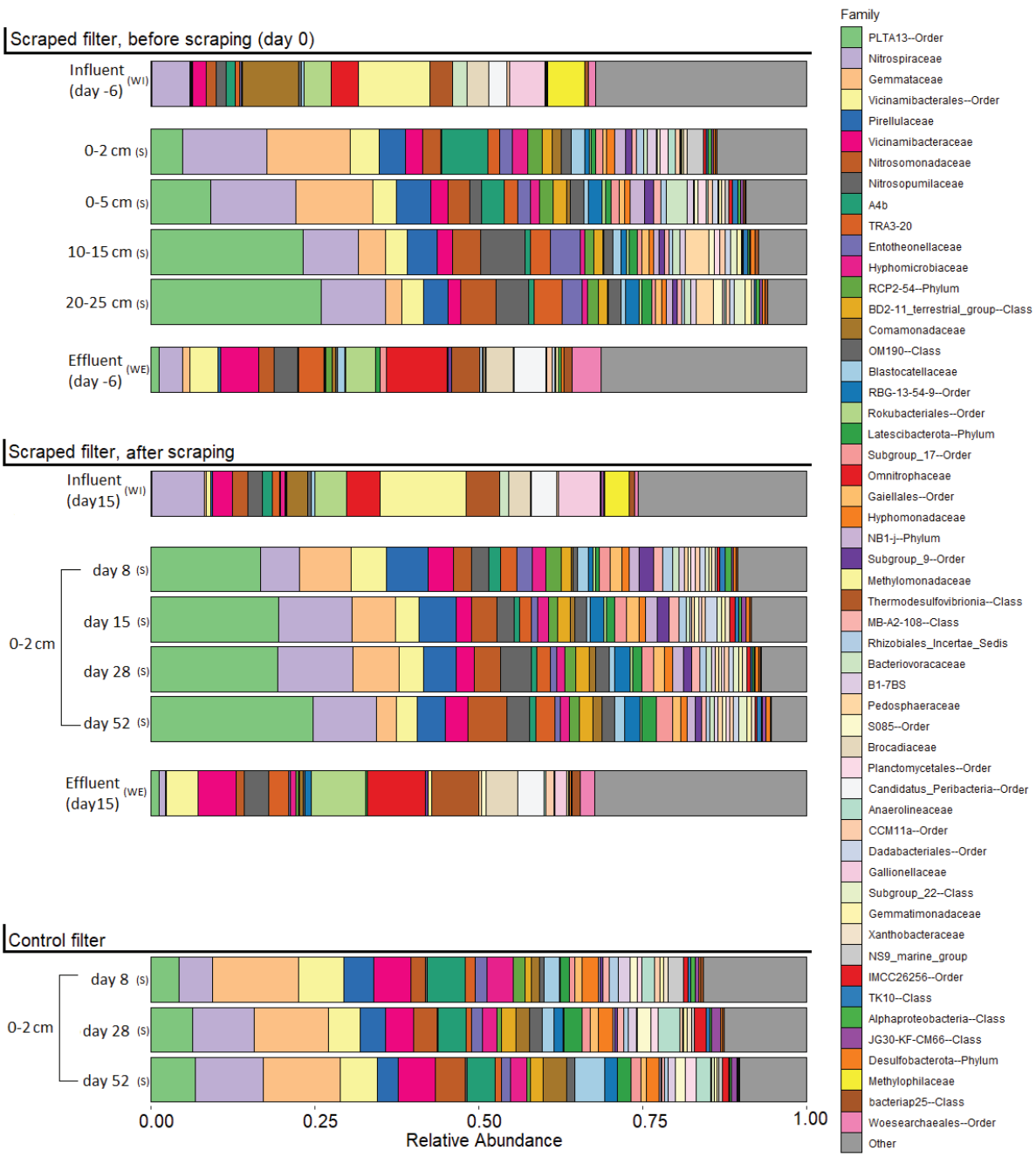

Figure 5 Microbial community composition bar plot of sand in scraped and control filters at different depths (scraped filter) and at different time points. Relative abundance of the top 53 taxa at family level is shown as the average of two duplicate biological replicates. For taxa at the family-level that are classified only at higher taxonomic levels (order, class, phylum), these classifications are indicated.

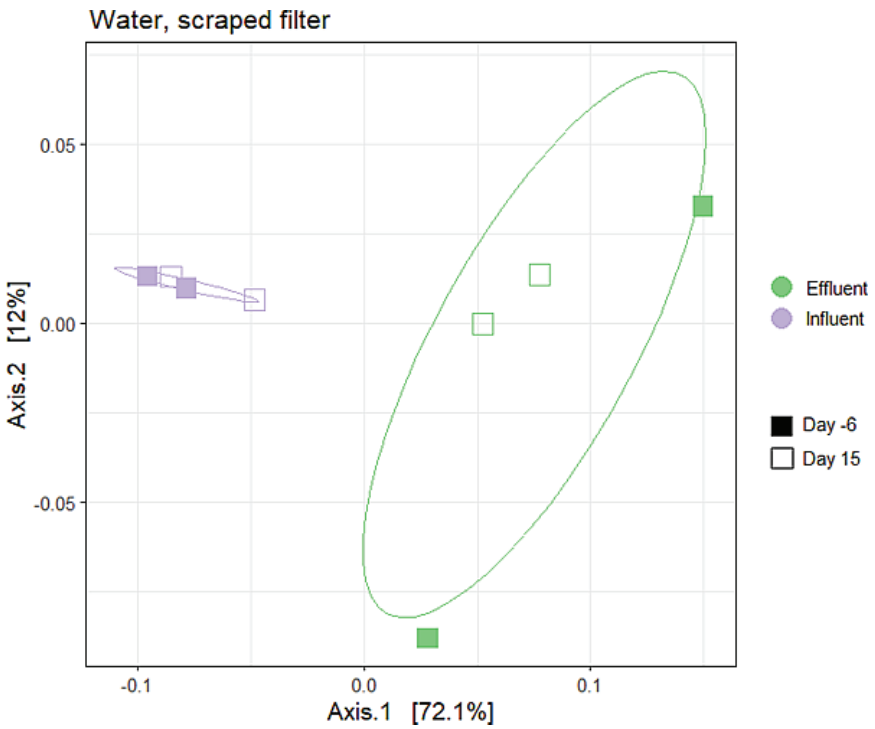

Figure 6 PCoA plot showing the Beta Diversity (Weighted UniFrac) analysis of water samples from the scraped filter before (day -6) and 15 days after scraping.

3.3.3 Concentrations of DOC, NH_4^+ and NO_3^-

The influent DOC concentration ranged from 2.4-3.7 mg/L during the monitoring period of 37 days (Fig. 7). On day -1, both filters reduced the DOC concentration by 0.6-0.7 mg/L, with most of the removal in the top 5 cm. After scraping, the depth profiles of DOC remained consistent with the concentrations measured before scraping or in the control SSF. Thus, no DOC release in the top layers was observed due to scraping, which contrasts with the ICC_W and $cATP_W$ data. A slight increase was noted in the middle layers, also seen in the control filter until day 28, suggesting the release was independent of scraping. However, this released DOC fraction was subsequently removed in the deeper layers. These observations suggest that DOC release in the deeper layers might be important to understand the overall DOC removal mechanisms.

NH_4^+ concentration in the influent was low and ranged from 5.8-8.1 µg N/L, while NO_3^- was between 1.41-1.61 mg N/L. The NH_4^+ concentration during the sampling period was close to the detection limit of 5 µg/L. NH_4^+ decreased in the first 55 cm and then stabilized. NO_3^- significantly increased in the deeper layers ($p=0.0005$) (Fig. 8). Both NH_4^+ and NO_3^- concentrations were not significantly different ($p=0.09$) between the scraped and control SSF. The depth profiles of NH_4^+ and NO_3^-, thus, remained stable after scraping, indicating that NH_4^+ removal was not controlled by the top layer biofilms alone.

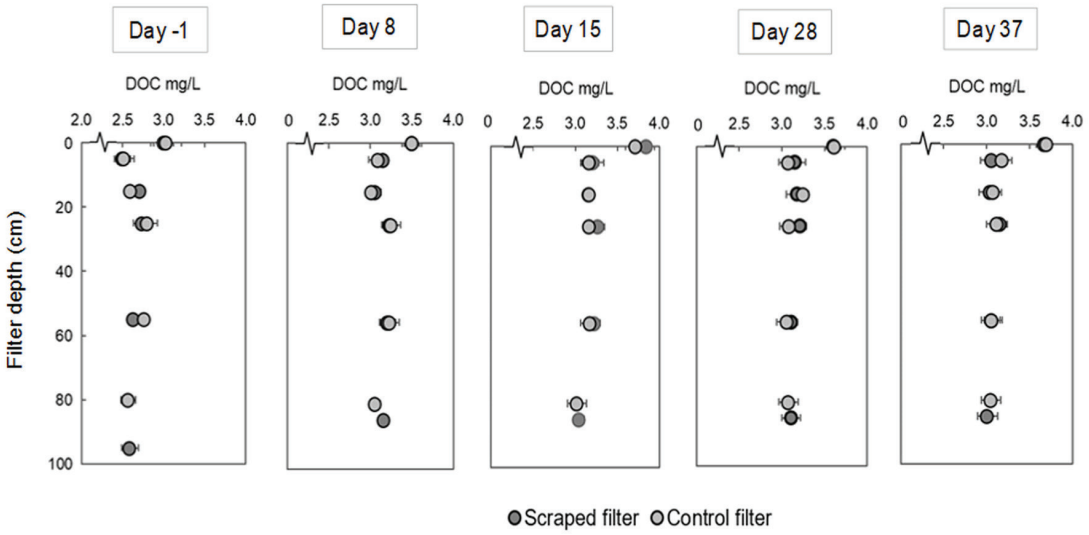

Figure 7 Depth profiles of DOC in scraped and control filters during filter operation. Measurements were carried out in triplicates; error bars represent standard deviation

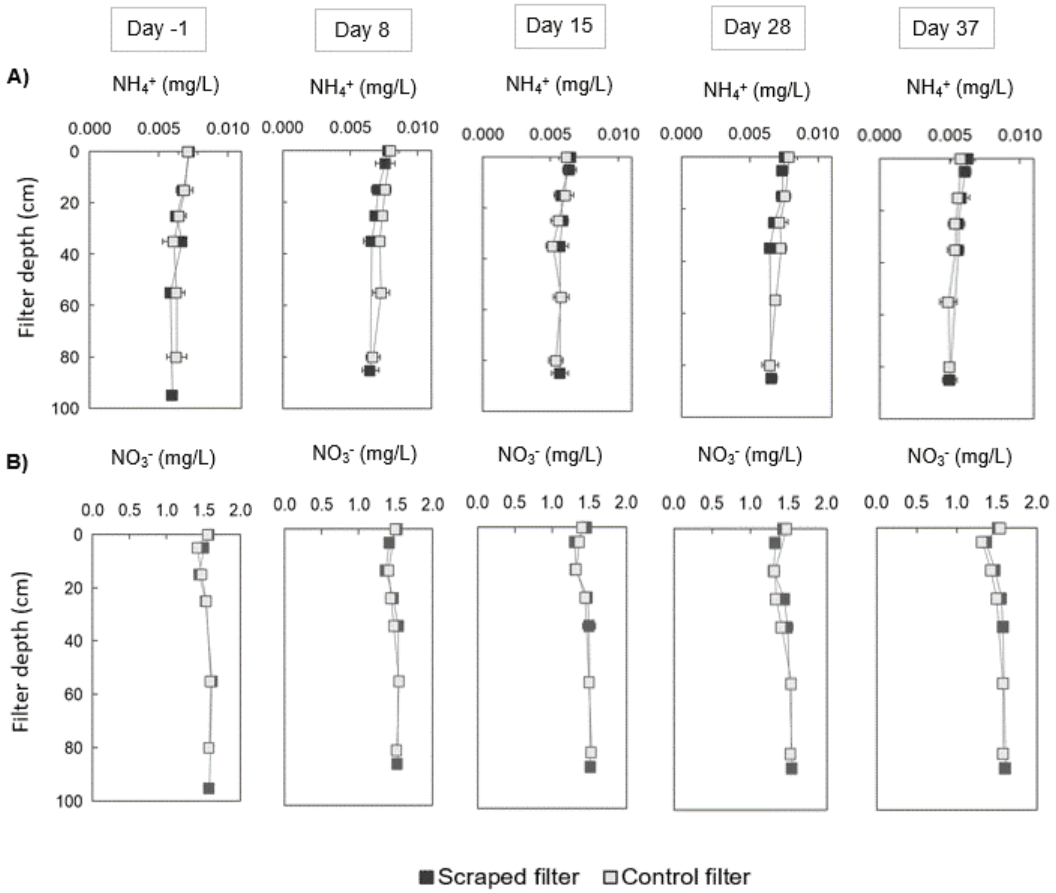

Figure 8 Depth profiles of NH_4^+ (A) and NO_3^- (B) in scraped and control filters during filter operation. Measurements were carried out in triplicates; error bars represent standard deviation

3.4 Discussion

3.4.1 Filter recovery after scraping

This research examined operating scraped and unscraped mature full-scale SSFs along the filter depth to examine the recovery processes after scraping. $cATP_w$, HNA-ICC_w and LNA-ICC_w in water from the top layers increased immediately after scraping. This deterioration of $cATP_w$ and ICC_w could be attributed to bacterial sloughing of the filter biofilm (Sousi et al., 2020) and/or reduced retention of microbial biomass in the water from top layers after the *Schmutzdecke* removal. Straining in the *Schmutzdecke* has been observed to be a key retention mechanism for bacteria (Hijnen et al., 2004; Hijnen et al., 2007; Trikannad et al., 2023). However, biomass released from the top layers after scraping was retained in the deeper layers. This highlights the role of physical-chemical and biological processes in the sand bed and the adaptability of mature filters to *Schmutzdecke* loss. In contrast, newer filters have been shown to be strongly impacted by scraping, resulting in poor removal of total organic carbon and bacterial indicators (Chan et al., 2018; Collins and Unger, 2006; Haig et al., 2011; Hijnen et al., 2004). This contrast may be due to differences in maturity of microbial communities across filters (Abkar et al., 2024). In newer filters without established biofilms in the sand bed, effluent quality is more dependent on the *Schmutzdecke* layer (Chan et al., 2018; Collins and Unger, 2006; Hijnen et al., 2004). Therefore, depth profiles must be monitored to assess disruption and/or recovery of microbial biomass after scraping.

In DWTPs where SSF is the final treatment step (van der Kooij et al., 2017), understanding the impact of scraping on disinfection is vital to ensure microbial safety of produced drinking water, necessitating the analysis of fecal indicators and pathogens in the effluent. Pathogen removal was not explored in this research, as these organisms were not detected in the influent. Previously, deeper layers of mature SSFs have shown substantial bacteria and virus removal capacity as the *Schmutzdecke* (Trikannad et al., 2024). Chan et al. reported no breakthrough of coliform and *E.coli* in the effluent after scraping of mature full-scale SSFs (Chan et al., 2018). However, future research should examine scraping effects on virus, bacteria and protozoa removal and explore how pathogen removal processes recover in new and mature full-scale SSFs.

Scraping reduced biomass in the top sand layers, as previously reported by De Souza et al. (2021). Yet, biomass redeveloped after scraping as expected due to high nutrient levels in the influent, compared to biomass concentration. The altered microbial community composition resembled that of the deeper layers. This change is not attributed to a shift in the community composition, but to scraping of top 10 cm of the sand bed, which exposed deeper layers to the surface. Despite a shift in the relative abundances of various microbial groups, certain dominant taxa such as PLTA13, *Nitrospiraceae*, *Gemmataceae*, *Vicinamibacteriales*, *Pirellulaceae*, *Vicinamibacteriaceae*, *Nitrosomonadaceae*, *Nitrosopumilaceae* and A4B

remained prevalent in the top layers even after scraping. A previous lab-scale investigation found depth stratification of bacterial community after scraping (De Souza et al., 2021). In the present study with mature full-scale SSFs, the dominant taxa were not confined to the *Schmutzdecke*, but extended beyond the top 10 to 15 cm. Although microbial biomass in the top layer was reduced after scraping, the relative abundance of the dominant groups remained unchanged. Therefore, the integration of relative and absolute abundances of microbial community using 16S rRNA gene amplicon sequencing, qPCR and ATP methods offers a comprehensive view of the dynamics of microbial abundance and diversity within the SSFs.

Despite disturbances from scraping, the microbial community composition in filter effluent before and after scraping was similar, indicating the system's resilience to short-term disruptions. Moreover, both before and after scraping, the effluent microbial community differed significantly from the influent ($p=0.031$) and its biomass content (measured with qPCR) was still lower than in the influent, proving the capability of SSFs to retain bacterial biomass within 15 days after scraping. These findings highlight the resilience and robustness of mature SSF microbial communities and the contribution of the deepest layers of the sand bed in maintaining the treatment efficiency after the removal of the top layer.

3.4.2 DOC and NH_4^+ removal processes

The SSFs consistently reduced DOC by 0.5 mg/L, with scraping showing no adverse effect on DOC levels at varying filter depths. However, the decrease in DOC was not solely due to the easily biodegradable organic carbon fractions. The influent and effluent data (Table 1) show that the influent AOC concentration of 5.4 µg C/L, already within the guideline value of 10 µg C/L for biostable water (Hijnen et al., 1992) decreased to 3.6 µg C/L in the effluent. This suggests that the removed DOC contained complex, recalcitrant organic carbon fractions, such as polysaccharides and humic substances, similar to previous findings (Lautenschlager et al., 2014; Campos et al., 2002). Since fractions like humics are difficult to degrade in SSFs, physical-chemical processes alongside microbial processes might have contributed to DOC removal (Haig et al., 2011). DOC release in the middle layers has been reported previously in biological filtration systems, linked to biofilm proliferation and breakdown of particulate organic carbon into DOC (Bar-Zeev et al., 2012; Perujo et al., 2018). Furthermore, the concentration of released DOC may be reduced in the deeper layers by a combination of physical-chemical and microbial processes.

Heterotrophs play a crucial role in the carbon cycle by metabolizing BDOC. Various microbial groups including those with cultivated heterotrophic species such as *Gemmataceae*, and *Vicinamibacteraceae* (Kulichevskaya et al., 2017; Huber et al., 2018) dominated the microbial community across all filter depths (Fig. 5). This might indicate the potential ability of the SSF microbial community to degrade BDOC

and produce biologically stable drinking water throughout the filter depth. However, specific microorganisms within these dominant groups responsible for BDOC degradation are difficult to pinpoint due to the unclassified nature of many genera. Identifying these microbes is essential for a clearer understanding of the carbon cycle and for enhancing water treatment techniques. Yet, it's important to note that 16S rRNA gene amplicon sequencing, while useful, has its limitations in providing comprehensive functional insights due to its inability to fully capture microbial functionality. More advanced techniques such as metagenomics, metatranscriptomics and proteomics offer more detailed insight into the functional potential of the microbial community and could be used to determine microbial roles in decomposing organic substances. Furthermore, innovative approaches like bioorthogonal non-canonical amino acid tagging combined with fluorescence-activated cell sorting (BONCAT-FACS) (Couradeau et al., 2019; Hatzenpichler et al., 2016) and cultivation methods might help to identify microbes responsible for BDOC degradation. However, mimicking low BDOC levels in SSF influent poses significant analytical challenges.

NH_4^+ removal occurred over the filter depth, indicating the occurrence of nitrification. Nitrospiraceae (dominated by the genus *Nitrospira*), *Nitrosomonadaceae* and *Nitrosopumilaceae* families, capable of oxidizing ammonia and/or nitrite were observed in the filter sand (Daims et al., 2015; Jung et al., 2022). The dominance of *Nitrospira* indicates direct NH_4^+ oxidation to NO_3^- as members of this genus have been shown for their capacity to perform complete oxidation of ammonia, also referred to as comammox metabolism (Daims et al., 2015; Haukelidsaeter et al., 2023; van Kessel et al., 2015). *Nitrospiraceae*, *Nitrosomonadaceae* and *Nitrosopumilaceae* were not only present in the filter but also in the influent which might be a carryover from the preceding rapid sand filtration step where NH_4^+ is actively removed and continued to persist throughout the filter bed. *Nitrosopumilaceae* are known to thrive at lower ammonia concentrations compared to *Nitrospiraceae* and *Nitrosomonadacae* (Jung et al., 2022). Therefore, the increased relative abundance of *Nitrosopumilaceae* in deeper layers suggests NH_4^+ depletion from its removal in the top layers. The diversity of microbial communities enhances NH_4^+ removal, adapting to varying NH_4^+ concentrations and environmental conditions. Therefore, it is important to preserve microbial diversity in the filter to improve water treatment effectiveness.

3.4.3 Implications for practice

SSFs in this study received pre-treated influent from managed aquifer recharge (infiltration of pretreated river water in the dunes and subsequent abstraction) and rapid sand filtration. This has greatly reduced microbial and organic load and thereby the extent of clogging in SSFs. Since deeper layers of full-scale SSF were unaltered during scraping for over 67 years, microbial communities and purification processes remained resilient in the sand bed. Thus, deeper layer biofilms should be retained in the filter by avoiding repetitive scraping. Backwashing may be used as an alternative to traditional

scraping to preserve biomass within the filter for quick recovery of full filter function.

Future research could examine removal of pathogens and biological stability indicators such as microbial growth potential and biofouling potential. This evaluation is important to clarify if mature SSFs, especially under low-loading conditions, require a ripening period or not. Whereas, in young filters without optimally performing biofilms in the deep sand bed, a ripening period might be necessary to recover filter performance. The ripening of these young filters may be accelerated by biostimulation with nutrients, inoculation with specific microbial communities or filter media from mature SSFs. It is essential to note that the hypotheses outlined here are starting points that require further experimental validation. They provide a basis for future research to rigorously test and confirm these initial observations.

This research showed that recovery of microbial activity and ecology after scraping can be effectively monitored using rapid ATP and FCM, and 16S rRNA gene sequencing on influent, sand and effluent samples. Further, relying solely on effluent quality analyses is not sufficient to understand filter status, as deeper layers balance scraping effect. Therefore, depth profiles of previously mentioned microbial biomass parameters could be monitored to assess recovery and optimize SSF maintenance, thereby reducing costs and water loss.

3.5 Conclusions

This study compared the performance of scraped and unscraped mature full-scale SSFs to evaluate the recovery of microbial biomass and communities, and the removal of DOC and NH_4^+ after scraping. The main findings were:

- Scraping reduced microbial biomass on filter sand but did not alter the dominant prokaryotic taxa.
- ATP and flow cytometry analysis revealed temporary disruption in top layers after scraping when monitored over the height in mature SSFs.
- Stable effluent concentrations of DOC, NH_4^+, cATPw and ICCw and consistent microbial community composition throughout ripening showed that deeper layer biofilms offset any scraping effect.
- Further research on the effects of scraping on fecal pathogens removal and biological stability parameters (e.g., regrowth potential) in mature SSFs is recommended to assess the need for filter ripening.

3.6 Supplementary information

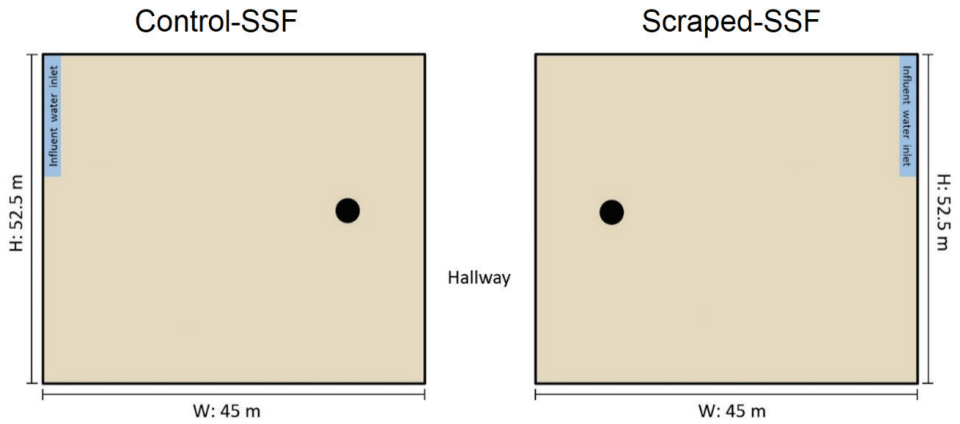

Figure S1. Planimetry on control and scraped SSFs with sand sampling point as a black dot

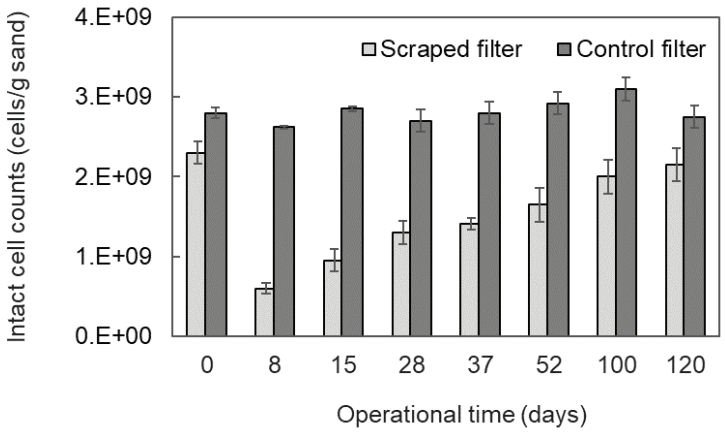

Figure S2 Intact cell counts in the top sand layer (0-2cm) of control and scraped filter during operation after scraping

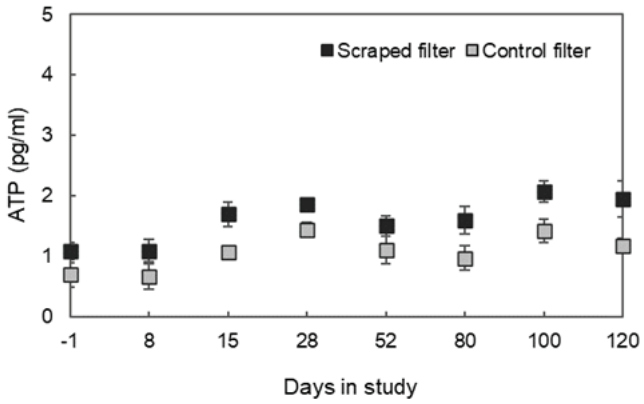

Figure S3 Effluent concentration of (A) $cATP_w$ and (B) ICC_w in scraped and control filters during the sampling period

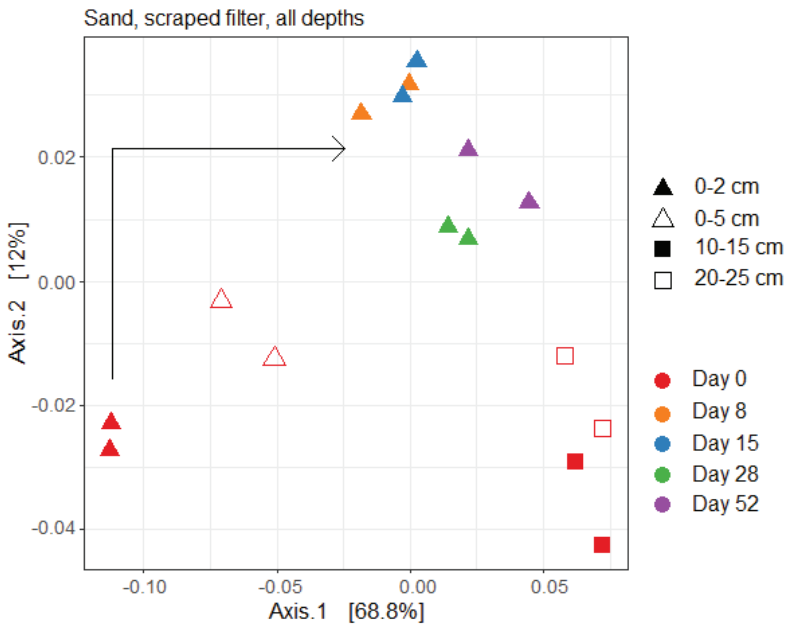

Fig S4 Temporal and spatial variation in Beta Diversity (Weighted UniFrac) analysis of sand samples from different depths collected from the scraped filter.

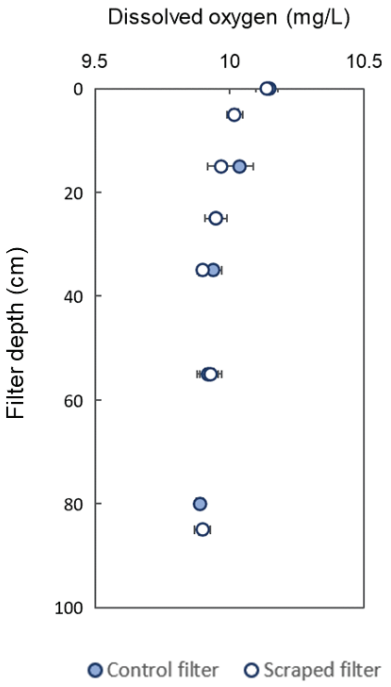

Figure S5 Depth profiles of dissolved oxygen (DO) in scraped and control filters

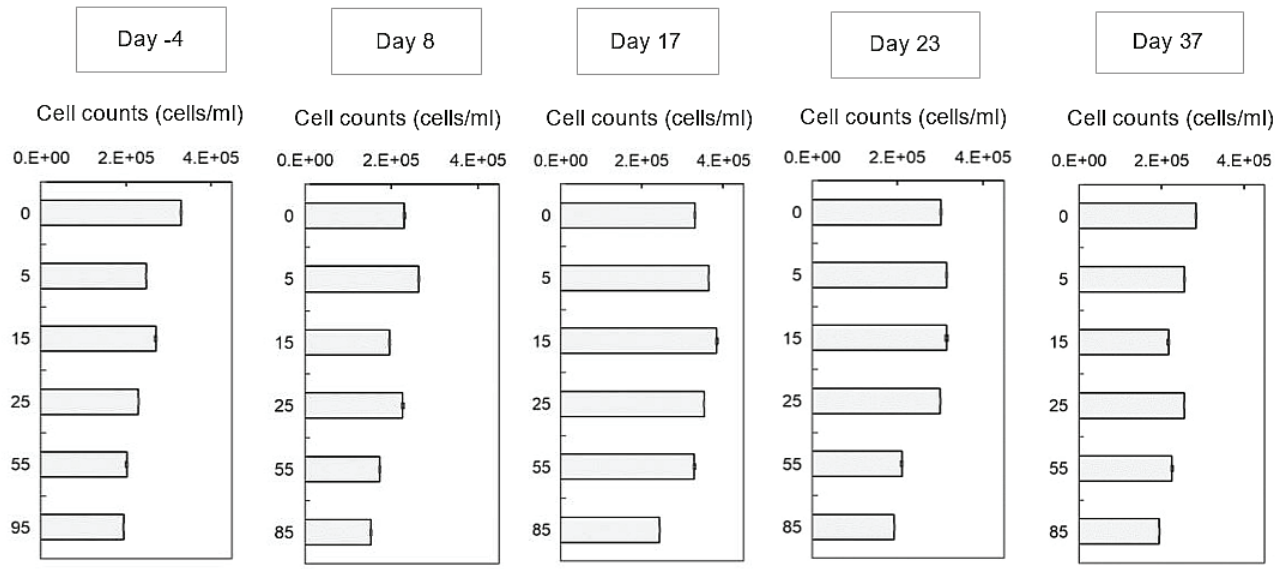

Figure S6 Depth profiles of total cell counts in scraped filter during the sampling period

Table S1 Taxa at family level present at relative abundance > 1.5% for each sample type sand, water influent, and water effluent. Taxa that are present in all sample types are highlighted in green, whereas taxa that are present only in one specific sample type are shown highlighted in grey.

Water influent*	% relative abundance	Sand**	% relative abundance	Water effluent***	% relative abundance
Methylomonadaceae	11.9	PLTA13—Order	12.9	*Omnitrophaceae*	9.2
Nitrospiraceae (Nitrospira)	6.9	*Nitrospiraceae (Nitrospira)*	9.5	Rokubacteriales--Order	6.4
Comamonadaceae	5.9	*Gemmataceae*	9.1	Thermodesulfovibrionia--Class	5.8
Gallionellaceae	5.8	Vicinamibacterales—Order	4.6	*Vicinamibacteraceae*	5.8
Methylophilaceae	4.7	*Pirellulaceae*	4.6	Vicinamibacterales--Order	4.6
Omnitrophaceae	4.6	*Vicinamibacteraceae*	3.8	*Brocadiaceae*	4.5
Rokubacteriales--Order	4.4	*Nitrosomonadaceae*	3.7	Candidatus_Peribacteria--Order	4.4
Thermodesulfovibrionia--Class	4.3	A4b	3.2	*Nitrosopumilaceae*	3.7
Candidatus_Peribacteria--Order	3.3	*Hyphomicrobiaceae*	2.2	Rhodospirillales--Order	3.5
Brocadiaceae	3.3	*Blastocatellaceae*	1.9	TRA3-20	3.4
Vicinamibacteraceae	2.5	BD2-11_terrestrial_group--Class	1.8	Woesearchaeales--Order	3.4
env.OPS_17	2.1	TRA3-20	1.8	*Nitrospiraceae (Nitrospira)*	2.2
Crocinitomicaceae	2.0	*Nitrosopumilaceae*	1.8	SAR202_clade--Order	1.9
Nitrosomonadaceae	1.9	Latescibacterota--Phylum	1.5	*Nitrosomonadaceae*	1.7
Nitrosopumilaceae	1.9	Subgroup_17--Order	1.5	*Methylomirabilaceae*	1.7
Bacteriovoracaceae	1.8	RCP2-54--Phylum	1.5	Omnitrophales--Order	1.5
Methylomirabilaceae	1.7	*Hyphomonaaceae*	1.5		
Micavibrionales--Order	1.5	OM190--Class	1.5		
		Entotheonellaceae	1.5		

*Average of all WI samples day -6 and day 15, scraped filter
**Average of all sand samples from scraped and control filter, from all depths, overtime
***Average of all WE samples day -6 and day 15, scraped filter

*Table S2 (A-D). p-values from statistical tests on the qPCR data tested with one-way ANOVA with Bonferroni post-hoc correction. A) Comparison of sand samples from scraped filter at different depths, B and C) pairwise comparison of sand samples from 0-2 cm of scraped and control filter overtime, D) comparison between influent and effluent water samples on before and after scraping from the scraped filter. * indicate a p ≤ 0.05.*

A

Scraped filter (before scraping)	0-2 cm	0-5 cm	10-15 cm
0-5 cm	0.073	-	-
10-15 cm	0.020 *	0.789	-
20-25 cm	0.016 *	0.478	1.00

B

Scraped filter	Day 0	Day 8	Day 15	Day 28
Day 8	0.007 *	-	-	-
Day 15	0.011 *	1	-	-
Day 28	0.009 *	1	1	-
Day 52	0.005 *	1	1	1

C

Control filter	Day 8	Day 28
Day 28	0.62	-
Day 52	1	0.44

D

Scraped filter		
Influent vs effluent	Day -6	0.024*
	Day 15	0.015*

References

Abkar, L., Moghaddam, H. S., & Fowler, S. J. (2024). Microbial ecology of drinking water from source to tap. Science of The Total Environment, 908, 168077.

Adomat, Y., Orzechowski, G. H., Pelger, M., Haas, R., Bartak, R., Nagy-Kovacs, Z. A., ... & Grischek, T. (2020). New methods for microbiological monitoring at riverbank filtration sites. Water, 12(2), 584. Ahlmann-Eltze. C, I. Patil, ggsignif: R Package for Displaying Significance Brackets for'ggplot2, PsyArxiv (2021).

Apprill, S. McNally, R. Parsons, L. Weber, Minor revision to V4 region SSU rRNA 806R gene primer greatly increases detection of SAR11 bacterioplankton, Aqua, Microb. Ecol. 75 (2) (2015) 129–137.

Bai, X., Dinkla, I. J., & Muyzer, G. (2022). Microbial ecology of biofiltration used for producing safe drinking water. Applied Microbiology and Biotechnology, 106(13-16), 4813- 4829.

Bar-Zeev, E., Belkin, N., Liberman, B., Berman, T., & Berman-Frank, I. (2012). Rapid sand filtration pretreatment for SWRO: Microbial maturation dynamics and filtration efficiency of organic matter. Desalination, 286, 120-130.
Barnett. D. G, I.C. Arts, J. Penders, microViz: an R package for microbiome data visualization and statistics, J. of Open Sour. Softw. 6 (63) (2021) 3201.

Brandt, M. J., Johnson, K. M., Elphinston, A. J., & Ratnayaka, D. D. (2017). Specialized and advanced water treatment processes. Twort's water supply, 407-473 Campos, L. C., Su, M. F. J., Graham, N. J. D., & Smith, S. R. (2002). Biomass development in slow sand filters. Water research, 36(18), 4543-4551.

Chan, S., Pullerits, K., Riechelmann, J., Persson, K. M., Rådström, P., & Paul, C. J. (2018). Monitoring biofilm function in new and matured full-scale slow sand filters using flow cytometric histogram image comparison (CHIC). Water research, 138, 27-36.

Collins, M Robin; Unger, M. (2008). Assessing Escherichia coli removal in the *Schmutzdecke*. Journal of American Water Works Association, 100(12), 60–73.

Couradeau, E., Sasse, J., Goudeau, D., Nath, N., Hazen, T. C., Bowen, B. P., ... & Northen, T. R. (2019). Probing the active fraction of soil microbiomes using BONCAT-FACS. Nature communications, 10(1), 2770.

Daims, H., Lebedeva, E. V., Pjevac, P., Han, P., Herbold, C., Albertsen, M., & Wagner, M. (2015). Complete nitrification by Nitrospira bacteria. Nature, 528(7583), 504-509.

De Souza, F. H., Roecker, P. B., Silveira, D. D., Sens, M. L., & Campos, L. C. (2021). Influence of slow sand filter cleaning process type on filter media biomass: backwashing versus scraping. Water Research, 189, 116581.

de Vera, G. A., & Wert, E. C. (2019). Using discrete and online ATP measurements to evaluate regrowth potential following ozonation and (non) biological drinking water treatment. Water research, 154, 377-386.

Haig, S. J., Collins, G., Davies, R. L., Dorea, C. C., & Quince, C. (2011). Biological aspects of slow sand filtration: past, present and future. Water Science and Technology: Water Supply, 11(4), 468-472.

Haig, S. J., Quince, C., Davies, R. L., Dorea, C. C., & Collins, G. (2015). The relationship between microbial community evenness and function in slow sand filters. MBio, 6(5), e00729- 15.

Haig, S. J. (2014). Characterising the functional ecology of slow sand filters through environmental genomics (Doctoral dissertation, University of Glasgow)

Hammes, F., Berger, C., Köster, O., & Egli, T. (2010). Assessing biological stability of drinking water without disinfectant residuals in a full-scale water supply system. Journal of Water Supply: Research and Technology-AQUA, 59(1), 31-40.

Hatzenpichler, R., Connon, S. A., Goudeau, D., Malmstrom, R. R., Woyke, T., & Orphan, V. J. (2016). Visualizing in situ translational activity for identifying and sorting slow-growing archaeal– bacterial consortia. Proceedings of the National Academy of Sciences, 113(28), E4069-E4078.

Haukelidsaeter, S., Boersma, A. S., Kirwan, L., Corbetta, A., Gorres, I. D., Lenstra, W. K., ... & Slomp, C. P. (2023). Influence of filter age on Fe, Mn and NH4+ removal in dual media rapid sand filters used for drinking water production. Water Research, 120184.

Hijnen, W. A., Schijven, J. F., Bonne, P., Visser, A., & Medema, G. J. (2004). Elimination of viruses, bacteria and protozoan oocysts by slow sand filtration. Water Science and Technology, 50 (1), 147-154.

Hijnen, W. A., Dullemont, Y. J., Schijven, J. F., Hanzens-Brouwer, A. J., Rosielle, M., & Medema, G. (2007). Removal and fate of Cryptosporidium parvum, Clostridium perfringens and small-sized centric diatoms (Stephanodiscus hantzschii) in slow sand filters. Water research, 41(10), 2151-2162.

Hijnen, W. A., & Van Der Kooij, D. (1992). AOC removal and accumulation of bacteria in experimental

sand filters. Revue des sciences de l'eau, 5, 17-32.

Hübner, U., Miehe, U., & Jekel, M. (2012). Optimized removal of dissolved organic carbon and trace organic contaminants during combined ozonation and artificial groundwater recharge. Water research, 46(18), 6059-6068

Huber, K. J., & Overmann, J. (2018). Vicinamibacteraceae fam. nov., the first described family within the subdivision 6 Acidobacteria. International journal of systematic and evolutionary microbiology, 68(7), 2331-2334.

Huisman, L., & Wood, W. E. (1974). Slow sand filtration. World Health Organization.

Jung, M. Y., Sedlacek, C. J., Kits, K. D., Mueller, A. J., Rhee, S. K., Hink, L., ... & Wagner, M. (2022). Ammonia-oxidizing archaea possess a wide range of cellular ammonia affinities. The ISME journal, 16(1), 272-283.

Kulichevskaya, I. S., Ivanova, A. A., Baulina, O. I., Rijpstra, W. I. C., Sinninghe Damsté, J. S., & Dedysh, S. N. (2017). Fimbriiglobus ruber gen. nov., sp. nov., a Gemmata-like planctomycete from Sphagnum peat bog and the proposal of Gemmataceae fam. nov. International Journal of Systematic and Evolutionary Microbiology, 67(2), 218-224.

Lautenschlager, K., Hwang, C., Ling, F., Liu, W. T., Boon, N., Köster, O., ... & Hammes, F. (2014). Abundance and composition of indigenous bacterial communities in a multi-step biofiltration-based drinking water treatment plant. Water research, 62, 40-52.

McLaren.M, speedyseq: Faster implementations of phyloseq functions. https://github.com/mikemc/speedyseq https://github.com/mikemc/speedyseq.

McMurdie. P.J, S. Holmes, phyloseq: an R package for reproducible interactive analysis and graphics of microbiome census data, PloS one 8 (4) (2013) e61217.

Oh, S., Hammes, F., & Liu, W. T. (2018). Metagenomic characterization of biofilter microbial communities in a full-scale drinking water treatment plant. Water research, 128, 278-285.

Parada. A.E, D.M. Needham, J.A. Fuhrman, Every base matters: assessing small subunit rRNA primers for marine microbiomes with mock communities, time series and global field samples, Environ. Microbiol. 18 (5) (2016) 1403–1414.

Park, J. W., Kim, H. C., Meyer, A. S., Kim, S., & Maeng, S. K. (2016). Influences of NOM composition and bacteriological characteristics on biological stability in a full-scale drinking water treatment plant. Chemosphere, 160, 189-198

Perujo, N., Romaní, A. M., & Sánchez-Vila, X. (2018). Bilayer infiltration system combines benefits from both coarse and fine sands promoting nutrient accumulation in sediments and increasing removal rates. Environmental science & technology, 52(10), 5734-5743.

Piche, A., Campbell, A., Cleary, S., Douglas, I., & Basu, O. D. (2019). Investigation of backwash strategy on headloss development and particle release in drinking water biofiltration. Journal of Water Process Engineering, 32, 100895

Prest, E. I., Hammes, F., Kötzsch, S., Van Loosdrecht, M. C. M., & Vrouwenvelder, J. S. (2016). A systematic approach for the assessment of bacterial growth-controlling factors linked to biological stability of drinking water in distribution systems. Water Science and Technology: Water Supply, 16(4), 865-880.

Prest, E. I., Hammes, F., Kötzsch, S., van Loosdrecht, M. C., & Vrouwenvelder, J. S. (2013). Monitoring microbiological changes in drinking water systems using a fast and reproducible flow cytometric method. Water research, 47 (19), 7131-7142.

Poncheewin. W, G.D. Hermes, Van Dam, J.J. Koehorst, H. Smidt, P.J. Schaap, NGTax 2.0: a semantic framework for high-throughput amplicon analysis, Front. In Gen. 10 (2020) 1366.

Quast. C, E. Pruesse, P. Yilmaz, J. Gerken, T. Schweer, P. Yarza, J. Peplies, F.O. Glockner, ¨The SILVA ribosomal RNA gene database project: improved data processing and web-based tools, Nucleic Acids Res. 41 (D1) (2013) D590–D596.

Ramiro-Garcia. J, G.D. Hermes, C. Giatsis, D. Sipkema, E.G. Zoetendal, P.J. Schaap, H. Smidt, NG-Tax, a highly accurate and validated pipeline for analysis of 16SrRNA amplicons from complex biomes F1000Res., (2016).

Schurer, R., Hijnen, W. A. M., & van der Wal, A. (2022). The significance of the biomass subfraction of high-MW organic carbon for the microbial growth and maintenance potential of disinfectant-free drinking water produced from surface water. Water Research, 209, 11789

Sousi, M., Liu, G., Salinas-Rodriguez, S. G., Chen, L., Dusseldorp, J., Wessels, P., ... & van der Meer, W. (2020). Multi-parametric assessment of biological stability of drinking water produced from

groundwater: Reverse osmosis vs. conventional treatment. Water research, 186, 116317.

Symons, G. E. (2006). Water treatment through the ages. Journal-American Water Works Association, 98(3), 87-98.
Tatari, K., Smets, B. F., & Albrechtsen, H. J. (2013). A novel bench-scale column assay to investigate site-specific nitrification biokinetics in biological rapid sand filters. Water research, 47(16), 6380-6387.

Tatari, K., Smets, B. F., & Albrechtsen, H. J. (2013). A novel bench-scale column assay to investigate site-specific nitrification biokinetics in biological rapid sand filters. Water research, 47(16), 6380-6387.

Trikannad, S. A., van Halem, D., Foppen, J. W., & van der Hoek, J. P. (2023). The contribution of deeper layers in slow sand filters to pathogens removal. Water Research, 237, 119994.

van der Kooij, D., Veenendaal, H. R., van der Mark, E. J., & Dignum, M. (2017). Assessment of the microbial growth potential of slow sand filtrate with the biomass production potential test in comparison with the assimilable organic carbon method. Water research, 125, 270-279.

van der Wielen, P. W., Brouwer-Hanzens, A., Italiaander, R., & Hijnen, W. A. (2023). Initiating guidance values for novel biological stability parameters in drinking water to control regrowth in the distribution system. Science of the Total Environment, 871, 161930

Van Kessel, M. A., Speth, D. R., Albertsen, M., Nielsen, P. H., Op den Camp, H. J., Kartal, B., & Lücker, S. (2015). Complete nitrification by a single microorganism. Nature, 528(7583), 555-559.

Velten, S., Boller, M., Köster, O., Helbing, J., Weilenmann, H. U., & Hammes, F. (2011). Development of biomass in a drinking water granular active carbon (GAC) filter. Water research, 45(19), 6347-6354.

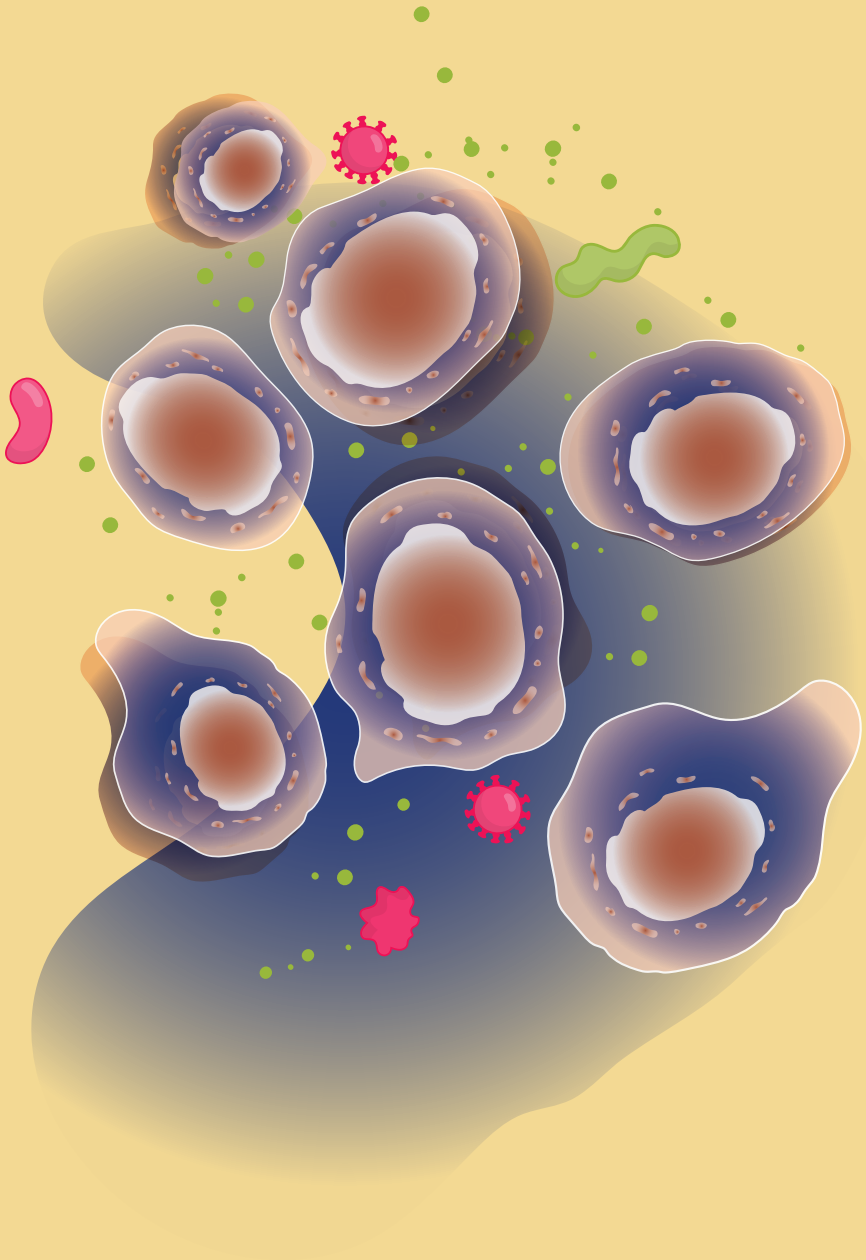

Chapter 4

Biodegradable organic carbon release in deep bed of slow sand filters

This chapter is based on:
Trikannad, S. A., van der Hoek, J. P., & van Halem, D. (2024). Biodegradable organic carbon release in deep bed of slow sand filters. (In preparation)

Abstract

Slow sand filters (SSFs), popular for their disinfection capabilities, are also widely recognised for removing biological stability parameters such as dissolved organic carbon (DOC) and ammonium (NH_4^+). This study investigated the biochemical processes influencing DOC release in mature full-scale and young experimental SSFs. The *Schmutzdecke* layer decreased the easily biodegradable fraction of DOC (low molecular-weight acids and building blocks), along with a slight decrease in NH_4^+, phosphate and dissolved oxygen (DO), due to heterotrophic activity. The deeper layers, completely removed NH_4^+ by nitrification, as confirmed by the DO consumption and nitrogen balance. This was accompanied by a slight decrease in the slowly degradable fraction of DOC (biopolymers). Upon complete nitrification at 55 cm depth, DOC release was consistently observed as easily biodegradable acids and neutrals. This release was observed in both full-scale and lab-scale SSFs, indicating that it is relevant for practice and independent of biofilm maturity. The underlying mechanism needs further investigation, but it is hypothesized to be a product of starving nitrifiers under NH_4^+ and NO_2^- limitation conditions in the deeper filter bed, or due to the conversion of slowly degradable carbon into easily biodegradable carbon. Either way, the bottom filter layers effectively captured the released DOC, highlighting the critical role of deep sand bed in removing biological stability parameters and maintaining effluent quality. This study marks the first report of DOC release in the deeper layers of SSFs, urging further research to understand the impact of DOC cycling on removal processes in filters.

4.1 Introduction

Water utilities are concerned about biodegradable fraction of dissolved organic carbon (DOC) in drinking water as it can diminish the biological stability of finished water and serve as a precursor to the formation of organic disinfection byproducts (DBPs) (Terry et al., 2024). In countries like the Netherlands, where disinfectants are not used during treatment or distribution (Prest et al., 2016; Sousi et al., 2020), removal of biodegradable fraction of DOC is crucial to prevent microbial regrowth in the distribution network. Slow sand filters (SSFs), popular for their disinfection capabilities, are increasingly recognised for improving DOC and ammonium (NH_4^+) removal.

NH_4^+ removal by nitrification occurs over the filter depth in SSFs (Trikannad et al., 2024). Ammonia and/or nitrite oxidising families such as *Nitrospiraceae* (dominated by the genus *Nitrospira*), *Nitrosomonadaceae* and *Nitrosopumilaceae* families have been found in the sand bed (Bai et al., 2022; Chen et al., 2021; Haig et al., 2015). *Nitrosopumilaceae* known to thrive at very low ammonia concentrations was abundant in the deeper depths where NH_4^+ was almost completely depleted (Trikannad et al., 2024).

SSFs remove refractory (i.e. poorly biodegradable) compounds, in addition to easily and slowly biodegradable organic carbon using physical-chemical and biological processes (Brandt et al., 2017; Haig et al., 2011; Schurer et al., 2022). Therefore, the collective removal of these compounds is measured by DOC. Heterotrophic bacteria that develop on sand play a critical role in metabolizing the biodegradable fraction of DOC. Heterotrophic microbial groups such as *Gemmataceae* and *Vicinamibacteraceae* were found at different depths of SSFs (Bai et al., 2022; Chen et al., 2021; Haig et al., 2015; Trikannad et al., 2024), highlighting the removal capability of biodegradable fraction of DOC in the entire sand bed. However, a release of DOC in the sand bed of biological filtration systems has been reported previously (Bar-Zeev et al., 2012; Perujo et al., 2018). Recently, a slight increase in DOC was also noted in the deeper layers of mature full-scale SSFs, operating under low loading conditions (Trikannad et al., 2024).

In this study, we investigate the DOC release and what the source and composition is of the released DOC. For this, duplicate full-scale and lab-scale filters were sampled to monitor the fate of DOC, alongside various chemical parameters, at different filter depths. The contribution of various organic carbon fractions to DOC changes was examined using liquid chromatography with organic carbon detection (LC-OCD) analysis.

4.2 Materials and methods

4.2.1 Description and sampling of full-scale SSFs

The drinking water treatment plant in Scheveningen (The Netherlands) of drinking water company

Dunea receives raw water from the river Meuse and is further treated by managed aquifer recharge in the dunes, pellet softening, aeration and rapid sand filtration with powdered activated carbon dosing. Further, the water flows through slow sand filters designed as a final polishing step before distribution to remove microbial growth-promoting compounds such as DOC and NH_4^+. The two mature full-scale SSFs examined in this study are from the same production line and have been producing drinking water for the last 28 years without sand replacement. Here on, these two mature filters will be referred to as F-SSF1 and F-SSF2. The sand depth was 95 cm and 85 cm for F-SSF1 and F-SSF2, respectively, and the filters are operated at an average hydraulic loading rate of 0.4 $m^3/m^2/h$. Specific operational and design parameters for the full-scale SSFs are shown in Table S1.

The water used to measure chemical parameters was sampled from both filters at influent, effluent and at five different depths of 5, 20, 30, 45 and 65 cm (measured from the top of the sand bed). The water was collected using sampling ports provided on the filter wall with 30 cm long pipes penetrating the sand bed. The samples were collected once a week over 5 months.

4.2.2 Operation and sampling of laboratory SSFs

Duplicate laboratory columns with diameter of 4 cm were operated for 6 months. The sand bed height was 85 cm, with an additional 5 cm under-drainage (5-7 mm gravel) to allow free passage of filtered water were operated. The two laboratory columns, referred to as L-SSF1 and L-SSF2 from here on consisted of freshly washed sand with an effective grain size of 0.45 mm (uniformity coefficient (UC)=1.63) and 0.9 mm (UC=1.51), respectively. The columns were operated at room temperature (19-21^oC), at an average hydraulic loading rate of 0.5 $m^3/m^2/h$.

Tap water resulting from a multistage treatment scheme at a Dutch drinking water treatment plant was used as the influent for the laboratory filters. DOC in tap water was 1.7 mg/L, comprising mainly of neutrals, building blocks, biopolymers, and humics (Table S2). This remaining DOC was not degraded even after multistage treatment, indicating their recalcitrant nature. The concentrations of NH_4^+ and PO_4^3 were below 0.01 mg/L. Hence, each filter was supplied with non-chlorinated tap water, dosed with easily biodegradable carbon as a mixture of carboxylic acids, sodium acetate ($NaC_2H_3O_2$), sodium oxalate ($Na_2C_2O_4$) and sodium formate ($NaCHO_2$) (1:1:1), NH_4^+ as ammonia chloride (NH_4Cl) (Merck chemicals) and PO_4^{3-} as potassium dihydrogen phosphate ($KH_2PO_4^-$) (Merck chemicals) (Table S3)

A supernatant water layer of 80 cm was maintained above the sand layer. The filters were covered with aluminium foil to exclude light and avoid algal growth. The water samples were collected from influent, effluent and five different depths of 5, 20, 35, 55 and 65 cm using sampling ports provided along the height of the columns. The samples were collected once a week over 6 months.

4.2.3 Analytical methods

4.2.3.1 DOC

DOC was measured with a Shimadzu TOC-V$_{CPH/CPN}$ analyser (Limit of Detection [LOD]=0.1 mg/L) immediately or within one day after sampling. 30 mL of sample was filtered through 0.45 µm filters (SPARTAN™, Whatman, Germany) that had been flushed twice with demineralized water.

Liquid chromatography-organic carbon detection (LC-OCD) analysis (reporting limit- 0.1 mg/L) was performed at Het Waterlaboratorium (Haarlem, Netherlands) to quantify different carbon fractions as described by Sousi et al., (2020). The carbon fractions were distinguished based on their molecular weight (MW), and they are (from largest to smallest): biopolymers (proteins and polysaccharides), humic substances, building blocks, low molecular weight acids, and neutrals. The DOC changes were only examined in laboratory SSFs, since low AOC concentration in mature filters posed analytical challenges.

4.2.3.2 NH_4^+, NO_2^- and NO_3^-

The concentrations of NH_4^+ (LOD=0.01 mg N/L), NO_2^- (LOD = 0.01 mg N/L) and NO_3^- (LOD=0.1 mg N/L) and PO_4^{3-} (LOD = 0.005 mg/L) in the filtered water (<0.22 µm) samples were determined using Ion Chromatography (Dionex ICS-2100, Thermo, USA) equipped with an AS17-Column.

4.2.3.3 pH and DO

Dissolved oxygen (DO) concentrations, pH and temperature were measured directly in the water from sampling ports using a HQ40D portable multimeter (HACH), with a tube from each tap leading directly into a 500 ml polypropylene bottle that overflowed continuously.

4.2.4 Calculation of carbon released from biomass

The heterotrophic and nitrifying biomass produced in experimental SSFs were calculated from their respective biomass yield and substrates utilized as follows (Equation 1):

$$\textit{Biomass produced (X) = Biomass yield (Y) x Substrate utilized (S)} \quad (1)$$

Where, yield (Y) was considered as 0.71 gVSS/g sodium acetate for heterotrophs (Metcalf and Eddy, 1991; Randall et al., 1992) and 0.2 gVSS/g NH_4^+-N for nitrifiers (Rittmann and McCarty, 2001). For heterotrophs, the reduced DOC concentration, consisting solely of easily biodegradable carbon compounds, was considered as the substrate. Meanwhile, the substrate for nitrifiers was the NH_4^+-N

consumed during nitrification. Based on the biomass concentration, the carbon content in biomass was calculated considering a biomass composition of $CH_{1.8}O_{0.5}N_{0.2}$.

4.2.5 Statistical analysis

Statistical analysis was performed on all quantitative data using one-way ANOVA, followed by the Bonferroni post-hoc correction.

4.3 Results

4.3.1 DOC release observed in mature full-scale SSFs

Figure 1 shows the DOC concentrations over depth in mature SSFs. In the top 5 cm, DOC concentrations decreased by 0.6-0.8 mg C/L. Deeper into the filter bed, between 20-60 cm, a significant increase in DOC concentration ($p<0.05$) was noted in both filters. The released DOC concentration was around 0.36 mg C/L in both full-scale filters. The released DOC fraction was subsequently removed in the deeper layers. Hence, the release would have remained unnoticed if merely effluent DOC concentrations were monitored. This variation of DOC over depth was consistently observed throughout the 4-month sampling period. It should be noted that these full-scale filters are positioned at the end of an extensive treatment train, amongst other treatment steps, after dune passage and rapid sand filters. Consequently, the fraction of easily biodegradable organic carbon will be low in these waters (AOC< 5 µgC/L), i.e., oligotrophic conditions, making it challenging to study carbon cycling in such full-scale filters.

Concentrations of NH_4^+, DO and pH decreased with depth (Figure S1). Despite low NH_4^+-N concentration (<0.01 mg N/L) in the influent, a minor decrease was noted between 5- 55 cm. Both DO and pH slightly decreased in the top 40 cm and then stabilized in the deeper depths.

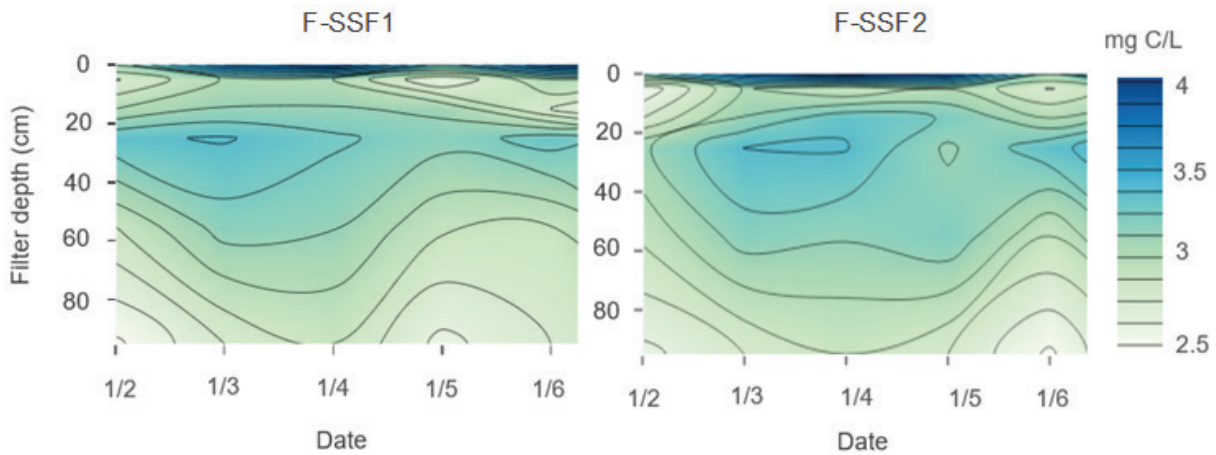

Figure 1 Depth profiles of DOC in mature full-scale SSFs: (A) F-SSF1 and (B) F-SSF2 between February and June 2022. Measurements were carried out in triplicates

4.3.2 Laboratory SSFs mirror full-scale findings

Figure 2 shows the DOC concentrations over the height of young SSFs for the experimental period of 123 days. In the first 60 days, DOC removal was minor (<5%), but after 80 days the columns reached a stable DOC removal of 22-25%. Majority of DOC was removed (0.63 mg/L) in the first 5 cm, with subsequent stable conditions down to the 55 cm sampling port. At this depth, a sudden increase in DOC concentrations was observed with an average of 0.31 mg/L higher than the concentration in the preceding depth. This observation corresponds to the observed release in the mature SSFs. The released DOC was removed again in the deeper layers, similarly to the removal observed in the top 5 cm. The total biomass on sand measured by tATP (Figure S2) showed an increasing trend with time for sand samples taken from the top, middle and bottom layers. This confirms biofilm growth throughout the filter and underlines the importance of biological processes in the observed DOC removal at all depths. The onset of DOC release after 2 months in the laboratory filters with fresh filter sand, illustrates that DOC release in the deeper layers was independent of biofilm maturity and occurred in both mature and young SSFs.

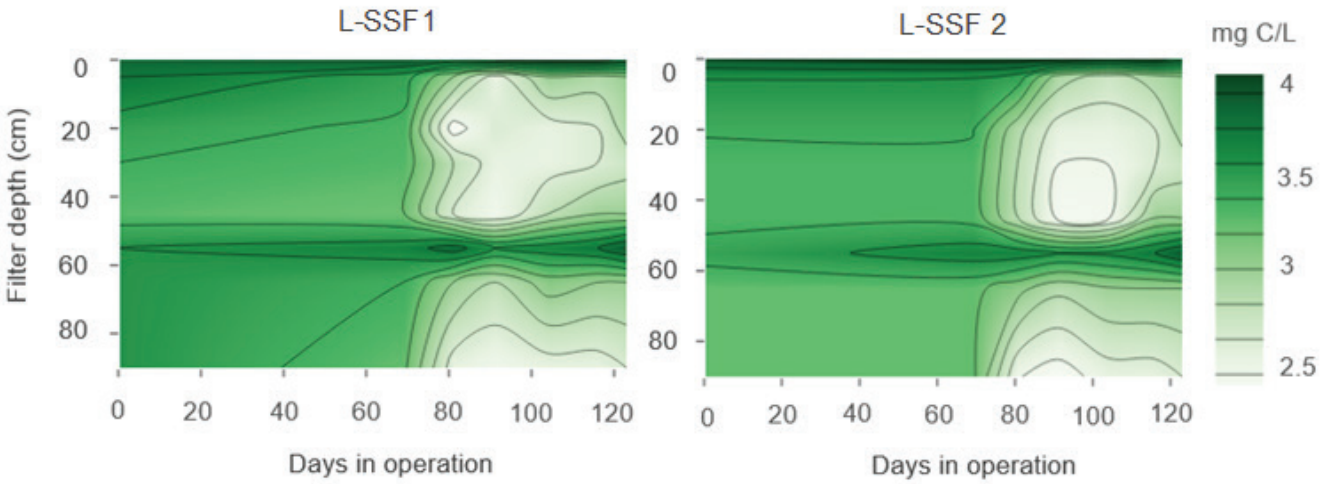

Figure 2 Depth profiles of DOC in laboratory SSFs: (A) L-SSF1 and (B) L-SSF2 over time of operation. Measurements were carried out in triplicates

4.3.3 Nitrification and PO_4^{3-} removal in filters

Figure 3 shows the depth profiles of DOC, NH_4^+, PO_4^{3-} and pH at steady state in the laboratory SSFs (day 120-123 of operation). Most of the DOC removal was observed in the top 5 cm, followed by a sharp release in the deeper layers. NH_4^+ removal commenced below 5 cm depth and was completely removed (0.98 mg/L) from the effluent, achieving >87% of removal already after 45 cm. Simultaneously, NO_2^- and NO_3^- concentrations increased, as well as a drop in pH and DO (Figures 3 and S3), together indicating nitrification. It is noteworthy that 0.21 mg/L of NH_4^+-N was not recovered as NO_2^--N or NO_3^--N in the

effluent, i.e., the removal could not be linked to nitrification. This corresponds to the observed DO consumption, which is too low for complete nitrification of incoming NH_4^+-N. The PO_4^{3-}-P concentration was low in the influent (0.04 mg/L), yet a significant decrease ($p<0.05$) of 0.02 mg/L and 0.01 mg/L was noted in the top 5 cm and between 55-90 cm depths, respectively.

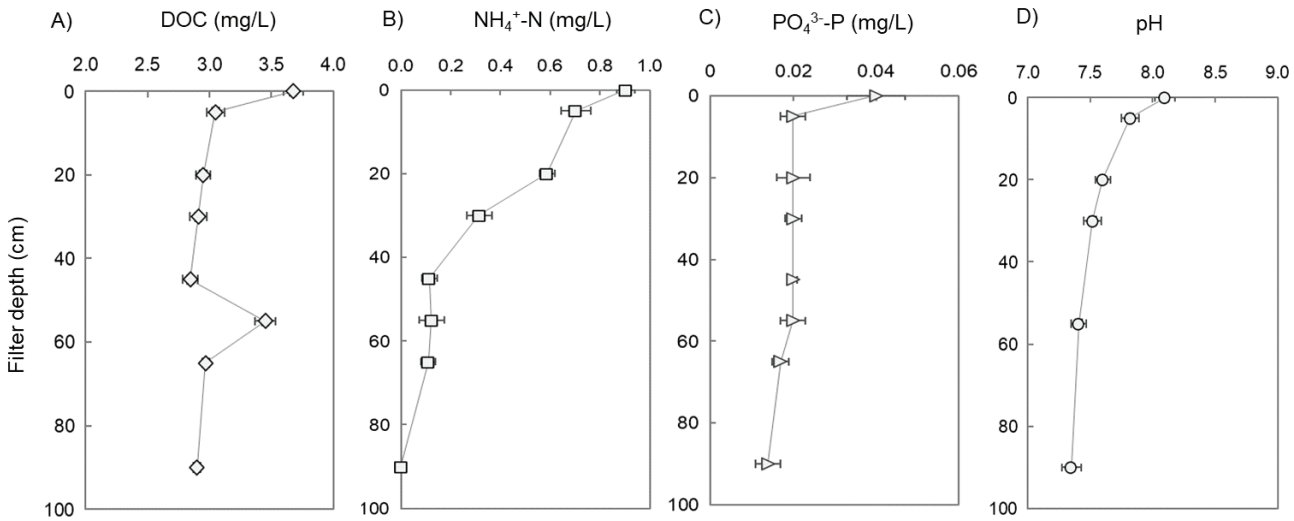

Figure 3 Depth profiles of (A) DOC (B) NH_4^+-N, (C) PO_3^- and (D) pH on the last four days (120-123 of operation) of the experiment in laboratory SSFs. Measurements were carried out in triplicates

4.3.4 Biodegradable organic carbon

LC-OCD analysis was used to identify the contribution of various organic carbon fractions to DOC changes in the laboratory SSFs after 106 days of operation. The influent DOC was composed of low molecular weight (LMW) acids (0.24 mg/L), LMW neutrals (0.35 mg/L), building blocks (1 mg/L), biopolymers (0.16 mg/L) and humic substances (0.92 mg/L). The concentration of acids and building blocks in the influent was higher than the levels in tap water (background) (Figure 4) due to the dosing of easily biodegradable carbon.

DOC removal in the top 5 cm was due to the decrease in acids (0.23 mg/L) and building blocks (0.6 mg/L). Biopolymers concentration decreased linearly between 20-90 cm, up to a total removal of 0.1 mg/L in the effluent. The release DOC concentration (0.83 mg/L) at 55 cm depth was caused by an increase in acids (0.09 mg/L) and neutrals (0.81 mg/L). The concentration of neutrals at 55 cm exceeded that of the influent, suggesting that processes within the sand bed contributed to the increase. The released acids and neutrals were subsequently removed between 55-90 cm. Noteworthy, the (background) concentrations of humic substances and neutrals in the influent stayed consistent throughout the filter depth, implying that these compounds were not removed by both physical-chemical and biological processes.

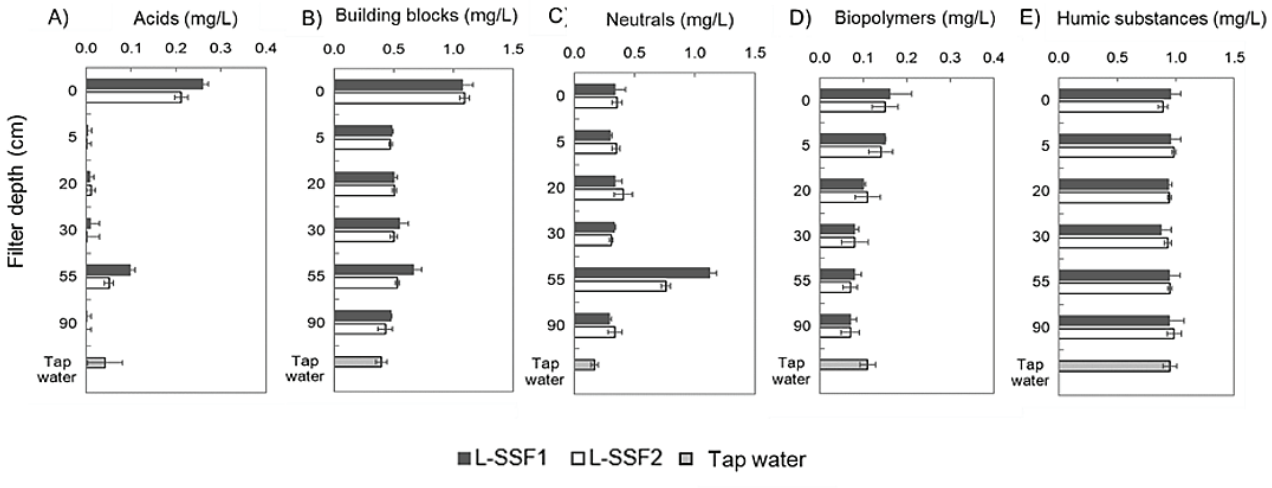

Figure 4 Concentrations of a) Acids, b) Building blocks, c) Neutrals, d) Biopolymers, e) Humic substances in tap water and the over depth of laboratory SSFs after 106 days of operation

4.4 Discussion

4.4.1 Release of LMW organic carbon in SSFs

In mature full-scale filters, DOC release was consistently observed at 20-60 cm depth. Also, after a start-up period of 2 months, the young laboratory SSFs started demonstrating stable release of DOC at 55 cm. These observations in both young and mature SSFs, suggest that DOC release in SSFs is independent of biofilm maturity. Figure 5 shows a schematic illustration of the proposed processes occurring at different filter depths. The top 5 cm, in SSF literature commonly referred to as the *Schmutzdecke*, was found to consistently remove easily biodegradable fractions such as acids and building blocks. The stochiometric calculations showed that the DO decrease in this layer was similar to the estimated oxygen needed to degrade the observed change in DOC. Thus, DOC removal is attributed to the activity of heterotrophs that utilise these compounds for assimilation and respiration (Law & Lamb, 2001; Lehtola et al., 2001). Although neutrals could serve as a substrate for microbial growth (Lautenschlager et al., 2014), the steady levels between 0-40 cm indicate their recalcitrant characteristics. The nitrogen balance (Table S4) at 5 cm indicated that only a fraction of NH_4^+ (0.05 mgN/L) was converted to NO_2^- and NO_3^-. This indicates that the remaining NH_4^+ (0.21 mgN/L) may be assimilated by the fast-growing heterotrophic bacteria (Butturini et al., 2000). The finding that

heterotrophic bacterial growth processes predominate in the top layer is further supported by the elemental molar ratio of removed DOC, NH_4^+, and PO_4^{3-} closely matching the microbial growth ratio of 100:10:1 (LeChevallier et al., 1996). Nitrification primarily occurs beyond the Schmutzdecke, at a lower depth than DOC removal, leading to deeper infiltration of NH_4^+ and NO_2^-. The spatial separation between DOC and NH_4^+ removal is probably due to the different growth rates of both microbial groups removing these compounds (Fdz-Polanco et al., 2000).

The acids and neutrals, released at 55 cm, were completely removed in the subsequent sand layers, together with a fraction of PO_4^{3-}. Neutrals did not decrease beyond the concentration of non-biodegradable fraction present in tap water. Similarly, humic substances remained unchanged over depth. These observations suggest that both physical-chemical and biological processes in SSFs were unsuccessful in removing the complex and recalcitrant neutrals and humic substances present in tap water. However, the removal of released DOC in the bottom layer can be attributed to physical-chemical and biological processes. This shows that provided a sufficient filter depth, the observed DOC cycling does not threaten effluent quality, but can even boost PO_3^- removal to ultra-low levels. In addition, the released, supplementary carbon source could enhance heterotrophic activity and potentially promote co-removal of other contaminants from drinking water, such as organic micropollutants (Wang et al., 2022).

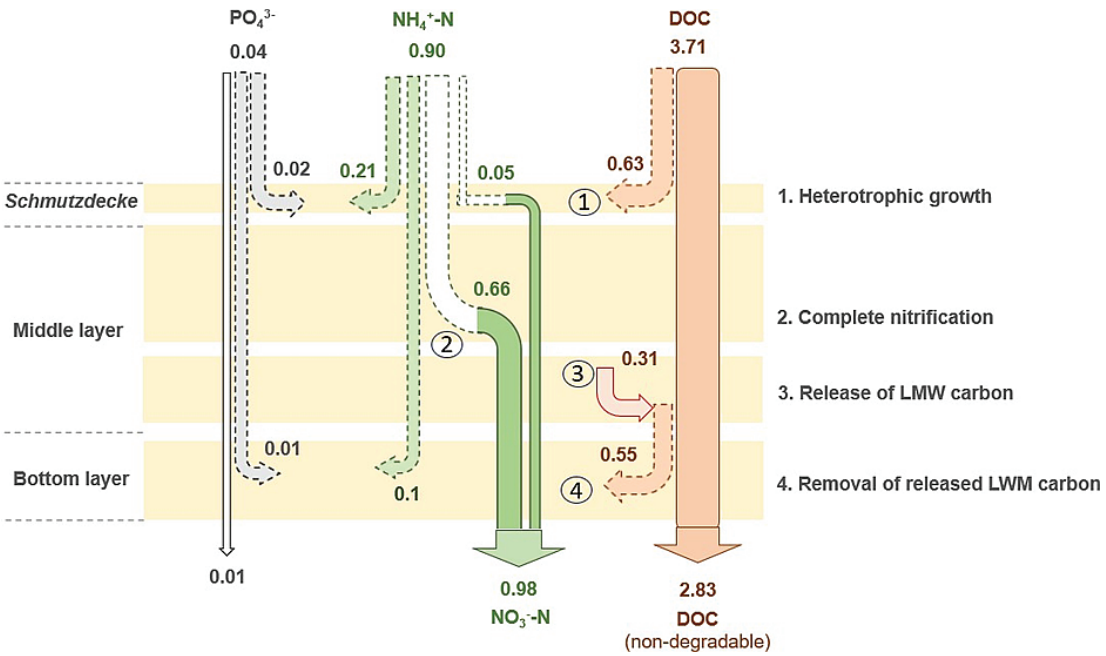

Figure 5 Schematic illustration of fate of DOC, NH_4^+ and PO_4^{3-}(mg/L) at different filter depths between days 120- 123 of operation. Coloured dotted arrows indicate the consumption of NH_4^+ and PO_4^{3-} for heterotrophic growth, while white dotted arrows indicate the consumption of NH_4^+ by nitrification.

4.4.2 Source of released DOC

The release of easily biodegradable compounds in the deeper layers of filters in this study may be explained by several mechanisms. One explanation could be that the released DOC originated from decaying bacterial cells. As water flows through the filter, released cells from biofilms are retained in the sand bed at a deeper depth (Chan et al., 2018; Trikannad et al., 2024). This biomass may release DOC as soluble metabolic by-products and/or during cell decay (Perujo et al., 2018). These decay processes may produce labile DOC which could be taken up by other microorganisms in the bottom layers of the filter, stimulating microbial proliferation (Bar-Zeev et al., 2012).

The specific filter depth of DOC release more or less coincides with the depth of complete nitrification; both in the mature and young filters. Hence, nitrifiers may be released in the middle layer of the filter bed and transported downwards to the depths where NH_4^+ and NO_2^- are limiting. Consequently, these retained cells may release LMW acids and neutrals due to starvation. Nitrifiers have been found to produce organic carbon, providing a carbon source for microorganisms in environments with limited carbon (Zhang et al., 2021). Rosenqvist et al., observed that in drinking water distribution systems (DWDS), when monochloramine (MCA) was suddenly cut off, *Nitrospira* associated with MCA metabolism began to die off. This necromass then served as a nutrient source for heterotrophic bacteria, enabling their proliferation (Rosenqvist et al., 2023). The major occurrence of nitrification in this middle layer is supported by the increase of NO_3^- and decrease in pH. Also, an earlier study revealed that microbial families, including *Nitrospiraceae*, *Nitrosomonadaceae*, and *Nitrosopumilaceae*, capable of NH_4^+ and/or NO_2^- oxidation, were present in the deeper layers of SSFs (Trikannad et al., 2024). Moreover, organic carbon excreted by nitrifiers has been shown to enhance the degradation of previously inert organic matter (Kuzyakov et al., 2000). Although this is a plausible explanation for the observed DOC release, the estimated organic carbon released from the total nitrifying biomass is 0.11 mg C/L in the laboratory filters. Hence, even if all nitrifiers would decay, which is highly unlikely, this could not account for the 0.31 mg C/L of released DOC. When considering decay of heterotrophic cells, the estimated organic carbon released from the total heterotrophic biomass produced is higher, at 0.34 mg C/L. A possible explanation is that in a steady-state condition where no biomass accumulates, the produced biomass decays and accounts for the released DOC. While this is theoretically possible, it is practically unlikely. Moreover, released cells would have to be transported from the Schmutzdecke to collectively decay at a depth of 55 cm, which is also not a likely scenario.

Another explanation could be that slowly degradable carbons are converted to easily degradable carbons, i.e., biopolymers are converted into easily biodegradable acids and neutrals. Biopolymers have been found to serve as substrates for microorganisms when present at low concentration in oligotrophic conditions (Sack et al., 2014; Chen et al., 2016). Lautenschlager et al., reported that polysaccharides may

be biologically removed in the deeper layers of SSFs due to the long residence time between substrates (in water) and biofilm in the sand bed (Lautenschlager et al., 2014). The observed biopolymer removal decreased by 0.1 mg/L over the depth, which does not align with the sudden peak in DOC release. Additionally, the overall biopolymer removal was low at <200ug/L, making it unlikely that this was the source of the observed DOC release peak.

Irrespective of the release pathway, this is the first study to highlight DOC release in the deeper bed of SSFs, both in full-scale and lab-scale SSFs, suggesting that this is a process occurring widely in filters. Therefore, further investigation is recommended to fully comprehend the impact of DOC cycling on removal processes in filters.

4.5 Conclusions

This study investigated the biochemical processes influencing DOC release in the deeper layers of SSFs using mature full-scale and young experimental SSFs. The *Schmutzdecke* layer reduced the easily biodegradable fraction of DOC (acids and building blocks), NH_4^+ , PO_4^{3-} and DO due to heterotrophic activity. The deeper layers completely removed NH_4^+ by nitrification as confirmed by the DO consumption and nitrogen balance. This was accompanied by a slight decrease in the slowly degradable fraction of DOC (biopolymers). Upon complete nitrification at 55 cm depth, DOC release was consistently observed as easily biodegradable acids and neutrals. This release was observed in both full-scale and lab-scale SSFs, showing its practical relevance and independence from biofilm maturity. The underlying mechanism needs further investigation, but is hypothesized to be a product of starving nitrifiers under NH_4^+ and NO_2^- limitation conditions in the deeper filter bed, or to be due to the conversion of slowly degradable carbon into easily biodegradable carbon. Either way, the bottom filter layers effectively captured the released DOC, highlighting the critical role of deep sand bed in removing biological stability parameters and maintaining effluent quality. This study marks the first report of DOC release in the deeper layers of SSFs, urging further research to understand the impact of DOC cycling on removal processes in filters.

4.6 Supplementary information

Table S1 Operational parameters of full-scale SSFs 1 and 2 at the drinking water treatment

	Unit	F-SSF1	F-SSF2
Filter bed height	m	0.95	0.8
Height of supernatant	m	1	1
Filter area	m^2	2383	2359
Filtration rate	m/h	0.4	0.4
Sand grain size	mm	0.3-0.6	0.3-0.6
Age of sand	years	28	28
Time since last scraping	years	5.3	4.6

Table S2 Dissolved organic carbon (DOC) composition in tap water determined by Liquid chromatography – organic carbon detection (LC-OCD)

DOC composition in tap water	
Fractions	**Concentration (mg/L)**
Low molecular-weight acids	0.042 ± 0.039
Low molecular-weight neutrals	0.210 ± 0.028
Building blocks	0.397 ± 0.046
Biopolymers	0.110 ± 0.018
Humics	0.951 ± 0.057

Table S3 Composition and concentration of compounds dosed in tap water

Parameter	Dosed concentration (mg/L)	Compound	Chemical concentration (mg/L)
DOC	0.85	Sodium acetate ($NaC_2H_3O_2$)	1.607
		Sodium formate ($NaCHO_2$)	1.606
		Sodium oxalate ($Na_2C_2O_4$)	1.582
NH_4^+-N	1	Ammonium chloride (NH_4Cl)	3.821
PO_4^{3-}-P	0.05	Pottasium dihydrogen phosphate (KH_2PO_4)	0.281

Table S4 Mass balances of NH_4^+, NO^- and NO^- at different depths calculated using data from the last four days of the experiment in laboratory SSFs

	Depths	Δ NH_4^+ (mg/L)	Δ NO_2^- (mg/L)	Δ NO_3^- (mg/L)	ΔN
Laboratory SSFs	Top (5 cm)	-0.26	0.01	0.04	-0.21
	Middle (55 cm)	-0.66	0.06	0.64	0.04
	Bottom (90 cm)	-0.08	0.01	0.22	0.16

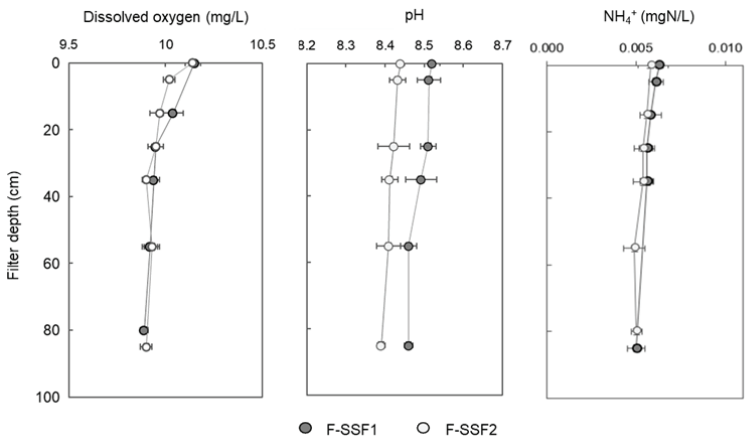

Figure S1 Depth profiles of (A) dissolved oxygen, (B) pH and (C) NH_4^+ in full-scale SSFs. Measurements were carried out in triplicates

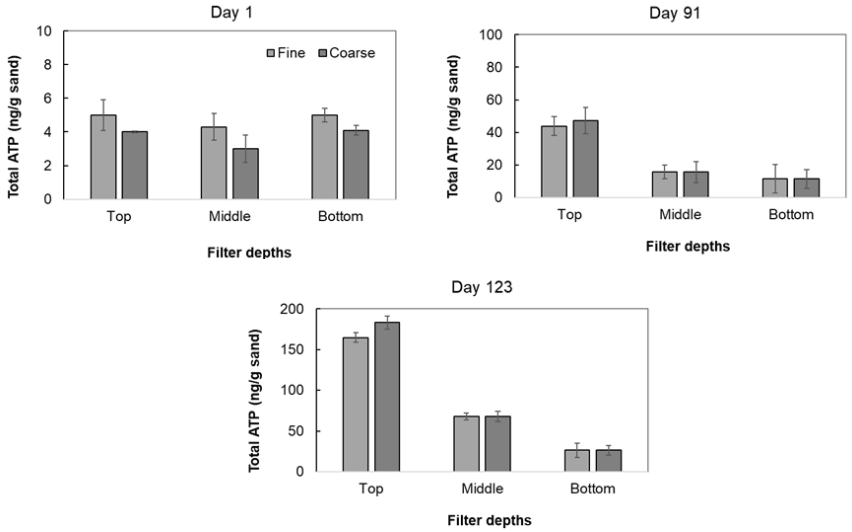

Figure S2 Total biomass on sand determined by total ATP from top, middle and bottom layers of laboratory SSFs over time of operation

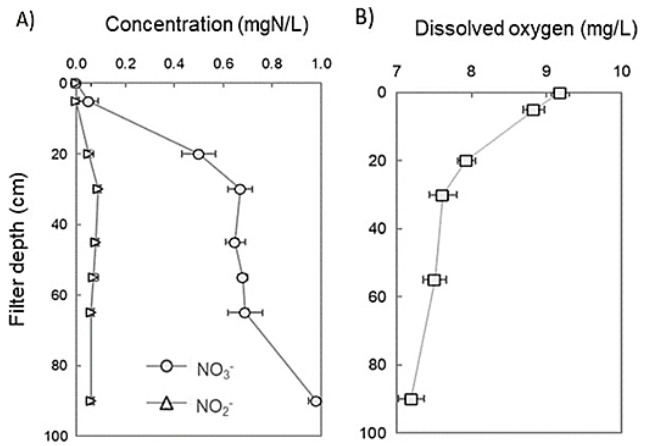

Figure S3 Depth profiles of (A) NO^- and NO^- and (B) dissolved oxygen on the last four days of the experiment in laboratory SSFs. Measurements were carried out in triplicates

References

Bai, X., Dinkla, I. J. T., & Muyzer, G. (2022). Microbial ecology of biofiltration used for producing safe drinking water. Applied Microbiology and Biotechnology, 106(13–16), 4813– 4829.

Bar-Zeev, E., Belkin, N., Liberman, B., Berman, T., & Berman-Frank, I. (2012a). Rapid sand filtration pretreatment for SWRO: Microbial maturation dynamics and filtration efficiency of organic matter. Desalination, 286, 120–130.

Brandt, M. J., Johnson, K. M., Elphinston, A. J., & Ratnayaka, D. D. (2017). Specialized and Advanced Water Treatment Processes. In Twort's Water Supply.

Butturini, A., Battin, T. J., & Sabater, F. (2000). Nitrification in stream sediment biofilms: The role of ammonium concentration and DOC quality. Water Research, 34(2), 629–639.

Chen, F., Peldszus, S., Elhadidy, A. M., Legge, R. L., Van Dyke, M. I., & Huck, P. M. (2016). Kinetics of natural organic matter (NOM) removal during drinking water biofiltration using different NOM characterization approaches. Water Research, 104, 361–370.

Chen, L., Zhai, Y., van der Mark, E., Liu, G., van der Meer, W., & Medema, G. (2021). Microbial community assembly and metabolic function in top layers of slow sand filters for drinking water production. Journal of Cleaner Production, 126342.

Fdz-Polanco, F., Méndez, E., Urueña, M. A., Villaverde, S., & García, P. A. (2000). Spatial distribution of heterotrophs and nitrifiers in a submerged biofilter for nitrification. Water Research, 34(16), 4081–4089.

Haig, S. J., Collins, G., Davies, R. L., Dorea, C. C., & Quince, C. (2011). Biological aspects of slow sand filtration: Past, present and future. Water Science and Technology: Water Supply, 11(4), 468–472.

Haig, Sarah Jane, Quince, C., Davies, R. L., Dorea, C. C., & Collinsa, G. (2015). The relationship between microbial community evenness and function in slow sand filters. MBio, 6(5).

Kuzyakov, Y., Friedel, J.K., Stahr, K., 2000. Review of mechanisms and quantification of priming effects. Soil Biol. Biochem. 32 (11-12), 1485–1498

Lautenschlager, K., Hwang, C., Ling, F., Liu, W. T., Boon, N., Köster, O., Egli, T., & Hammes, F. (2014).

Abundance and composition of indigenous bacterial communities in a multi-step biofiltration-based drinking water treatment plant. Water Research, 62, 40–52.

Law, S. P., & Lamb, A. J. (2001). Visualisation of the establishment of a heterotrophic biofilm. Biofilm, 6(1), 1–17.
LeChevallier, M. W., Welch, N. J., and Smith, D. B. (1996). Full-scale studies of factors related to coliform regrowth in drinking water. Appl. Environ.Microbiol. 62, 2201–2211.

Lehtola, M. J., Miettinen, I. T., Vartiainen, T., Myllykangas, T., & Martikainen, P. J. (2001). Microbially available organic carbon, phosphorus, and microbial growth in ozonated drinking water. Water Research, 35(7), 1635–1640.
Metcalf, L., Eddy, H. P., & Tchobanoglous, G. (1991). Wastewater engineering: treatment, disposal, and reuse (Vol. 4). New York: McGraw-Hill.

Perujo, N., Romaní, A. M., & Sanchez-Vila, X. (2018). Bilayer Infiltration System Combines Benefits from Both Coarse and Fine Sands Promoting Nutrient Accumulation in Sediments and Increasing Removal Rates. Environmental Science and Technology, 52(10), 5734–5743.

Prest, E. I., Hammes, F., van Loosdrecht, M. C. M., & Vrouwenvelder, J. S. (2016). Biological stability of drinking water: Controlling factors, methods, and challenges. In Frontiers in Microbiology (Vol. 7, Issue FEB, p. 45). Frontiers Media S.A.

Randall C. W., Barnard J. L. and Stensel H. D. (1992) Design and Retrofit of Wastewater Treatment Plant for Biological Nutrient Removal. Technomic, Lancaster, Basel.

Reinthaler, T., van Aken, H.M., Herndl, G.J., 2010. Major contribution of autotrophy to microbial carbon cycling in the deep North Atlantic's interior. Deep Sea Res. Part II 57 (16), 1572–1580

Rittmann, B. E., & McCarty, P. L. (2001). Environmental biotechnology: principles and applications.

Rosenqvist, T., Danielsson, M., Schleich, C., Ahlinder, J., Brindefalk, B., Pullerits, K., ... & Paul, C. J. (2023). Succession of bacterial biofilm communities following removal of chloramine from a full-scale drinking water distribution system. Npj Clean Water, 6(1), 41.

Sack, E. L., van der Wielen, P. W., & van der Kooij, D. (2014). Polysaccharides and proteins added to flowing drinking water at microgram-per-liter levels promote the formation of biofilms predominated by Bacteroidetes and Proteobacteria. Applied and environmental microbiology, 80(8), 2360-2371.

Schurer, R. T. significance of the biomass subfraction of high-M. organic carbon for the microbial growth and maintenance potential of disinfectant-free drinking water produced from surface water, Hijnen, W. A. M., & van der Wal, A. (2022). The significance of the biomass subfraction of high-MW organic carbon for the microbial growth and maintenance potential of disinfectant-free drinking water produced from surface water. Water Research, 209, 117898.

Sousi, M., Liu, G., Salinas-Rodriguez, S. G., Chen, L., Dusseldorp, J., Wessels, P., Schippers, J. C., Kennedy, M. D., & van der Meer, W. (2020). Multi-parametric assessment of biological stability of drinking water produced from groundwater: Reverse osmosis vs. conventional treatment. Water Research, 186, 116317.

Swan, B.K., Martinez-Garcia, M., Preston, C.M., Sczyrba, A., Woyke, T., Lamy, D., Reinthaler, T., Poulton, N.J., Masland, E.D.P., Gomez, M.L., Sieracki, M.E., DeLong, E.F., Herndl, G.J., Stepanauskas, R., 2011. Potential for chemolithoautotrophy among ubiquitous bacteria lineages in the dark ocean. Science 333 (6047), 1296–1300.

Terry, L. G., Peterson, E., & Summers, R. S. (2024). Organic matter biofiltration performance modeling: Influence of influent water quality, operating conditions, and biomass. Water Research, 249(August 2023), 121006.

Trikannad, S. A., Attiani, V., van der Wielen, P. W., Smidt, H., van der Hoek, J. P., & van Halem, D. (2024). Recovery of microbial biomass and purification performance after scraping of full-scale slow sand filters. Journal of Water Process Engineering, 60, 105101.

Wang, J., Poursat, B. A. J., Feng, J., de Ridder, D., Zhang, C., van der Wal, A., & Sutton, N. B. (2022). Exploring organic micropollutant biodegradation under dynamic substrate loading in rapid sand filters. Water Research, 221(July), 118832.

Zhang, L., Chen, M., Chen, X., Wang, J., Zhang, Y., Xiao, X., Hu, C., Liu, J., Zhang, R., Xu, D., Jiao, N., & Zhang, Y. (2021). Nitrifiers drive successions of particulate organic matter and microbial community composition in a starved macrocosm. Environment International, 157, 106776.

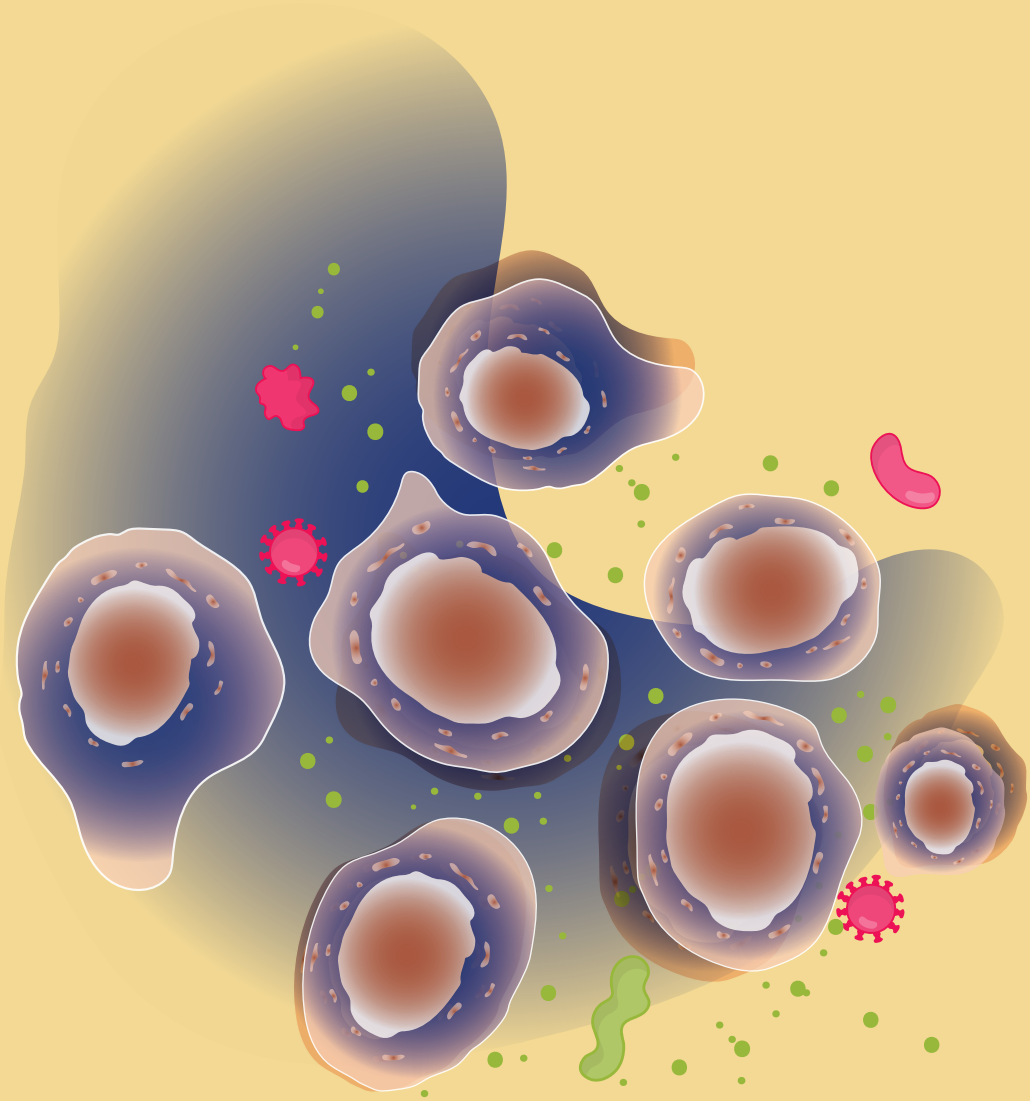

Chapter 5

Dissolved organic carbon and ammonium removal kinetics study to redesign slow sand filters

This chapter is based on:
Trikannad, S. A., Huang, Y., van Halem, D., & van der Hoek, J. P. (2024). Dissolved organic carbon and ammonium removal kinetics study to redesign slow sand filters. (In preparation)

Abstract

Slow sand filters (SSFs) historically applied to produce biostable drinking water are limited by large surface footprints due to low flow rates, fine sand grains, and lengthy downtimes after cleaning. This research brings new knowledge on operational strategies to enhance the removal of biodegradable fraction of dissolved organic carbon (DOC) and ammonium (NH_4^+) in experimental sand filters, using kinetic models to evaluate removal rates. Removal rates of both DOC (k=0.681-0.723 min^{-1}) and NH_4^+ (k=0.135-0.139 min^{-1}) were similar for coarse sand (0.8-1.2 mm) and fine sand (0.3-0.6 mm), indicating that the area occupied by biofilm on sand is limiting rather than the sand grain surface area itself. Higher loading rate increased removal rates of both DOC (k=0.891-0.895 min^{-1}) and NH_4^+ (k=0.706-0.728 min^{-1}), suggesting enhanced activity of growing biofilms. Backwashing restored the removal rate of DOC within 10 days, but NH_4^+ recovery extended beyond this period, however regular backwash cycles will probably reduce this downtime, as commonly observed in RSFs.

This study demonstrated that operating filters under a novel range of operational conditions can boost the efficiency of drinking water filters designed for biological stability purposes. Future research is recommended to verify the applicability of these findings in low-loaded polishing filters, assessing their impact on other parameters related to biological stability, such as regrowth potential and assimilable organic carbon (AOC).

5.1 Introduction

Slow sand filters (SSFs) are robust technologies widely used in drinking water production to remove turbidity, pathogens, organic matter and chemical contaminants (Haig et al., 2011). Globally, these filters are used either as a single-stage treatment or as a final polishing step in multi-stage treatment schemes in drinking water treatment plants (DWTPs) (van der Kooij et al., 2017; Mauclaire et al., 2004). Control of biodegradable fraction of dissolved organic carbon (DOC) and ammonium (NH_4^+) is critical for drinking water utilities to prevent microbial regrowth in the distribution network and the formation of organic disinfection byproducts (Lopato et al., 2013; Terry & Summers, 2018). SSFs remove biodegradable fraction of DOC and NH_4^+ biologically, with heterotrophic bacteria mineralizing biodegradable organic carbon and nitrifying bacteria oxidizing NH_4^+ (Lee et al., 2014; Lehtola et al., 2001).

Biological processes in porous media filters are shaped by process variables such as sand grain size, substrate loading rates and flow rates (Lee et al., 2014; Perujo et al., 2017). Fine sand (0.15-0.40 mm) is recommended for SSFs to enhance water quality by better straining and adsorption of pathogens due to its narrow pores and large specific surface area (Bai et al., 2016; Hijnen et al., 2010). However, grain size distribution also affects microbial processes in the filter by controlling the distribution of electron donors and acceptors (Ellis & Aydin, 1995; Perujo et al., 2018). In addition, the small grain interstices of fine sand increases flow resistance, resulting in low flow rates (Haig et al., 2011); for instance, a typical full-scale SSF in Europe operates at flow rates of 0.1-0.4 $m^3/m^2/h$, compared to rapid sand filters (RSFs) that operate at 5-15 $m^3/m^2/h$ (Brandt et al., 2017; Ratnayaka et al., 2009). Flow rates and substrate loading rates impact the distribution and interaction of microbial processes (Lee et al., 2014; Perujo et al., 2018; Wang et al., 2022). Higher loading rates (described by the product of flow rate and influent concentration of substrate) increase substrate availability of substrates deep in the filter, but shorten the contact time between water and biofilm and/or sand (Perujo et al., 2017).

In current practice, SSFs are not backwashed like RSFs are. Instead, to prevent clogging, they are periodically scraped to remove the *Schmutzdecke* layer (de Souza et al., 2021a). This procedure leads to significant downtime for *Schmutzdecke* restoration (Chan et al., 2018). The downtime demands more surface area or an additional filter in multi-SSF setups to maintain the required volumetric capacity. Sand grain size and uniformity coefficient (UC) influence backwashing efficiency, e.g., fine sand can accelerate headloss, but is more easily fluidized, requiring lower backwash velocities (Bellamy et al., 1985; Dharmarajah et al., 1986). Backwashing has been shown to successfully restore the removal of turbidity and coliforms (de Souza et al., 2021a), however, the impact on removal of NH_4^+ and the biodegradable fraction of DOC remains unexplored.

This study aimed to investigate the removal kinetics of biodegradable fraction of DOC and NH_4^+ at

different operational strategies to redesign SSFs. Experimental sand filters with different grain sizes and loading rates, as well as backwashing, were assessed using kinetic models.

5.2 Materials and Methods

5.2.1 Lab-scale filter set-up and operation

The lab-scale SSF module consisted of four columns, 210 cm in length and 4 cm in diameter (Figure 1). The columns were filled with a support layer of 5 cm gravel (granule size: 5–7 mm) and 85 cm of working sand layer (quartz sand). Two grain sizes: fine sand (0.3-0.6 mm; d_{10}= 0.45 mm; uniformity coefficient (UC)=1.63) and coarse sand (0.8-1.2 mm; d_{10}=0.9 mm; UC=1.51) were used in F1-F2 and C1-C2 filters, respectively. The specific surface area of fine sand and coarse sand was 2.71×10^{-3} m^2/g sand and 2.14×10^{-3} m^2/g sand, respectively.

The specific sand surface area (A_s) was approximated by (Langenbach et al., 2010):

$$A_s = 6000/d_s\,(1-p) \quad (1)$$

where p is the porosity and d_s is the specific grain diameter (Langenbach et al., 2010):

$$d_s = d_{10}(1+2\log\log U) \quad (2)$$

where U is the uniformity coefficient (U).

Typically, DOC in water comprises of refractory (i.e. poorly biodegradable) carbon, biodegradable carbon and easily assimilable organic carbon (AOC) (Brandt et al., 2017; Schurer et al., 2022). The tap water contained 2.8 mg C/L of DOC (mostly refractory carbon, Table S1), and NH_4^+ and PO_4^{3-} concentrations were below 0.01 mg/L. Hence, experimental filters were supplied with non-chlorinated tap water dosed with easily biodegradable carbon compounds as a mixture of carboxylic acids-sodium acetate ($NaC_2H_3O_2$), sodium oxalate ($Na_2C_2O_4$) and sodium formate ($NaCHO_2$) (1:1:1), NH_4^+ as ammonia chloride (NH_4Cl) (Merck chemicals) and PO_4^{3-} as potassium dihydrogen phosphate (KH_2PO^{4-}) (Merck chemicals) (Table S2).The filters were operated for 135 days to evaluate the removal of biodegradable fraction of DOC and NH_4^+ under three different operational conditions (Table 1 and Figure 1):

1. Reference: F1, F2, C1 and C2 filters were operated at a hydraulic loading rate (HLR) of 0.5 m/h (flow rate-0.63 L/h) with influent concentrations of 0.85 mg C/L for DOC and 1 mg N/L for NH_4^+. The loading rates (determined by the product of flow rate and influent concentration) were 0.54 mg C/h and 0.63 mg/h for DOC and NH_4^+, respectively.

2. High loading rate: After 123 days of operation in the reference condition, the loading rates in F1 and

C1 filters were increased by raising HLR to 2 m/h (flow rate 2.5 L/h) and influent concentrations to 1.8 mg C/L for DOC and 2 mg N/L for NH_4^+. This resulted in loading rates of 4.5 mg C/h for DOC and 5 mg N/L for NH_4^+.

3. Backwashing: F2 and C2 filters operating in the reference condition were backwashed after 123 days using tap water at 20% expansion for 5 minutes. Filters were operated in the original reference condition after backwashing.

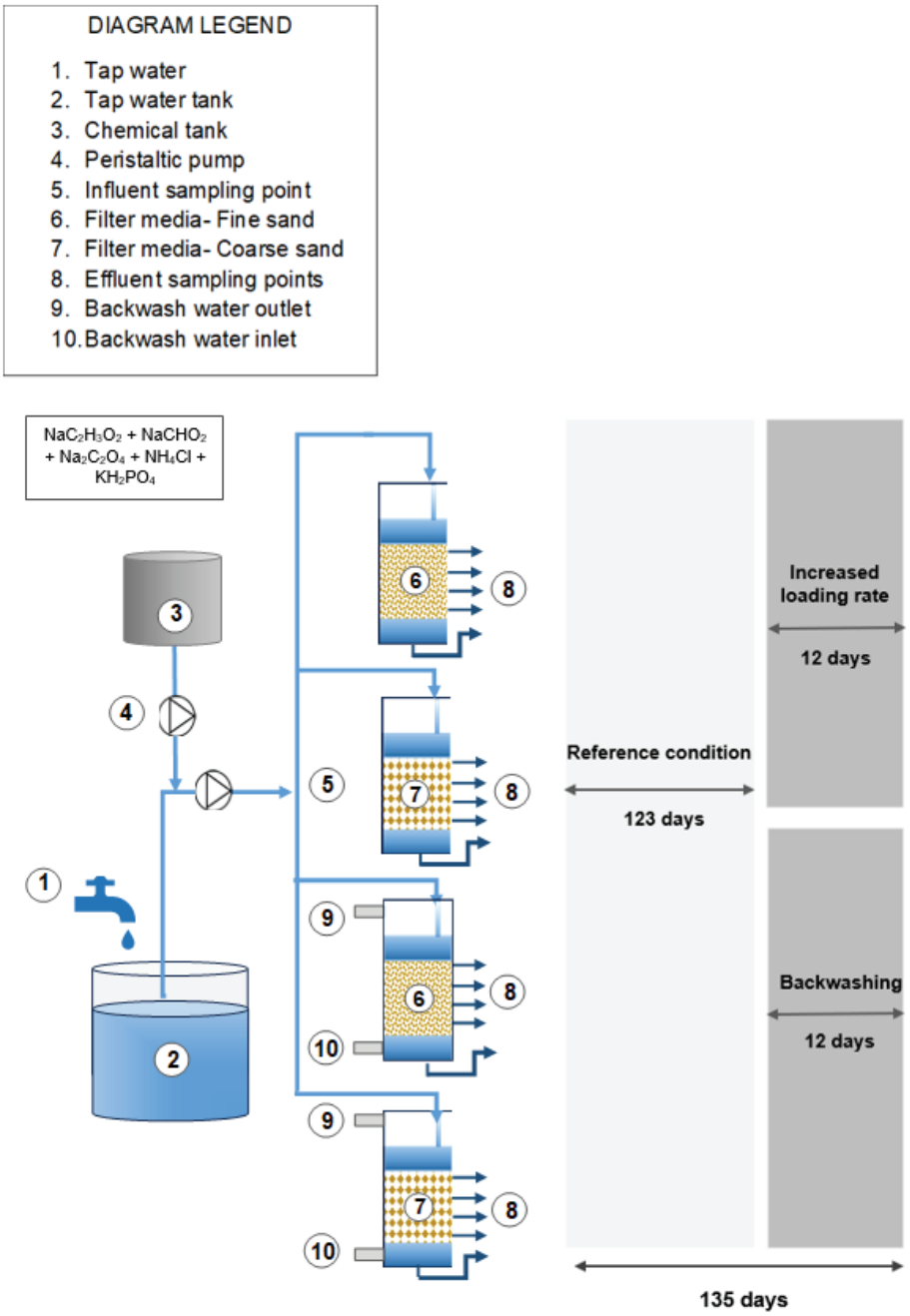

Figure 1 Schematic representation of laboratory scale SSFs

Table 1 Operational parameters for each experimental condition

Condition / Operational parameter	Reference (123 days)				Increased loading rate (12 days)		Backwash (12 days)	
	F1	F2	C1	C2	F1	C1	F2	C2
Hydraulic loading rate (m/h)	0.5				2.0		0.5	
Flow rate (L/h)	0.63				2.50		0.63	
	DOC							
Concentration (mg C/L)	0.85				1.80		0.85	
Loading rate (mg C/h)	0.54				4.50		0.54	
	NH_4^+							
Concentration (mg N/L)	1.0				2.0		1.0	
Loading rate (mg N/h)	0.63				5.0		0.63	

(The loading rates and concentrations of DOC and NH_4^+ are shown by mg C/h or mg C/L and mg NH_4^+-N/h or mg NH_4^+-N/L)

5.2.2 Analytical methods

The collected water samples were filtered through 0.45 µm syringe filters and then stored at 4°C before measurement. The reduction in the biodegradable fraction of DOC was measured using TOC-LCPH analyser (Limit of Detection [LOD]=0.1 mg/L) with an ASI-L autosampler (Shimadzu, Japan). Nitrite (NO_2^-) (LOD=0.01 mg N/L), nitrate (NO_3^-) (LOD=0.1 mg N/L), ammonium (NH_4^+) (LOD=0.01 mg N/L), and phosphate (PO_4^{3-}) (LOD=0.001 mg/L) ions were measured by Ion Chromatography (Dionex ICS-2100, Thermo, USA) equipped with an AS17- Column. DO, pH, electrical conductivity (EC) and temperature were measured with WTW electrodes (SenTix 940, TerraCon925 and FDO925, respectively).

Microbial activity on sand was measured by total ATP (tATP), using 1 g of wet media sample, following the Deposit and Surface Analysis test kit method from LuminUltra Technologies (Nemani et al., 2018). The measurements were read using a luminometer.

5.2.3 Environmental Scanning Electron Microscope

Fine sand and coarse sand from operating SSFs were inspected with Environmental Scanning Electron Microscope (ESEM). The combination of Philips XL30 ESEM and Tungsten filament electron microscope enabled up to 50,000x magnification at a 0 to 100% humidity range.

5.2.4 Kinetic modelling

Kinetic models were used to determine removal rates of the biodegradable fraction of DOC and NH_4^+ under various operational conditions. Based on the DOC and NH_4^+ depth profiles, the removal in the first 45 cm was considered for the model as tailing of removal (>99.7%) beyond this depth did not provide information for the model. Literature shows that NH_4^+ removal in biological filters follows first-order kinetics (Lopato et al., 2013; Tatari et al., 2013). Whereas, the removal of biodegradable organic matter can switch between first and second- order kinetics (Chen et al., 2016; Terry et al., 2024).

The first-order and second-order models are described using Equation (3) and (4), respectively.

$$C = C_0 * exp^{-k_1 t} \quad (1)$$

$$1/[C] = k_2 t + 1/[C_0] \quad (2)$$

where k_1 and k_2 (min^{-1}) are the first and second-order rate constants, respectively, t (min) is the hydraulic retention time (HRT), C_0 (mg/L) is the influent concentration at time 0 and C (mg/L) is the effluent concentration at time t.

In this study, the best-fitting model was determined by comparing correlation coefficient (R^2) values of first and second-order models. NH_4^+ rate constants were determined using first-order model due to higher R^2 values (0.81-0.99) compared to second-order model (0.4-0.98). Whereas, DOC rate constants were determined using second-order model due to its higher R^2 values (0.87-0.99) compared to first-order model (0.53-0.98).

5.2.5 Statistical analysis

The student's test (t-test) was carried out to identify the significance of differences for DOC and NH_4^+ removal among different columns and removal kinetic constants under different operational conditions.

5.3 Results

5.3.1 Effect of grain size on DOC and NH_4^+ removal

Figure 2 shows the rate constants (*k*) for biodegradable fraction of DOC and NH_4^+ removal over time of filter operation. The increase in k values for DOC and NH_4^+ aligns with the increasing trend of total biomass (measured by tATP) on sand with time (Figure S1), indicating the contribution of biological removal processes. The removal of biodegradable fraction of DOC and NH_4^+ commenced after days 50 and 80, respectively, indicating that DOC removal started prior to NH_4^+.

After 123 days of operation, *k* values for DOC were 0.723 min^{-1} and 0.681 min^{-1} in fine sand and coarse sand filters, respectively. For NH_4^+, *k* values of 0.139 min^{-1} and 0.135 min^{-1} were obtained for fine sand and coarse sand filters, respectively. The rate constants of DOC and NH_4^+ were statistically similar in both filters throughout the reference condition ($p>0.05$).

Figure 3 shows the depth profiles on day 123 for biodegradable fraction of DOC and NH_4^+ removal for both grain sizes. DOC was reduced to <0.1 mg/L in the first 50 cm, with predominant removal in the top 5 cm of the filter. Similarly, NH_4^+ was completely removed in the first 50 cm, but this occurred deeper in the bed below DOC removal. The decrease of NH_4^+ over depth was accompanied by a simultaneous increase in NO_2^- and NO_3^- (Figure S2 and S3). Removal rates for the investigated sand grain sizes were statistically similar ($p>0.05$) indicating that available grain surface area was not a limiting factor.

ESEM observations in Figure 4 show that the biofilms on fine and coarse sand grains were thin and patchy, suggesting that in both filters residual sand grain surface was available for biofilm colonization.

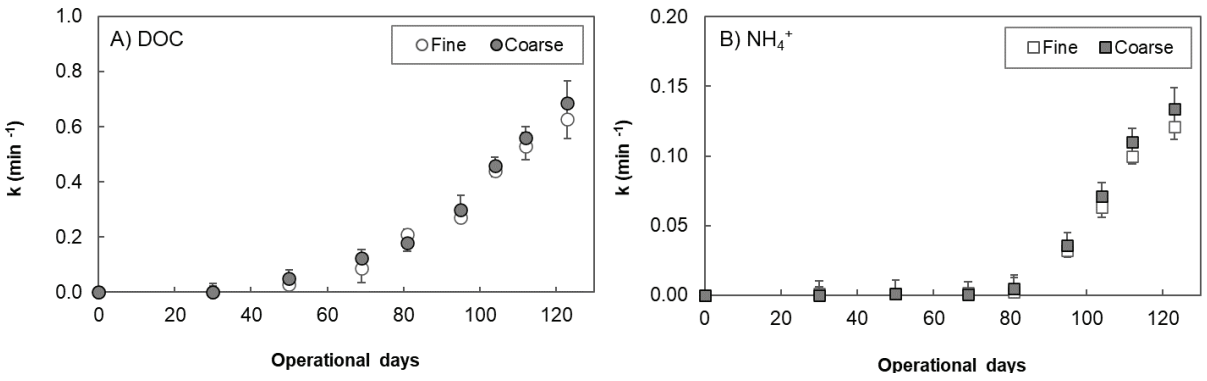

Figure 2 Removal rates of biodegradable fraction of DOC (A) and NH_4^+ (B) determined by second and first-order models, respectively in fine and coarse filters during operation under reference condition.

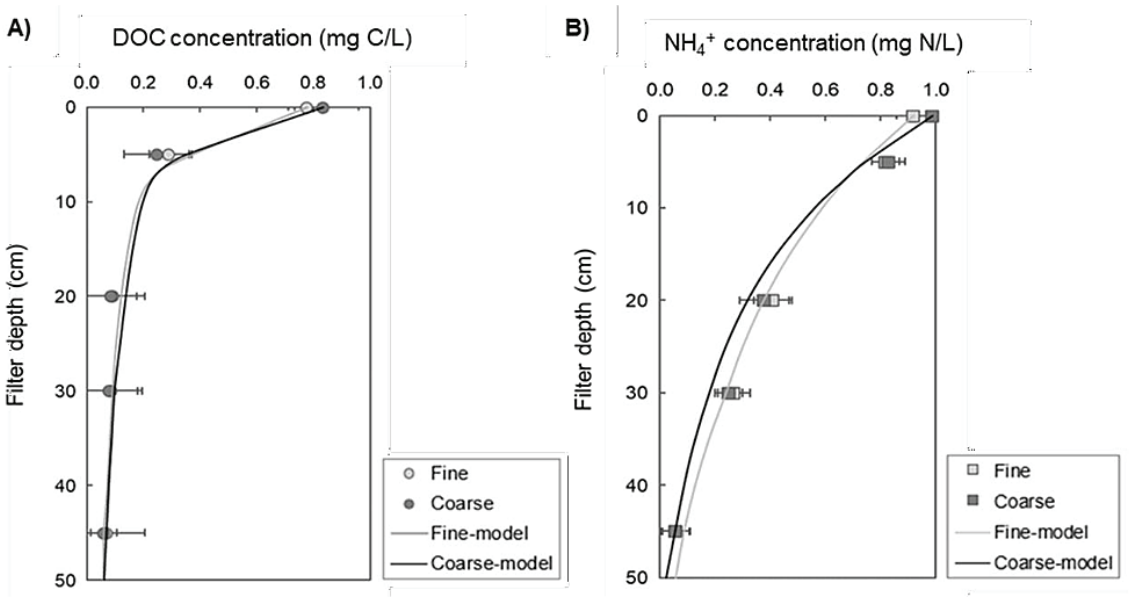

Figure 3 Depth profiles of biodegradable fraction of DOC (A) and NH_4^+ (B) in fine and coarse filters on day 123 of operation under reference condition. DOC and NH_4^+ removal are described by second and first-order kinetic

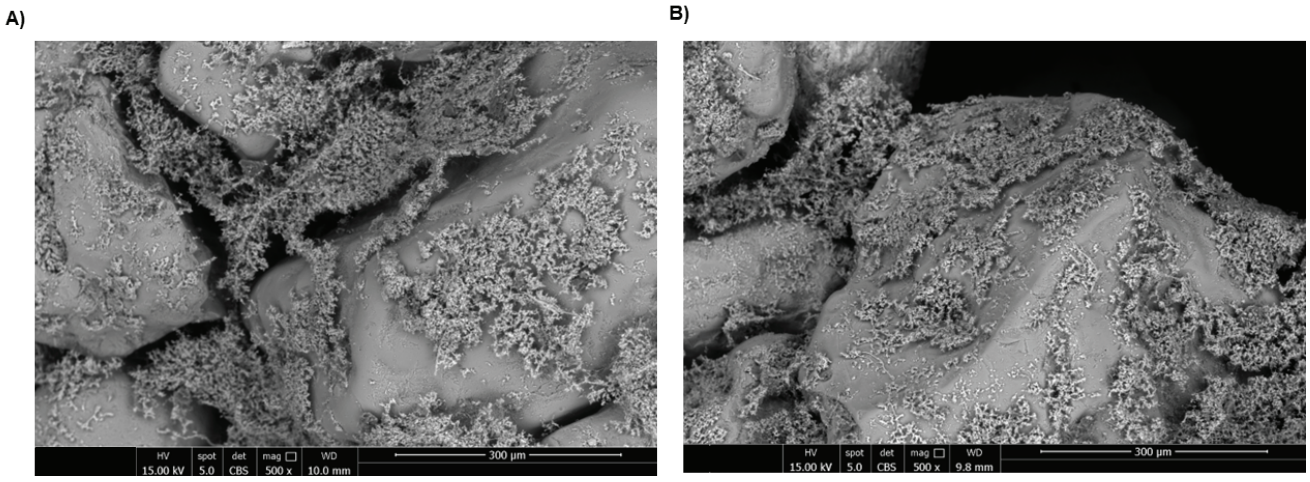

Figure 4 Environmental Scanning Electron Microscopy (ESEM) images of biofilm covered fine sand (A) and coarse sand (B)

5.3.2 DOC and NH_4^+ removal at higher loading rates

The loading rate of DOC and NH_4^+ was increased from 0.54 to 4.5 mg C/h and 0.63 to 5 mg N/h, respectively, by increasing both influent concentration and HLR. Hence, at a higher loading rate, the contact time per filter depth was shorter than in the reference condition.

A higher loading rate pushed the biodegradable fraction of DOC deeper in the filter bed, as seen by higher concentrations at specific depths (Figure 5A), i.e., DOC removal per centimeter of sand bed decreased. The *k* values decreased from 0.723 min^{-1} and 0.681 min^{-1} in the reference condition to 0.328 min^{-1} and 0.305 min^{-1}, for fine sand and coarse sand filters respectively (Figure 6A). After 10 days of the loading increase, DOC removal moved upwards in the filter, with an increase of *k* values by 2.7-3 fold to 0.895 min^{-1} and 0.891 min^{-1} for fine sand and coarse sand filters, respectively.

In contrast to DOC, NH_4^+ removal did not show a drop in rate constant after one day (Figure 5B). *k* values increased from 0.139 min^{-1} and 0.135 min-$^{-1}$ in the reference condition to 0.347 min^{-1} and 0.379 min^{-1} in fine sand and coarse sand filters, respectively (Figure 6B). After 10 days, the removal moved further upward in the filter with *k* values of 0.706 min^{-1} and 0.728 min^{-1} in fine sand and coarse sand filters, respectively.

The higher loading rate did not result in a difference in the removal rate between the fine and coarse sand filters, indicating that both granular media can host rapidly growing biofilms that support higher removal rates of the biodegradable fraction of DOC and NH_4^+.

5.3.3 DOC and NH_4^+ removal after backwashing

SSFs with fine sand and coarse sand operating under the reference condition were backwashed for 5 minutes at 20% expansion.

The removal rate constant of biodegradable fraction of DOC decreased after backwashing, with consequent deep infiltration into the filter (Figure 7A). The *k* values dropped from 0.723 and 0.681 min^{-1} to 0.133 and 0.155 min^{-1} in fine sand and coarse sand filters, respectively (Figure 8A). However, within 10 days after backwashing, *k* values increased to 1.148 and 1.161 min^{-1}, in fine sand and coarse sand filters respectively, exceeding the reference condition.

While DOC removal rate constants recovered within 10 days of backwashing, NH_4^+ removal rate constants did not (Figure 7B). One day after backwash, *k* values dropped from 0.139 min- 1 and 0.135 min-1 to 0.048 min^{-1} and 0.043 min^{-1} in fine sand and coarse sand filters, respectively (Figure 8B). After 10

days, the *k* values slightly increased to 0.069 min^{-1} in fine sand and 0.071 min^{-1} in coarse sand filter, but remained below its initial values in the reference condition.

It is worth mentioning that backwashing partly retained the total biomass at different depths in fine sand and coarse sand filters (Figure S4). Backwashing affected the removal of DOC and NH_4^+ similarly in both fine and coarse sand filters ($p>0.05$).

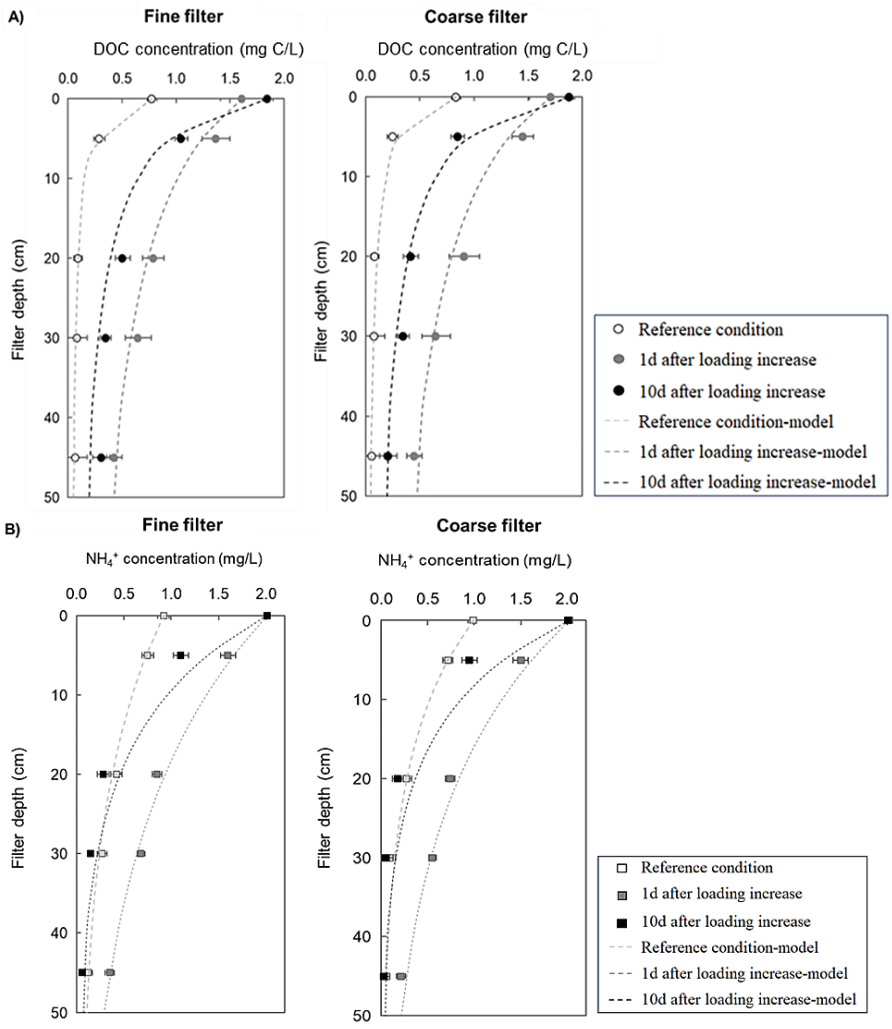

Figure 5 Depth profiles of biodegradable fraction of DOC (A) and NH_4^+ (B) at reference loading, and 1 day and 10 days after increasing the loading rate in fine and coarse filters. DOC and NH_4^+ removal was described by second and first-order kinetic models, respectively.

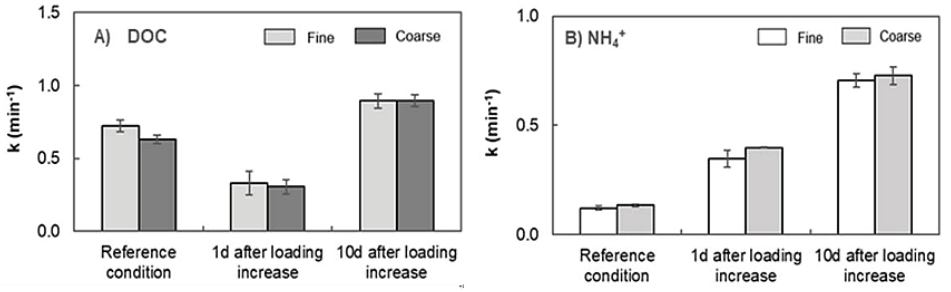

Figure 6 Removal rates of biodegradable fraction of DOC (A) and NH_4^+ (B) in reference condition, 1 day and 10 days after increasing the loading rate in fine and coarse sand filters.

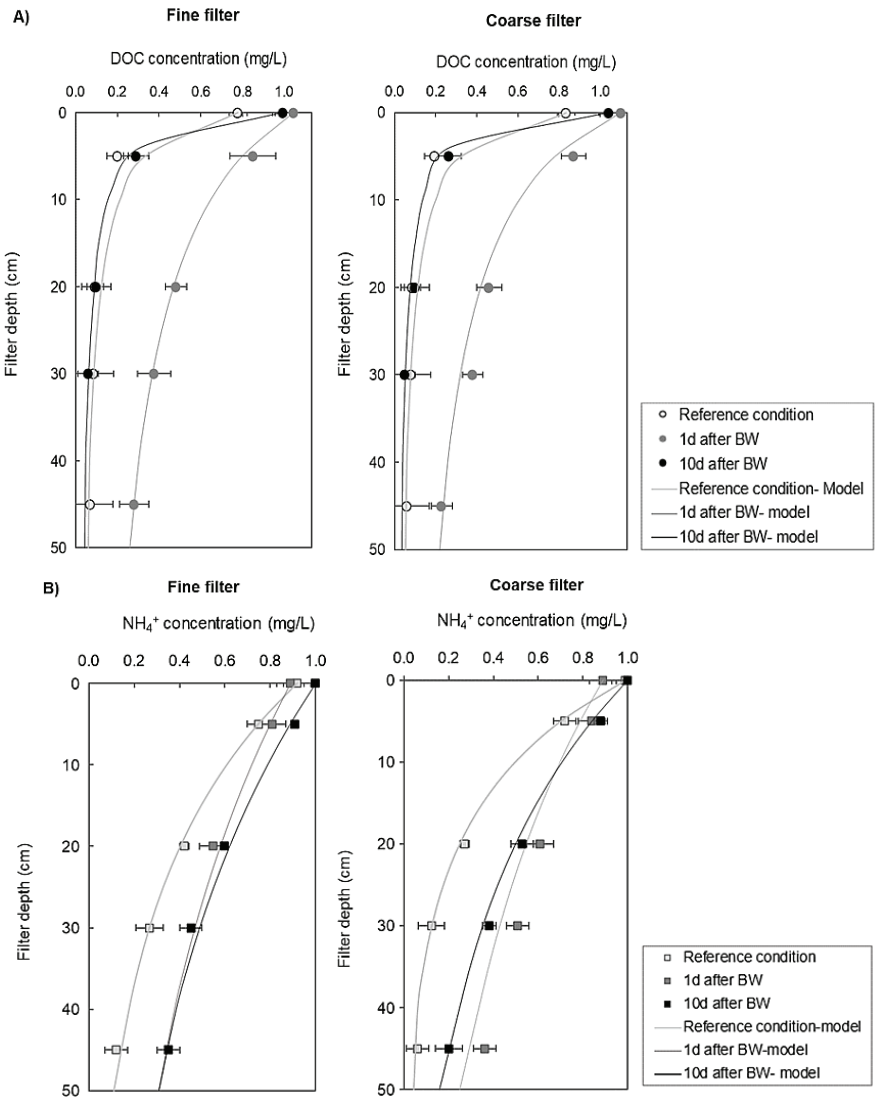

Figure 7 Depth profiles of biodegradable fraction of DOC (A) and NH_4^+ (B) during reference condition, 1 day and 10 days after backwashing (BW) in fine and coarse sand filters. The removal was described using second-order and first-order models for DOC and NH_4^+, respectively.

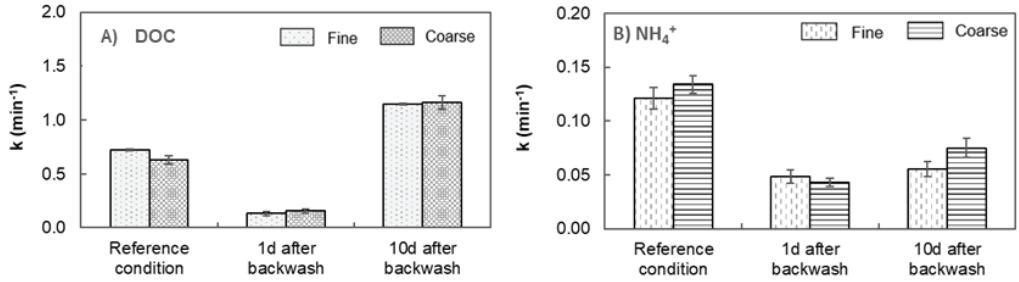

Figure 8 Removal rates of biodegradable fraction of DOC (A) and NH_4^+ (B) in reference condition, 1 day and 10 days after backwashing in fine and coarse sand filters.

5.4 Discussion

5.4.1 Similar removal rates in fine sand and coarse sand filters

Fine sand with grain size <0.5 mm is typically chosen for SSFs due to its large specific surface area and low porosity (Maiyo et al., 2023). Previously, fine grains and low flow were found to hinder microbial growth and organics removal (Essandoh et al., 2013) but coarse sand enhanced them by water exchange through larger pores (Dodds et al., 1996). On the contrary, Higashino et al., found coarse sand to reduce microbial oxygen uptake due to smaller sand surface area for biofilm development (Higashino et al., 2013). This study found statistically similar removal rate constants for fine sand (0.3-0.6 mm) and coarse sand (0.8-1.2 mm) filters, indicating that both systems are equally effective in removing DOC and NH_4^+.

The coarse sand grain size in this study, similar to the sand grain size in RSFs (Ratnayaka et al., 2009), had higher porosity and lower specific surface area than fine sand. The comparable performance of both filters suggests that the loss in surface area is not a limiting parameter within the investigated range of sand grain sizes. At the same flow rates, the coarse sand filter had a slightly longer HRT (22 minutes) than the fine filter (20 minutes) due to its higher water-holding capacity. This extended contact time likely boosts organic matter degradation and nitrification (Perez-Mercado et al., 2018; Perujo et al., 2017), potentially masking any loss in removal rate due to a smaller surface area in the coarse sand filter.

Biofilm coverage on sand grains could also explain the similar behaviour of fine sand and coarse sand filters. The biofilms developed on sand were thin and patchy, typical of oligotrophic environments which might have facilitated similar substrate access for microorganisms, irrespective of sand surface area (Hammes et al., 2011; Lee et al., 2014). Removal of the biodegradable fraction of DOC and NH_4^+ may be influenced by the surface area occupied by biofilm on sand, rather than the sand surface area. Hence, sand grain size is not a critical design parameter for the removal of biodegradable fraction of DOC and NH_4^+, as long as patchy biofilms develop on the sand grain. Further, enhanced removal at a higher loading rate highlights both increased activity of heterotrophs and nitrifiers in the existing biofilm (Lee et al., 2014; Tatari et al., 2014; Wang et al., 2022) and efficient utilisation of available surface area on sand by

growing biofilms. These observations indicate a surplus capacity for biodegradable fraction of DOC and NH_4^+ removal, suggesting that SSFs designed for the production of biologically stable drinking water could function efficiently at higher flow rates without compromising effluent quality. Operating filters under these high flow rate conditions reduces their physical footprint by a factor of four. To extend the applicability of these findings, future research is recommended at lower biodegradable fraction of DOC and NH_4^+ influent concentrations, typically found in polishing filters, ideally in combination with other biological stability parameters (e.g. regrowth potential).

5.4.2 Backwashing slow sand filters

In current practice, SSFs are not backwashed. Instead, to prevent clogging, they are periodically scraped to remove the *Schmutzdecke layer* (de Souza et al., 2021a). This procedure leads to significant downtime for *Schmutzdecke* restoration (Chan et al., 2018). The downtime demands more surface area or an additional filter in multi-SSF setups to maintain the required volumetric capacity. This study showed that both fine sand and coarse sand filters restored the removal capability of biodegradable fraction of DOC within 10 days of backwashing. In contrast, NH_4^+ recovery extended beyond this period, probably due to the redistribution of nitrification activity over filter depth and/or loss of nitrifying biomass from backwashing. However, backwashing regularly will result in a more uniform biofilm with nitrifies across filter depth and likely result in direct recovery as commonly observed in RSFs (Corbera-Rubio et al., 2023). In comparison, the recovery period after traditional scraping can vary from days to weeks or be negligible, depending on filter maturity and age (Abkar et al., 2024).

Until now, backwashing of large-scale SSFs has been challenged by complicated design (de Souza et al., 2021b). Moreover, backwashing was not considered viable until recently as it would disturb the *Schmutzdecke*, the primary barrier for contaminants and decrease filter efficiency. This study showed that biodegradable fraction of DOC and NH_4^+ can be effectively removed in the deeper layers, even at higher loading rates. While *Schmutzdecke* enhances the straining of larger-sized microorganisms such as pathogenic bacteria and protozoa for disinfection (Hijnen et al., 2004; Trikannad et al., 2023), it is not as important for removing DOC and NH_4^+ to improve the biological stability of water. Under such an operational scenario, the filter is more similar to a RSF, e.g., NH_4^+ removal in groundwater filters. In addition, backwashing partly retained the total biomass on sand, which might have promoted the recovery of removal processes of biodegradable DOC within 10 days. The slower growth rate of nitrifiers compared to heterotrophs might have delayed the complete recovery of NH_4^+ after backwashing (Nogueira et al., 2003). When operating SSFs at higher loading rates, clogging might develop faster, making backwashing an attractive procedure to reduce filter downtime. Research into the head loss development in highly loaded filters after backwashing is recommended, possibly in combination with tracking faecal pathogen removal.

Although backwashing proves practical for small-scale systems due to ease of operation and smaller dimensions (de Souza et al., 2021a; de Souza et al., 2021b), implementation in full- scale filters needs careful consideration due to the extensive filter surface area. A promising strategy is to divide the filter bed into segments that can be backwashed individually, while continuously operating the rest of the filter to minimise downtime.

5.5 Conclusions

This study explored the potential of coarse sand, high loading rate and periodic backwashing in SSFs for the removal of biological stability parameters NH_4^+ and biodegradable fraction of DOC. Coarse sand is found to be as effective as fine sand in removing biodegradable fraction of DOC and NH_4^+, indicating that their removal processes are not limited by sand surface area. Patchy biofilms were developed on the sand surface, leaving residual sand surface area for process enhancement at higher loading rates. Backwashing completely restored the removal rate of biodegradable fraction of DOC within 10 days, while NH_4^+ recovery extended beyond this period, but regular backwash cycles will likely reduce this downtime, as commonly observed in RSFs. This study demonstrated that operating filters under a novel range of operational conditions can boost the efficiency of drinking water filters designed for biological stability purposes. Future research is recommended to verify the applicability of these findings in low-loaded polishing filters, assessing their impact on other parameters related to biological stability, such as regrowth potential and assimilable organic carbon (AOC).

5.6 Supplementary information

Table S1 Dissolved organic carbon (DOC) composition in tap water determined by liquid chromatography- organic carbon detection (LC-OCD)

DOC composition in tap water	
Fractions	**Concentration (mg/L)**
Low molecular-weight acids	0.042 ± 0.039
Low molecular-weight neutrals	0.210 ± 0.028
Building blocks	0.397 ± 0.046
Biopolymers	0.110 ± 0.018
Humics	0.951 ± 0.057

Table S2 Composition and concentration of compounds dosed in tap water

Condition	Parameter	Dosed concentration (mg/L)	Compound	Chemical concentration (mg/L)
Reference	DOC	0.85	Sodium acetate ($NaC_2H_3O_2$)	1.607
			Sodium formate ($NaCHO_2$)	1.606
			Sodium oxalate ($Na_2C_2O_4$)	1.582
	NH_4^+-N	1	Ammonium chloride (NH_4Cl)	3.821
	PO_4^{3-}-P	0.015	Pottasium dihydrogen phosphate (KH_2PO_4)	0.048
Increased loading rate	DOC	1.8	Sodium acetate ($NaC_2H_3O_2$)	3.402
			Sodium formate ($NaCHO_2$)	3.401
			Sodium oxalate ($Na_2C_2O_4$)	3.35
	NH_4^+-N	2	Ammonium chloride (NH_4Cl)	7.643
	PO_4^{3-}-P	0.03	Pottasium dihydrogen phosphate (KH_2PO_4)	0.169

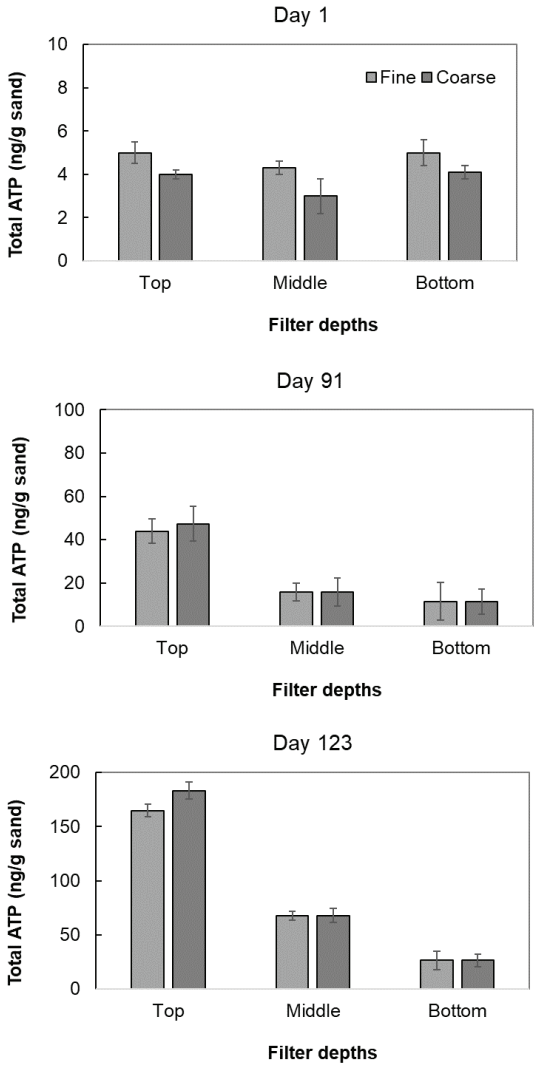

Figure S1 Total biomass on sand measured by Total ATP at different depths of fine and coarse filters over time during operation

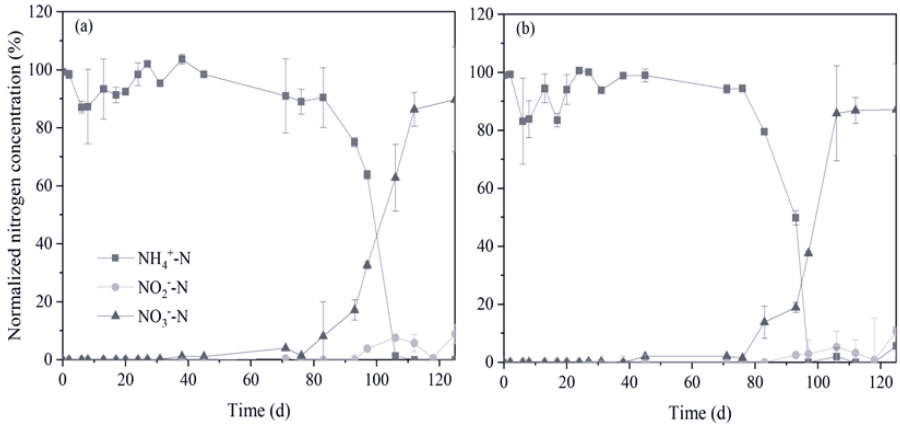

Figure S2 Temporal changes in NH_4^+, NO_3^- and NO_2^- in the effluents of fine (a) and coarse (b) columns under reference condition.

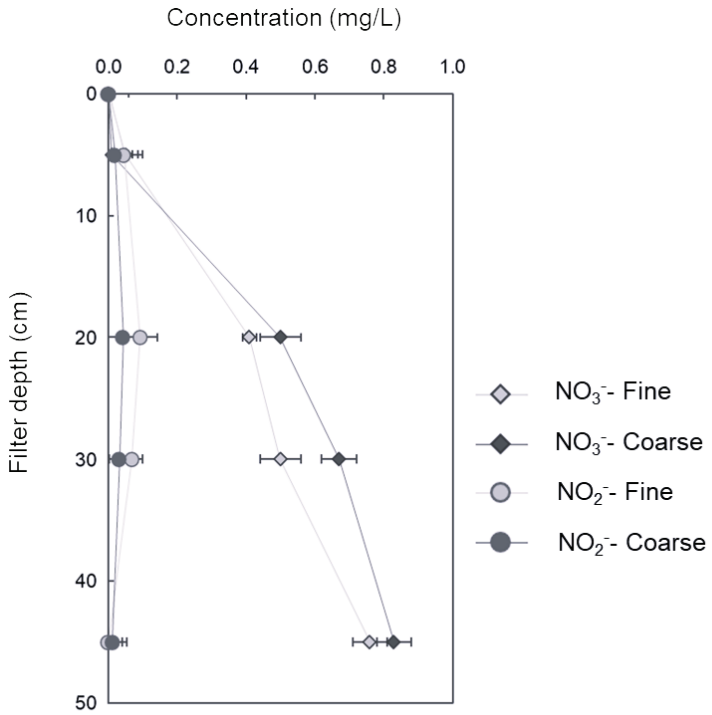

Figure S3 Depth profiles of NO_3^- and NO_2^- in fine and coarse columns after 123 days of operation under reference condition. NO_2^- concentrations were lower than 0.001 mg/L

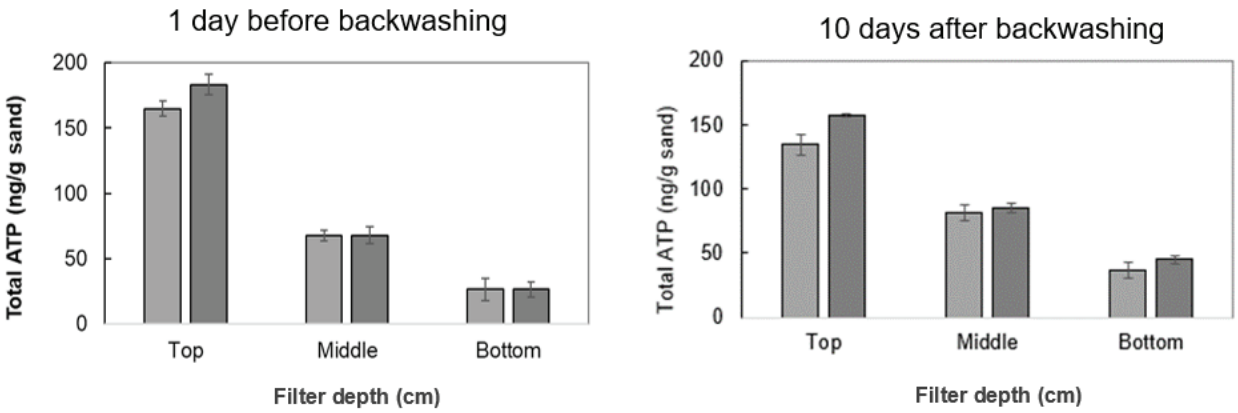

Figure S4 Microbial activity on sand measured by Total ATP in fine and coarse filters 10 days after increasing the loading rate and after backwashing

References

Abkar, L., Moghaddam, H. S., & Fowler, S. J. (2024). Microbial ecology of drinking water from source to tap. *Science of the Total Environment*, 908(October 2023), 168077.

Bai, H., Cochet, N., Pauss, A., & Lamy, E. (2016). Bacteria cell properties and grain size impact on bacteria transport and deposition in porous media. *Colloids and Surfaces B: Biointerfaces*, 139, 148–155.

Bai, X., Dinkla, I. J. T., & Muyzer, G. (2023). Shedding light on the total and active core microbiomes in slow sand filters for drinking water production. *Water Research*, 243(July), 120404.

Bellamy, W., Hendricks, D., Logsdon, G., 1985. Slow sand filtration: influences of selected process variables. Am. Water Works Assoc. 77 (12), 62–66

Brandt, M. J., Johnson, K. M., Elphinston, A. J., & Ratnayaka, D. D. (2017). Water Filtration.
In *Twort's Water Supply* (pp. 367–406). Elsevier.

Chan, S., Pullerits, K., Riechelmann, J., Persson, K. M., Rådström, P., & Paul, C. J. (2018). Monitoring biofilm function in new and matured full-scale slow sand filters using flow cytometric histogram image comparison (CHIC).
Water Research, 138, 27–36.

Chen, F., Peldszus, S., Elhadidy, A. M., Legge, R. L., Van Dyke, M. I., & Huck, P. M. (2016). Kinetics of natural organic matter (NOM) removal during drinking water biofiltration using different NOM characterization approaches.
Water Research, 104, 361–370.

Chen, L., Zhai, Y., van der Mark, E., Liu, G., van der Meer, W., & Medema, G. (2021). Microbial community assembly and metabolic function in top layers of slow sand filters for drinking water production. *Journal of Cleaner Production*, 126342.

Corbera-Rubio, F., Laureni, M., Koudijs, N., Müller, S., van Alen, T., Schoonenberg, F., ... & van Halem, D. (2023). Meta-omics profiling of full-scale groundwater rapid sand filters explains stratification of iron, ammonium and manganese removals. *Water Research*, 233, 119805.

Dharmarajah. A.H, J.L. Cleasby, Predicting the expansion behavior of filter media, J. Am. Water Work. Assoc. 78 (1986) 66–76

de Souza, F. H., Roecker, P. B., Silveira, D. D., Sens, M. L., & Campos, L. C. (2021a). Influence of slow sand filter cleaning process type on filter media biomass: backwashing versus scraping. *Water Research*, 189.

de Souza, Fernando Hymnô, Pizzolatti, B. S., & Sens, M. L. (2021b). Backwash as a simple operational alternative for small-scale slow sand filters: From conception to the current state of the art. *Journal of Water Process Engineering*, 40(December 2020), 101864.

Ellis, K. V., & Aydin, M. E. (1995). Penetration of solids and biological activity into slow sand filters. *Water Research*, 29(5), 1333–1341.

Essandoh, H. M., Tizaoui, C., & Mohamed, M. H. (2013). Removal of dissolved organic carbon and nitrogen during simulated soil aquifer treatment. *Water research*, 47(11), 3559-3572.

Haig, S. J., Collins, G., Davies, R. L., Dorea, C. C., & Quince, C. (2011). Biological aspects of slow sand filtration: Past, present and future. *Water Science and Technology: Water Supply*, 11(4), 468–472.

Hammes, F., Velten, S., Egli, T., & Juhna, T. (2011). Biotreatment of Drinking Water. *Comprehensive Biotechnology, Second Edition*, *6*(December 2017), 517–530.

Hijnen, W. A.M., Suylen, G. M. H., Bahlman, J. A., Brouwer-Hanzens, A., & Medema, G. J. (2010). GAC adsorption filters as barriers for viruses, bacteria and protozoan (oo)cysts in water treatment. *Water Research*, 44(4), 1224–1234.

Hijnen, Wim A.M., Schijven, J. F., Bonné, P., Visser, A., & Medema, G. J. (2004). Elimination of viruses, bacteria and protozoan oocysts by slow sand filtration. *Water Science and Technology*, 50(1), 147–154.

Higashino, M. (2013). Quantifying a significance of sediment particle size to hyporheic sedimentary oxygen demand with a permeable stream bed. Environmental Fluid Mechanics, 13(3), 227-241.

Hübner, U., Miehe, U., & Jekel, M. (2012). Optimized removal of dissolved organic carbon and trace organic contaminants during combined ozonation and artificial groundwater recharge. *Water Research*, 46(18), 6059–6068.

Langenbach, K., Kuschk, P., Horn, H., & Kästner, M. (2010). Modeling of slow sand filtration for disinfection of secondary clarifier effluent. *Water Research*, 44(1), 159–166.

Lee, C. O. (2014). Processes effecting nitrification performance in biological rapid sand filters.

Lehtola, M. J., Miettinen, I. T., Vartiainen, T., Myllykangas, T., & Martikainen, P. J. (2001). Microbially available organic carbon, phosphorus, and microbial growth in ozonated drinking water. *Water Research*, 35(7), 1635–1640.

Lopato, L., Röttgers, N., Binning, P. J., & Arvin, E. (2013). Heterogeneous Nitrification in a Full-Scale Rapid Sand Filter Treating Groundwater. *Journal of Environmental Engineering*, 139(3), 375–384.

Maiyo, J. K., Dasika, S., & Jafvert, C. T. (2023). Slow Sand Filters for the 21st Century: A Review. *International Journal of Environmental Research and Public Health*, 20(2).

Mauclaire, L., Schürmann, A., Thullner, M., Gammeter, S., & Zeyer, J. (2004). Sand filtration in a water treatment plant: Biological parameters responsible for clogging. *Journal of Water Supply: Research and Technology* - AQUA.

Nemani, V. A., McKie, M. J., Taylor-Edmonds, L., & Andrews, R. C. (2018). Impact of biofilter operation on microbial community structure and performance. *Journal of Water Process Engineering*, 24, 35–41.

Nogueira, R., Melo, L. F., Purkhold, U., Wuertz, S., & Wagner, M. (2002). Nitrifying and heterotrophic population dynamics in biofilm reactors: effects of hydraulic retention time and the presence of organic carbon. *Water research*, 36(2), 469-481.

Perez-Mercado, L. F., Lalander, C., Berger, C., & Dalahmeh, S. S. (2018). Potential of biochar filters for onsite wastewater treatment: Effects of biochar type, physical properties and operating conditions. *Water (Switzerland)*, 10(12).

Perujo, N., Romaní, A. M., & Sanchez-Vila, X. (2018). Bilayer Infiltration System Combines Benefits from Both Coarse and Fine Sands Promoting Nutrient Accumulation in Sediments and Increasing Removal Rates. *Environmental Science and Technology*, 52(10), 5734–5743.

Perujo, N., Sanchez-Vila, X., Proia, L., & Romaní, A. M. (2017). Interaction between Physical Heterogeneity and Microbial Processes in Subsurface Sediments: A Laboratory-Scale Column Experiment. *Environmental Science and Technology*, 51(11), 6110–6119.

Ratnayaka, D. D., Brandt, M. J., & Johnson, K. M. (2009). Water Filtration Granular Media Filtration. In *Water Supply* (pp. 315–350). Elsevier.

Schurer, R., Hijnen, W. A. M., & Van Der Wal, A. (2022). The significance of the biomass subfraction of

high-MW organic carbon for the microbial growth and maintenance potential of disinfectant-free drinking water produced from surface water. *Water Research*, 209, 117898.

Tatari, K., Smets, B. F., & Albrechtsen, H. J. (2013). A novel bench-scale column assay to investigate site-specific nitrification biokinetics in biological rapid sand filters. *Water Research*, 47(16), 6380–6387.

Tatari, K. (2014). Nitrification biokinetics in rapid sand filters for drinking water treatment. DTU Environment.

Terry, L. G., Peterson, E., & Summers, R. S. (2024). Organic matter biofiltration performance modeling: Influence of influent water quality, operating conditions, and biomass. *Water Research*, 249(August 2023).

Terry, L. G., & Summers, R. S. (2018). Biodegradable organic matter and rapid-rate biofilter performance: A review. In *Water Research* (Vol. 128, pp. 234–245).

Trikannad, S. A., van Halem, D., Foppen, J. W., & van der Hoek, J. P. (2023). The contribution of deeper layers in slow sand filters to pathogens removal. *Water Research*, 237(April), 119994.

van der Kooij, D., Veenendaal, H. R., van der Mark, E. J., & Dignum, M. (2017). Assessment of the microbial growth potential of slow sand filtrate with the biomass production potential test in comparison with the assimilable organic carbon method. *Water research*, 125, 270-279.

Dodds, W. K., Randel, C. A., & Edler, C. C. (1996). Microcosms for Aquifer Research: Application to Colonization of Various Sized Particles by Ground-Water Microorganisms. Groundwater, 34(4), 756-759.

Wang, J., Poursat, B. A. J., Feng, J., de Ridder, D., Zhang, C., van der Wal, A., & Sutton, N. B. (2022). Exploring organic micropollutant biodegradation under dynamic substrate loading in rapid sand filters. *Water Research*, 221(July), 118832.

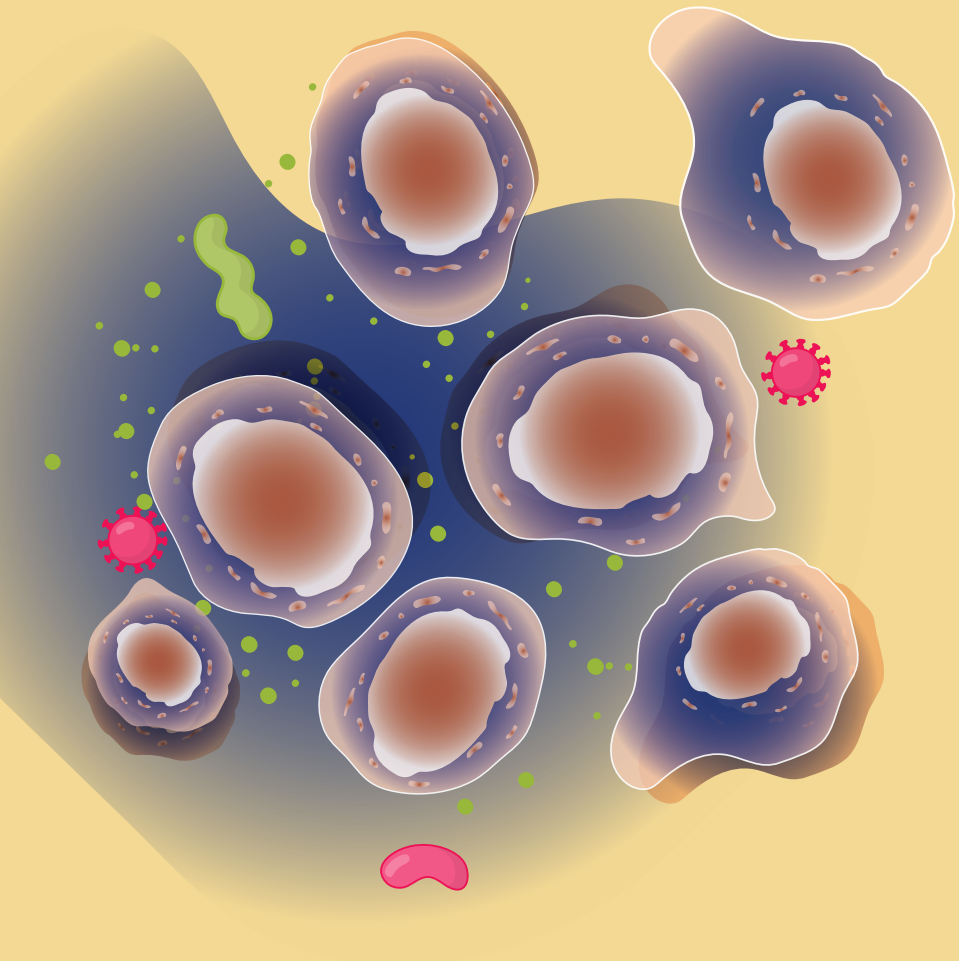

Chapter 6

Conclusions and Outlook

6.1 Main conclusion

The overall aim of this PhD thesis was to advance the understanding of physical-chemical and biological processes underlying disinfection and production of biologically stable drinking water in SSFs, focusing on the previously overlooked deeper layers rather than solely on the *Schmutzdecke*. Moreover, the aim was to identify process limitations and inform the redesigning of modern, polishing SSFs. The findings derived from each research question have collectively shaped the main conclusion of this thesis.

The processes underlying the removal of enteric pathogens, DOC and NH_4^+ are distinct yet effective across filter depths, and modern polishing SSFs have been found to operate more efficiently under a novel range of operational conditions.

This conclusion underlines that the treatment capacity in SSFs extends far beyond the traditional Schmutzdecke and filters can function efficiently when they are specifically designed and operated to harness the biological processes critical for disinfection and producing biologically stable drinking water. In any case, leveraging the full potential of the deep sand bed through new design rules and operational strategies can significantly enhance the efficiency of next-generation SSFs. The insights into the specific roles of various processes in the removal of pathogens, DOC and NH_4^+ have led to distinct conclusions for each function.

6.2 Disinfection by SSFs

The extensive depth of SSFs can inherently provide a multi-barrier approach to disinfection. Yet, the emphasis has been largely limited to the top *Schmutzdecke* layer, particularly in studies with young filters where this layer is more developed than the deep sand bed. In full-scale systems operating for several years, the *Schmutzdecke* is frequently regenerated but the deeper layers are left undisturbed. The disinfection capability of mature full-scale filters was quantified using an innovative experimental setup that used filter material from various depths (Chapter 2). The deeper layers were found to outperform the *Schmutzdecke* in removing *E.coli* WR1 and PhiX 174—surrogates for enteric bacteria and viruses, respectively due to the presence of well-established biofilms in the deep sand bed. Although the retention rate per cm bed height of *E.coli* WR1 and PhiX 174 was 3-4 times lower in the deeper layers than in the *Schmutzdecke*, the extensive height of the deep sand bed compensated for this difference, enhancing total removal.

Due to the overlapping action of physical-chemical and biological processes, it is complex to discern their independent effect. The contribution of these processes in bacteria and virus removal at different depths was quantified under three conditions in Chapter 2. First, the removal with active biofilm

determined the role of (micro)organisms (predation, grazing and the inactivation through enzymes). Second, inactive biofilm condition showed removal caused by biofilm alone (straining and attachment). Third, no biofilm condition determined removal exclusively by sand (straining and attachment). The results revealed that (micro) organism-led mechanisms were primarily responsible for the removal of *E.coli* WR1 in both the *Schmutzdecke* and deeper layers. This was supported by the observation that the relative abundance of dominant taxa within the prokaryotic community was similar across both the *Schmutzdecke* and deeper layers (Chapter 3). A similar observation with eukaryotic communities was reported previously (Stott et al., 2001; Haig et al., 2015). Further, straining and attachment in the biofilm and sand, served as secondary mechanisms in bacteria removal. Their retention by straining might have been enhanced particularly in the *Schmutzdecke* with narrow pore radii of 0.5-35 µm, resulting from increased collisions of bacteria with the biofilm. In contrast, PhiX removal was found to be largely influenced by attachment onto sand, aided by Brownian diffusion. Despite the natural repulsion between the negatively charged virus and sand surfaces at neutral pH, the presence of positively charged iron and manganese oxides on sand enhanced virus attachment. Virus removal subsequently occurred within the biofilm, likely through mechanisms such as grazing, inactivation by proteolytic enzymes, and binding to extracellular polymeric substances (EPS), similarly in both the *Schmutzdecke* and deeper layers.

This additional capacity of the deep sand bed in retaining microbial biomass was also revealed from the response of the deeper layers to *Schmutzdecke* scraping in mature SSFs (Chapter 3). Although scraping disturbed the functionality of the top layers and released microbial biomass, the deeper layers effectively captured it, demonstrating the robustness of the processes within the mature sand bed. Further, the resilience of microbial communities in these deeper layers was evident from the consistent microbial composition of the effluent, both before and after scraping.

6.3 Biological stability in SSFs

The polishing SSFs succeeded in removing both readily and slowly biodegradable carbon and NH_4^+, crucial for reducing the regrowth potential of drinking water (Chapters 3 and 5). The *Schmutzdecke* removed a major share of DOC but the removal processes were not limited to this layer. In the event of scraping, the deeper layers of full-scale filters assumed the function of the top layer in reducing the degradable fraction of DOC, ensuring consistent effluent quality. The presence of biological processes in the deeper layers was evident by the release of easily biodegradable carbon, including low molecular weight acids and neutrals (Chapter 4). This release occurred in both mature and young filters, regardless of biofilm maturity and was subsequently removed in the deep sand bed. The contribution of biological processes in DOC removal was supported by the prevalence of heterotrophic species like *Gemmataceae* and *Vicinamibacteraceae*, adept at degrading DOC and present throughout the *Schmutzdecke* and deeper layers.

Nitrification, primarily responsible for NH_4^+ removal, occurred below the *Schmutzdecke*, separated from DOC removal. Nitrifiers such as *Nitrospiraceae Nitrosomonadaceae* and *Nitrosopumilaceae* capable of adapting to varying NH_4^+ concentrations populated the deeper layers corresponding to the distribution of NH_4^+ with depth. The spatial separation of microbial communities in the sand bed was based on the distribution of chemical species and the growth rates of specific microbial groups, with heterotrophs dominating the top layers due to the high load of easily biodegradable carbon near the surface of the filter and their fast growth rate. In contrast, nitrifiers, which have a relatively slower growth rate, inhabited the deeper layers, allowing for the compartmentalization of different biological processes. The observed release of DOC in both young and mature filters occurred in these deeper layers, suggesting that the release might have been caused by two mechanisms: the release of carbon from starving nitrifiers due to NH_4^+ and NO_2^- limitation, or the conversion of slowly degradable carbon such as biopolymers into easily biodegradable carbon. However, this released carbon did not threaten the effluent quality as it was effectively captured in the bottom layers of the filter, indicating an interaction between physical-chemical and biological processes in the sand bed.

In experiments with laboratory filters, biological processes influencing DOC and NH_4^+ removal were found to be not limited by sand grain size within the investigated range of 0.3-1.2 mm. The patchy biofilms that developed on the sand grains ensured similar substrate access for microorganisms, regardless of sand surface area, and supported the removal of both DOC and NH_4^+. Even in the presence of shorter contact times and higher loading rates, the growing biofilms were able to utilize the available surface area of the sand grain effectively and achieve complete removal of biodegradable fraction of DOC and NH_4^+. These findings indicated that sand grain size and contact time no longer posed limitations for improving the performance of SSFs designed for biological stability. In these columns, redistributing the biological processes throughout the filter by backwashing was shown to restore performance within 10 days for DOC but took slightly longer for NH_4^+. The slower growth rate of nitrifiers compared to heterotrophs might have delayed the complete recovery of NH_4^+ removal after backwashing. Thus, SSFs designed for biological stability demonstrated the capability to perform efficiently when operated similarly to rapid rate biofilters.

6.4 Proposed design rules and operational conditions for modern SSFs

SSFs have been a reliable technology for drinking and wastewater treatment for decades now. Yet, their extensive land requirement has limited practitioners from widely adopting this sustainable technology in modern settings where land availability is limited and demand for clean water is escalating due to population growth. The results in this thesis suggest new design and operational strategies to reduce the physical footprint and improve the maintenance of SSFs. A primary focus among practitioners is better management of the *Schmutzdecke* to accelerate the ripening period after scraping. In polishing SSFs, like

in the Netherlands, that often handle influent with <10 µgC/L of AOC and undetectable pathogen indicators, using ATP and FCM in effluent monitoring can already shorten the current ripening of 6-9 weeks to less than 15 days. However, it is further necessary to identify reliable ripening indicators that correlate with both pathogenic indicators and biological stability parameters, in low-loaded influents.

An effective approach to accelerate the ripening period is to enhance and utilize the capacity of the deep sand bed, rather than focusing solely on the development of the *Schmutzdecke*. This implies that maintaining the current sand bed depth of approximately 1 meter is necessary, which acts as a multi-layered barrier to handle fluctuations in influent quality and disturbances after scraping. Moreover, these different depths support various microenvironments for multiple processes like nitrification and organic carbon degradation to occur, thereby removing a wide range of contaminants. In newly built filters, increasing the filtration rate can potentially shorten the ripening period by pushing a higher load of microbial growth-promoting compounds deeper into the sand bed. This encourages biological processes to develop not just at the surface but also deeper within the bed. This thesis proposes increasing the filtration rate by a factor of four, which considerably reduces the physical footprint, without compromising effluent quality in terms of DOC and NH_4^+. Further research is recommended to determine whether this approach can significantly reduce the ripening period by assessing overall effluent quality.

SSFs can benefit from frequent backwashing to maintain an even distribution of biological processes within the sand bed. The current use of fine sand, however, creates significant resistance to backwashing. The findings of this thesis reveal that the development of biological processes in SSFs is independent of the surface area of the sand grains. Therefore, for new SSFs, coarser sand (with grain sizes of 0.8-1.2 mm) is recommended as the filter media. This change facilitates easier backwashing, allowing for lower backwash velocities and promotes operation at higher filtration rates. In the start-up phase, filters can be frequently backwashed. For large, full-scale filters, it is effective to segment the sand bed vertically and backwash sections independently at suitable flow backwash velocities, allowing the rest of the filter to operate continuously. New SSFs could adopt a cascade design where the top layers are physically separated from the deep sand bed. This allows for frequent and targeted backwashing of the top layers where major clogging occurs, while the deeper sections continue to operate without interruption for extended periods. It is important to note that long-operating full-scale filters are typically scraped, and introducing backwashing could disrupt established processes and compromise performance. Therefore, further research into the effects of backwashing on ripening, clogging, and disinfection is recommended for both new and mature filters. Additionally, determining optimal backwashing parameters are essential.

6.5 Scope of SSFs beyond drinking water treatment

SSFs, known for their multi-barrier treatment capability and versatility in addressing a wide range of contaminants, are an excellent choice for integration into hybrid systems to enhance the performance of existing and/or novel water treatment technologies. For example, membrane biofouling is a persistent issue in many water treatment facilities. Typically, integrated or hybrid membrane systems use biocides like chlorine, ozone, and UV irradiation to manage this problem. However, the use of biocides can pose challenges for the membrane components and may result in environmental pollution. SSFs are ideally suited as a pre-treatment for membrane systems due to their potential to limit biofouling by removing microbial biomass, and growth- promoting compounds (AOC, PO_4^{3-}, NH_4^+) in water.

In the context of water reuse, SSFs stand out as a sustainable alternative to technologies such as ultrafiltration, reverse osmosis, and ozone treatment. These alternatives are often capital- intensive and complex, making them less suitable for low and middle-income countries where reclaimed water is emerging as a vital alternative water source. If the water has to serve high- end purposes, contaminants such as enteric pathogens, emerging contaminants such as pharmaceuticals and personal care products (PPCPs) and antimicrobial resistance need to be tackled. Recently, SSFs have been proven to be effective against at least two to three categories of these contaminants, particularly when integrated with systems such as activated carbon (Li et al., 2018; D'Alessio et al., 2015; Pompei et al., 2017). The adaptability of SSF under diverse environmental settings makes it a viable tertiary technology in a multi-barrier treatment scheme in both decentralized and centralized treatment. To maximize the potential of SSFs in modern water treatment and reuse scenarios, ongoing research into mechanisms for removing emerging contaminants and improved design and operation is crucial.

References

D'Alessio, M., Yoneyama, B., Kirs, M., Kisand, V., & Ray, C. (2015). Pharmaceutically active compounds: Their removal during slow sand filtration and their impact on slow sand filtration bacterial removal. Science of the Total Environment, 524, 124-135.

Haig, S. J., Quince, C., Davies, R. L., Dorea, C. C., & Collins, G. (2015). The relationship between microbial community evenness and function in slow sand filters. MBio, 6(5), e00729- 15.

Li, J., Zhou, Q., & Campos, L. C. (2018). The application of GAC sandwich slow sand filtration to remove pharmaceutical and personal care products. Science of the Total Environment, 635, 1182-1190.

Pompei, C. M., Ciric, L., Canales, M., Karu, K., Vieira, E. M., & Campos, L. C. (2017). Influence of PPCPs on the performance of intermittently operated slow sand filters for household water purification. Science of the total environment, 581, 174-185.

Stott, R., May, E., Matsushita, E., & Warren, A. (2001). Protozoan predation as a mechanism for the removal of Cryptosporidium oocysts from wastewaters in constructed wetlands. Water Science and Technology, 44(11-12), 191-198.

Summary

Slow sand filtration is one of the oldest water treatment technology widely applied globally across various scales from centralised systems to point-of-use treatment. The major functions of these filters include turbidity removal, disinfection and production of biologically stable drinking water. SSFs operate on the principle of percolation of water through a fine sand bed at low rates of 0.1-0.3 m/h without backwashing. This fosters the growth of a thick biofilm layer called the *Schmutzdecke* on the filter surface, and thinner biofilms in the remaining filter bed.

SSFs to date are operated as "black boxes" with limited understanding of the underlying processes contributing to treatment. This research aimed to unravel the physical-chemical and biological processes involved in disinfection and removal of biological stability parameters (dissolved organic carbon (DOC) and ammonium (NH_4^+) and by contributing to the development of new design rules for modern SSFs. Moving beyond the traditional focus on the *Schmutzdecke*, considerable attention was given to understanding the role of the entire filter system in removing enteric pathogens, DOC and NH_4^+. The insights from the depth-specific investigation in both full-scale SSFs at a Dutch drinking water utility and experimental filters in the laboratory yielded two main conclusions.

Conclusion 1: Removal of bacteria and viruses in SSFs is more effective in the deeper layers than in the Schmutzdecke, with distinct mechanisms for each at different depths

In column experiments with filter material from mature full-scale SSFs, the deeper layers were found to be more effective at removing *E.coli* WR1 and PhiX 174—surrogates for enteric bacteria and viruses, respectively, compared to the *Schmutzdecke*. The effectiveness of the deeper layers is attributed to well-established biofilms in filters operating for several years. Although, the deeper layers showed three to four times lower retention rates per cm bed height than in the *Schmutzdecke* for these surrogates, the extensive depth of the sand bed compensated for these lower values, enhancing total removal. Scraping of the *Schmutzdecke* in a full-scale SSF was found to disrupt the functionality of the top layers, leading to the release of biomass. However, this biomass was effectively captured by the deeper layers, which functioned as the ultimate barrier, ensuring a stable biomass concentration and microbial community composition in the effluent.

Bacteria and virus attenuation in the *Schmutzdecke* and deeper layers resulted from distinct biotic processes led by (micro)organisms in the biofilm and abiotic processes occurring within the biofilm and sand. *E.coli* WR1 was predominantly removed by (micro)organisms, likely through predation, grazing and enzyme-based inactivation, similarly in both the *Schmutzdecke* and deeper layers. Straining in the sand bed and attachment to the biofilm served as secondary mechanisms. The narrow pore radii (0.5-35 µm) in

the *Schmutzdecke* were particularly effective in trapping bacteria by increasing collisions with the biofilm. On the contrary, PhiX 174 was primarily removed by attachment to sand grains containing traces of iron and manganese oxides, aided by Brownian motion. Subsequently, its removal occurred due to (micro)organisms in the biofilm, likely through grazing and inactivation by proteolytic enzymes, and by attachment to extracellular polymeric substances (EPS) of biofilm in both the *Schmutzdecke* and deeper layers.

Conclusion 2: Dissolved organic carbon and ammonium removal in SSFs is spatially separated and not exclusive to the Schmutzdecke, and can be enhanced using a novel range of operational conditions

In both full-scale and laboratory SSFs, the removal of DOC and NH_4^+ was spatially separated in the filter, aided by distinct microbial communities and processes at different depths. The biodegradable fraction of DOC was mainly removed in the *Schmutzdecke* due to heterotrophic activity; however, its removal was not exclusive to this layer. After scraping of *Schmutzdecke*, the deeper layers of full-scale SSF effectively took over the function of eliminating both easily biodegradable and complex recalcitrant fractions of DOC. NH_4^+ slightly decreased in the *Schmutzdecke* due to assimilation by heterotrophic microorganisms, while a major removal occurred through nitrification at depths below the *Schmutzdecke*. The efficacy of these deeper layers in removing NH_4^+ was highlighted by the presence of nitrifiers capable of adapting to different NH_4^+ concentrations.

In the middle layers where nitrification was complete, both mature and young SSFs produced easily biodegradable carbon, independent of biofilm maturity. This phenomenon was hypothesized to result from two mechanisms: release of carbon from starving nitrifiers due to NH_4^+ and NO_2^- limitation or the conversion of slowly degradable carbon into easily biodegradable carbon. Nevertheless, the released DOC was effectively captured by processes in the deep sand bed, once again highlighting the critical role of deeper layers of SSFs in enhancing the biological stability of drinking water.

The removal kinetics study in experimental filters showed that DOC and NH_4^+ removal could be enhanced by adopting the operational conditions of rapid-rate biofilters. Using coarse sand (0.8-1.2 mm) as the filter medium did not limit microbial interactions and removal, indicating that a relatively small sand grain size, normally used in SSFs (0.3-1.2 mm), is not a crucial design parameter for DOC and NH_4^+ removal. Operating SSFs at a higher loading rate increased their removal efficacy, explained by sufficient utilisation of residual surface area on the sand grains by growing biofilms. Thus, filters targeting DOC and NH_4^+ removal can effectively operate at higher flow rates without compromising effluent quality. The backwashing of laboratory SSFs accelerated the recovery of DOC and NH_4^+ removal, due to the redistribution of biomass on sand after backwashing which probably enhanced the development of biological processes throughout the filter. Backwashing was thus identified as a potential strategy to

accelerate the ripening period, specifically for young SSFs designed from a biological stability perspective.

This dissertation offers a detailed insight into the key roles of distinct processes in disinfection and removal of biological stability parameters in SSFs, highlighting that biological processes extend beyond the traditionally valued *Schmutzdecke* into the deeper filter layers. A practical conclusion is that SSFs can benefit from preserving the sand bed height and minimizing invasive cleaning, thus protecting the biofilms in the deeper layers. Coarse sand and high loading rates do not compromise the effluent quality. This research shows the need to re-evaluate the traditional SSF design and operational strategies, to recognize the importance of both the *Schmutzdecke* and deeper layers. This is particularly important as the original design of SSFs dates back to a period when SSFs were part of a limited treatment scheme. In modern drinking water production, SSFs are used as final polishing step, operating under very low loads, justifying a new design.

Samenvatting

Langzame zandfiltratie is de oudste waterbehandelingstechnologie die wereldwijd op verschillende schaal wordt toegepast, van gecentraliseerde systemen tot en met huishoudelijk niveau. De belangrijkste functies van deze filters zijn het verwijderen van troebelheid, desinfectie en productie van biologisch stabiel drinkwater. Langzame zandfilters (LZFs) werken volgens het principe van percolatie van water door een fijn zandbed met lage snelheden van 0.1-0.3 m/u, zonder periodieke terugspoeling van het filterbed. Dit bevordert de groei van een dikke biofilmlaagop het filteroppervlak, de *Schmutzdecke*, en dunnere biofilms in de rest van het filterbed.

Tot op heden worden LZFs bedreven als "black boxes". Dit onderzoek richtte zich op het ontrafelen van de fysisch-chemische en biologische processen betrokken bij desinfectie en verwijdering van parameters voor biologische stabiliteit (opgeloste organische koolstof (DOC) en ammonium (NH_4^+) en daardoor bij te dragen aan het ontwikkelen van nieuwe ontwerpinzichten voor moderne LZFs. Verder kijkend dan de traditionele focus op de *Schmutzdecke*, werd vooral aandacht besteed aan het begrijpen van de rol van het gehele filtersysteem in het verwijderen van enterische pathogenen, DOC en NH_4^+. De inzichten uit onderzoek over de gehele hoogte van filters, in zowel full-scale LZFs bij een Nederlands drinkwaterbedrijf als in experimentele filters op laboratoriumschaal, leidden tot twee hoofdconclusies.

Conclusie 1: De verwijdering van bacteriën en virussen in LZFs is effectiever in de diepere lagen dan in de Schmutzdecke, met specifieke mechanismen voor de verschillende diepten

In kolomexperimenten met filtermateriaal van full-scale LZFs, bleken de diepere lagen effectiever te zijn in het verwijderen van *E.coli* WR1 en PhiX 174 - surrogaatparameters voor enterische bacteriën en virussen, respectievelijk - dan de *Schmutzdecke*. De effectiviteit van de diepere lagen wordt toegeschreven aan goed gevestigde biofilms in filters die al enkele jaren operationeel zijn. Hoewel de verwijdering per cm filter diepte voor deze surrogaatparameters drie tot vier keer lager was in de diepere lagen dan in de *Schmutzdecke*, compenseerde de totale hoogte van de diepere lagen van het zandbed deze lagere waarden, waardoor de totale verwijdering groter was. Het afschrapen van de *Schmutzdecke* in de full-scale LZFs bleek de functionaliteit van de bovenste lagen te verstoren, wat leidde tot de afgifte van biomassa. Deze biomassa werd echter effectief afgevangen in de diepere lagen, die fungeerden als de ultieme barrière, waardoor een stabiele biomassaconcentratie en microbiële gemeenschapssamenstelling in het effluent werd gewaarborgd.

De verwijdering van bacteriën en virussen in de *Schmutzdecke* en diepere lagen was het resultaat van specifieke biotische processen door (micro)organismen in de biofilm, en abiotische processen die plaatsvinden in de biofilm en het zandbed. *E.coli* WR1 werd voornamelijk verwijderd door

(micro)organismen, waarschijnlijk door predatie, begrazing en enzymatische inactivatie, op dezelfde manier in zowel de *Schmutzdecke* als in de diepere lagen. Zeving in het zandbed en hechting aan de biofilm dienden als secundaire mechanismen. De nauwe porieradii (0.5-35 µm) in de *Schmutzdecke* waren bijzonder effectief in het afvangen van bacteriën door het verhogen van botsingen met de biofilm. In tegenstelling werd PhiX 174 voornamelijk verwijderd door hechting aan zandkorrels die sporen van ijzer- en mangaanoxiden bevatten, in combinatie met Brownse beweging. Vervolgens vond de verwijdering plaats door (micro)organismen in de biofilm, waarschijnlijk door begrazing en inactivatie door proteolytische enzymen, en door hechting aan extracellulaire polymere stoffen (EPS) in de biofilm, zowel in de *Schmutzdecke* als in de diepere lagen.

Conclusie 2: De verwijdering van opgeloste organische koolstof en ammonium in LZFs is ruimtelijk gescheiden en niet exclusief voor de Schmutzdecke, en kan worden verbeterd door gebruik te maken van een nieuw scala aan bedrijfscondities

In zowel full-scale als laboratorium LZFs was de verwijdering van DOC en NH_4^+ ruimtelijk gescheiden van elkaar, ondersteund door specifieke microbiële gemeenschappen en processen op verschillende diepten. Het biologisch afbreekbare deel van DOC werd voornamelijk verwijderd in de *Schmutzdecke* door de activiteit van heterotrofe bacteriën, maar de verwijdering was niet exclusief voor deze laag. Na het afschrapen van de *Schmutzdecke* namen de diepere lagen van het full-scale LZF effectief het elimineren van zowel gemakkelijk biologisch afbreekbare als complexe recalcitrante fracties van DOC over. NH_4^+ nam licht af in de *Schmutzdecke* door assimilatie door heterotrofe microorganismen, terwijl een belangrijke verwijdering plaats vond door nitrificatie op diepten onder de *Schmutzdecke*. De effectiviteit van deze diepere lagen in het verwijderen van NH_4^+ werd benadrukt door de aanwezigheid van nitrificeerders die zich konden aanpassen aan verschillende NH_4^+ concentraties.

Op de filterdiepten waar de nitrificatie compleet was, produceerden zowel oudere als jonge LZFs gemakkelijk biologisch afbreekbare koolstof, onafhankelijk van de rijpheid van de biofilm. Twee mechanismen kunnen ten grondslag liggen aan dit fenomeen: de afgifte van koolstof door uitgehongerde nitrificeerders vanwege NH_4^+ en NO_2^- limitatie, of de omzetting van langzaam afbreekbare koolstof in gemakkelijk biologisch afbreekbare koolstof. Echter, de vrijgegeven DOC werd effectief opgevangen door processen dieper in het zandbed, wat nogmaals de cruciale rol van de diepere lagen van LZFs in het verbeteren van de biologische stabiliteit van drinkwater benadrukt.

De studie naar verwijderingskinetiek in laboratoriumfilters toonde aan dat de verwijdering van DOC en NH_4^+ kon worden verbeterd door de operationele condities van snelfilters toe te passen. Het gebruik van grof zand (0.8-1.2 mm) als filtermedium beperkte de microbiële interacties en verwijdering niet, wat aantoont dat een relatief kleine korreldiameter, normaliter gebruikt in LZFs (0.3 – 1.2 mm), geen

cruciale ontwerpparameter is voor DOC en NH_4^+ verwijdering. Het bedrijven van LZFs met een hogere belasting verhoogde de verwijderingsefficiëntie, wat verklaard kan worden door gebruik van het resterende oppervlak op de zandkorrels voor groei van biofilm. Op die manier kunnen filters, die gericht zijn op DOC en NH_4^+ verwijdering, effectief werken met hogere filtratiesnelheden zonder de effluentkwaliteit in gevaar te brengen. Het terugspoelen van laboratorium LZFs versnelde het herstel van DOC en NH_4^+ verwijdering, door de herverdeling van biomassa op zand na het terugspoelen, wat waarschijnlijk de ontwikkeling van biologische processen door het hele filter verbeterde. Terugspoelen is dus een potentiële strategie om de rijpingsperiode te versnellen, specifiek voor jonge LZFs ontworpen vanuit een perspectief van biologische stabiliteit.

Dit proefschrift biedt een gedetailleerd inzicht in de sleutelrollen van specifieke processen voor desinfectie en verwijdering van parameters voor biologische stabiliteit in LZFs, en toont aan dat biologische processen zich uitstrekken verder dan de traditioneel belangrijke *Schmutzdecke*, naar de diepere filterlagen. Een conclusie voor de praktijk is dat LZFs kunnen profiteren van het behoud van de zandbedhoogte en het minimaliseren van invasieve reiniging, waardoor de biofilms in de diepere lagen worden beschermd. Grof zand en hoge belastingen hebben geen nadelig effect op de effluentkwaliteit. Dit onderzoek benadrukt de noodzaak van een herziening van het traditionele LZF-ontwerp en bedrijfsvoering strategieën, die het belang van zowel de *Schmutzdecke* als de diepere lagen erkennen. Dit is des te belangrijk, omdat het oorspronkelijke ontwerp van LZFs veelal dateert uit de tijd dat LZFs onderdeel vormden ven een beperkt zuiveringsschema. In de moderne, hedendaagse drinkwaterproductie zijn LZFs vaak de laatste, zeer laagbelaste polishing stap, wat een nieuw ontwerp rechtvaardigt.

Biography

Shreya Ajith Trikannad was born in Mysore, India on 22nd November, 1995. With an interest in environmental science, she did her bachelors in Environmental Engineering at Sri Jayachamarajendra College of Engineering in Mysore, India. In 2017, she started her MSc in Delft University of Technology in the Netherlands, specialising in water quality and treatment. For her MSc thesis she investigated the removal of enteric pathogens and antibiotic-resistant bacteria from municipal effluent using low-voltage iron electrocoagulation, for which she won the Gijs Oskam prize. She also did an additional research to assess the fate of pathogens in (novel) secondary wastewater treatment technologies designed for water reclamation. In 2019, she started her PhD research under the guidance of Prof. Jan Peter van der Hoek and Prof. Doris van Halem. Her research focused on slow sand filters for drinking water treatment, as part of the broader Sand Filtration Programme. Her research contributed to a better understanding of removal processes at different depths of slow sand filters, promoting the development of novel design rules and operational strategies.

Shreya is currently doing her postdoctoral research at Eawag (Swiss Federal Institute of Aquatic Science and Technology) in Switzerland, in the group of Prof. Eberhard Morgenroth. Her research focuses on treatment technologies and monitoring approaches for pathogens control in decentralized water treatment and reuse systems for non-potable purposes.

List of publications

International refereed journals

Trikannad, S. A., van Halem, D., Foppen, J. W., & van der Hoek, J. P. (2023). The contribution of deeper layers in slow sand filters to pathogens removal. *Water Research*, 237, 119994.

Trikannad, S. A., Attiani, V., van der Wielen, P. W., Smidt, H., van der Hoek, J. P., & van Halem, D. (2024). Recovery of microbial biomass and purification performance after scraping of full-scale slow sand filters. *Journal of Water Process Engineering*, 60, 105101.

Bicudo, B., van Halem, D., Trikannad, S. A., Ferrero, G., & Medema, G. (2021). Low voltage iron electrocoagulation as a tertiary treatment of municipal wastewater: removal of enteric pathogen indicators and antibiotic-resistant bacteria. *Water Research*, 188, 116500.

Publications in preparation

Trikannad, S. A., Huang, Y., van Halem, D., & van der Hoek, J. P. (2024). Dissolved organic carbon and ammonium removal kinetics study to redesign slow sand filters. To be submitted.

Trikannad, S. A., van der Hoek, J. P., & van Halem, D. (2024). Biodegradable organic carbon release in deep bed of slow sand filters. To be submitted.

Attiani, V., Trikannad, S. A., van der Hoek, J. P., van Halem, D., van der Wielen, P. W., & Smidt, H., (2024). Accelerating the ripening period in slow sand filters by biostimulation. To be submitted.

Conference proceedings

Trikannad, S. A., van Halem, D., Foppen, J. W., & van der Hoek, J. P. (2022). The underestimated contribution of deeper layers in slow sand filters to pathogens removal, Young Water Professionals, Netherlands.